

Compounding Effects of Sea Level Rise and Fluvial Flooding

SUPPLEMENTARY MATERIALS

H.R. Moftakhari

Department of Civil and Environmental Engineering
University of California, Irvine (USA)

G. Salvadori

Dipartimento di Matematica e Fisica
Università del Salento, Lecce (Italy)

A. AghaKouchak

Department of Civil and Environmental Engineering
University of California, Irvine (USA)

B.F. Sanders

Department of Civil and Environmental Engineering
University of California, Irvine (USA)

R.A. Matthew

Blum Center for Poverty Alleviation
University of California, Irvine (USA)

June 20, 2017

1 Study Area and Data Resources

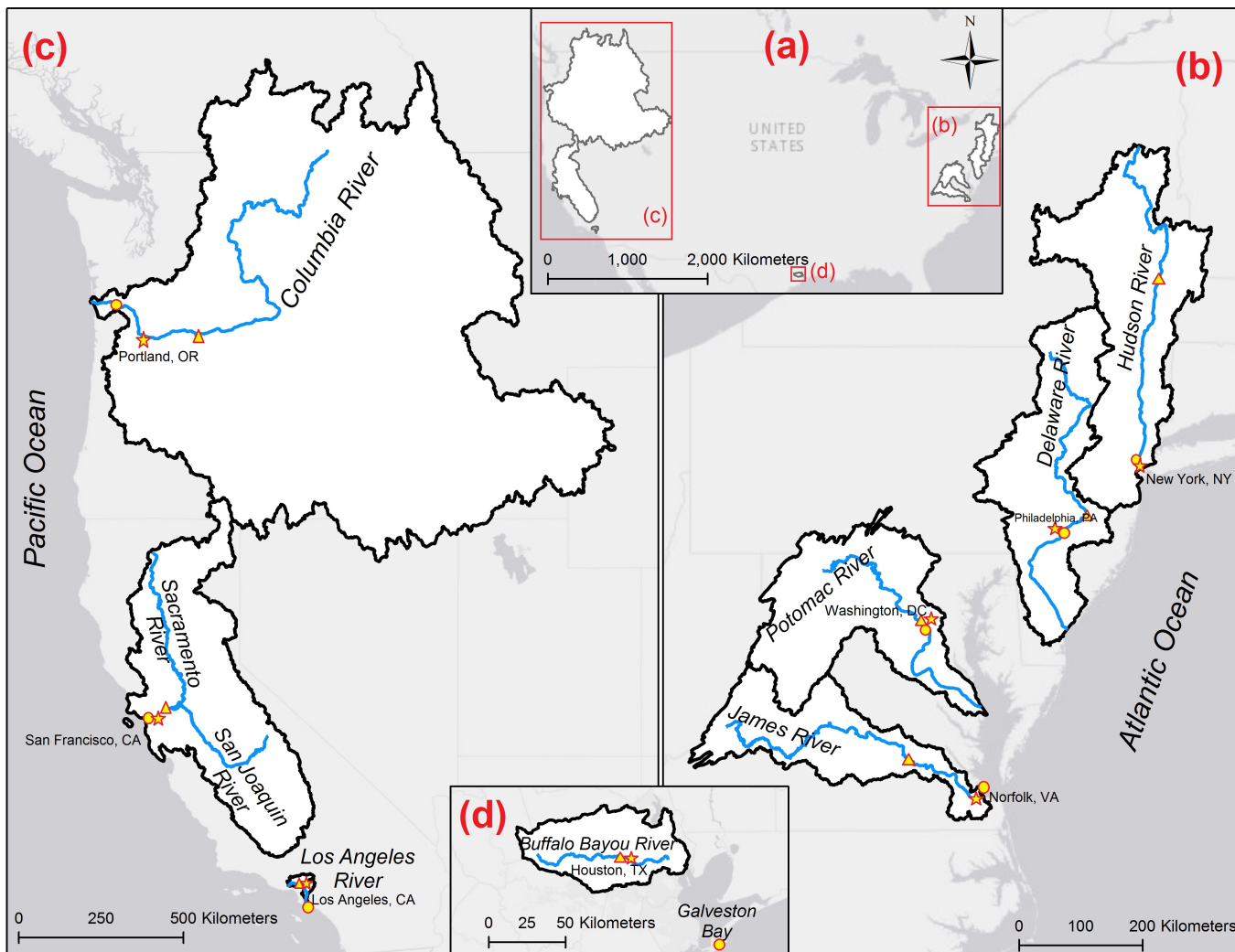


Figure SM.1: Locations of the selected coastal-estuarine systems; the white closed area show the watershed that drains freshwater into ocean at/near a tide gauge. The star, triangle, and circle marks show, respectively, the nearby major town, river flow measurement gauge, and tide gauge.

Table SM.1: Data info

Location	River Flow				Water Level		
	River Name	Measured by	Station ID	Length of Record (years)	Tide gauge	NOAA ID	Length of Record (years)
Houston, TX	Buffalo Bayou	USGS	08073500	70	Galveston	8771450	70
Los Angeles, CA	Los Angeles	USGS	11092450	84	Los Angeles	9410660	91
New York, NY	Hudson	USGS	01335754	128	Battery	8518750	89
Norfolk, VA	James	USGS	02037500	81	Sewells point	8638610	88
Philadelphia, PA	Delaware	USGS	01463500	103	Philadelphia	8545530	103
Portland, OR	Columbia	USGS	14105700	137	Astoria	9439040	90
San Francisco, CA	Delta Outflow	CDWR	Net Delta Outflow Index	85	San Francisco	9414290	157
Washington, DC	Potomac	USGS	01646500	85	Washington	8594900	84

Table SM.2: Previous studies on bivariate flood hazard analysis on a Country base

Study	Region	Variables	Method
Hawkes et al. [2002]	UK	Waves/Water level	Bivariate Normal and Empirical Copulas
Svensson and Jones [2002]	UK	Storm Surge/River Flow	Bivariate Extreme Value
Svensson and Jones [2004]	UK	Storm Surge/River Flow/Precipitation	Bivariate Extreme Value
Lamb et al. [2010]	UK	River Flow/Sea Level	Conditional Exceedence
Chini and Stansby [2012]	UK	Waves	Gumbel Copulas
Zheng et al. [2013]	Australia	Storm Surge/Precipitation	Bivariate Extreme Value
Zheng et al. [2014]	Australia	Storm Surge/Precipitation	Bivariate Extreme Value
Zheng et al. [2015b]	Australia	Storm Surge/Precipitation	Design Variable
Zheng et al. [2015a]	Australia	Storm Surge/Precipitation	Design Variable
van den Hurk et al. [2015]	Netherlands	Storm Surge/Precipitation	Physical Model Ensembles
Kew et al. [2013]	Netherlands	Storm Surge/River Flow	Physical Model Ensembles
Klerk et al. [2015]	Netherlands	Storm Surge/River Flow	Joint Tail Dependence
Li et al. [2014a]	Netherlands	Wave variables	Copulas and logistic models
Li et al. [2014b]	Netherlands	Wave variables	Copulas
De Michele et al. [2007]	Italy	Storm Surge Parameters	Vine Copulas
Salvadori et al. [2014]	Italy	Storm Surge Parameters	Khoudraji-Liebscher Copulas
Salvadori et al. [2015]	Italy	Storm Surge Parameters	Khoudraji-Liebscher Copulas and Struct function
Gouldby et al. [2014]	Spain	Offshore sea condition data	multivariate extremes model
Rueda et al. [2016]	Spain	Wave height, wave period, storm surge	Gaussian Copula
Wahl et al. [2012]	Germany	Storm Surge Height and Intensity	Archimedean Copulas
Bender et al. [2016]	Germany	River Flows	Archimedean Copulas
Lian et al. [2013]	China	Precipitation/Tidal Level	Elliptical and Archimedean Copulas
Corbella and Stretch [2012]	South Africa	Storm Parameters	Archimedean Copulas
Corbella and Stretch [2013]	South Africa	Storm Surge Parameters	Archimedean Copulas
Serafin and Ruggiero [2014]	USA	Wave, tide, non-tidal residuals	Conditional dependence
Wahl et al. [2015]	USA	Storm Surge/Precipitation	Extreme Value and Archimedean Copulas
Wahl et al. [2016]	USA	Wave/Water Level	Elliptical Copulas

2 Univariate Analysis

Each sub-section contains the following plots concerning the gauge site indicated by the sub-section name: namely, Houston, Los Angeles, New York, Norfolk, Philadelphia, Portland, San Francisco, and Washington. The variables considered are:

- **X:** River flow (discharge), in m^3/s [left column];
- **Y:** Water level, in m [right column].

The number of Bootstrap iterations is $B = 1000$. The legend of the figures is as follows.

1st row. Estimates of the AIC (Akaike Information Criterion) statistics, for all the distributions considered: viz., from left to right, Birnbaum-Saunders (BS), Exponential (Exp), Gamma (Gam), Generalized Extreme Value (GEV), Generalized Pareto (GP), Inverse Gaussian (InvG), Loglogistic (LogL), Lognormal (LogN), and Weibull (Weib). The *black* bar indicates the probability law selected via the AIC, i.e. the one yielding the smallest AIC statistics.

2nd row. Bootstrap estimates of the approximate p -Value of the Kolmogorov-Smirnov Goodness-of-Fit test, for all the univariate distributions considered. The *black* bar indicates the probability law selected via the AIC, and the horizontal *dashed* line the critical 5% level. A distribution is considered as admissible, at a 5% level, only if the corresponding p -Value is larger than 5%

3rd row. Empirical distribution function of the available data (*markers*) and corresponding fit (*solid* line) using the distribution selected via the AIC. The *dashed* lines indicate a 95% bootstrap confidence band.

4th row. Empirical distribution function of the available data (*markers*) and corresponding fit (*solid* line) using the GEV distribution. The *dashed* lines indicate a 95% bootstrap confidence band. In this work, only the GEV distribution is used, independently of the indications provided by the AIC procedure.

2.1 Houston, TX

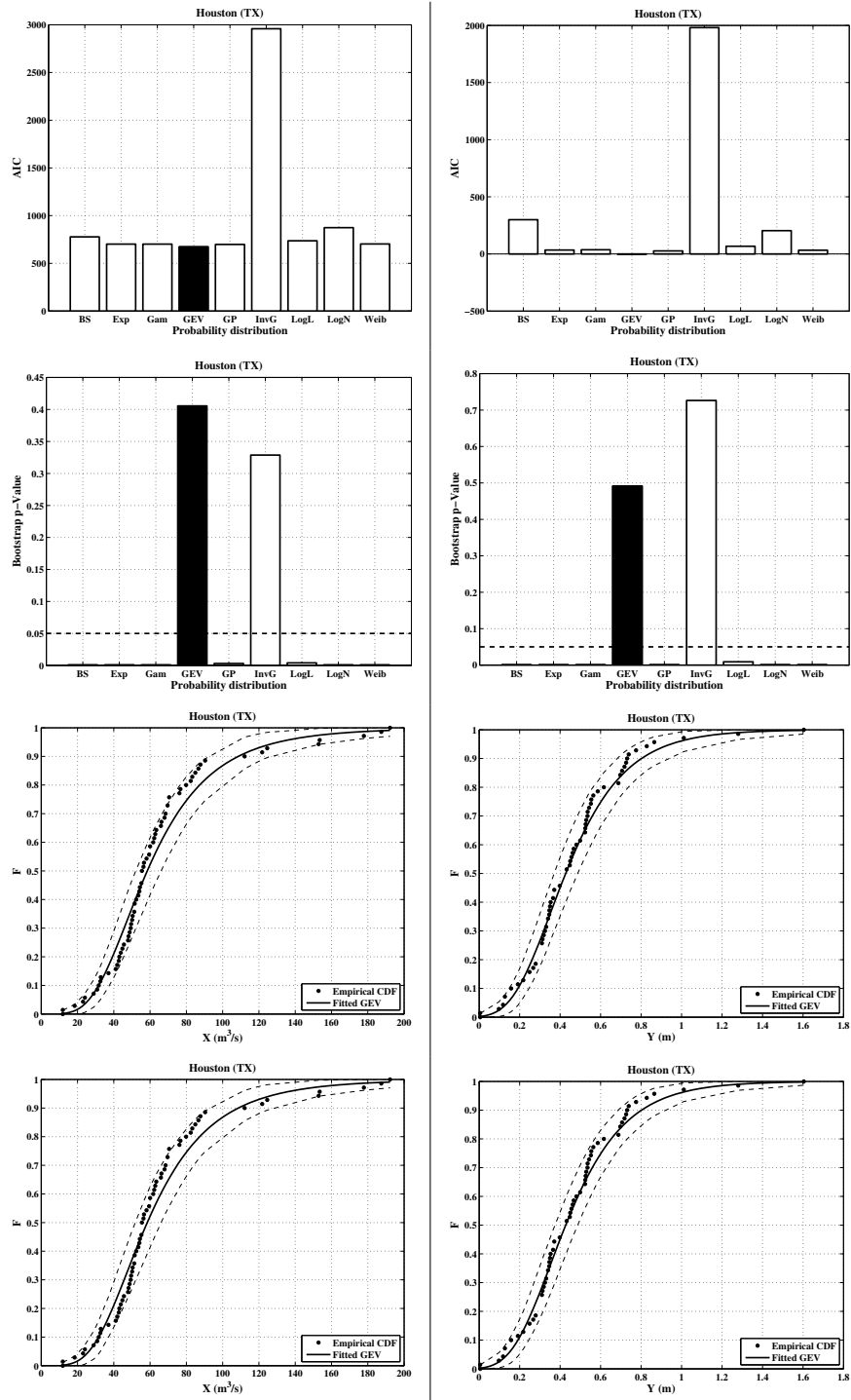


Figure SM.2: see text for explanation.

2.2 Los Angeles, CA

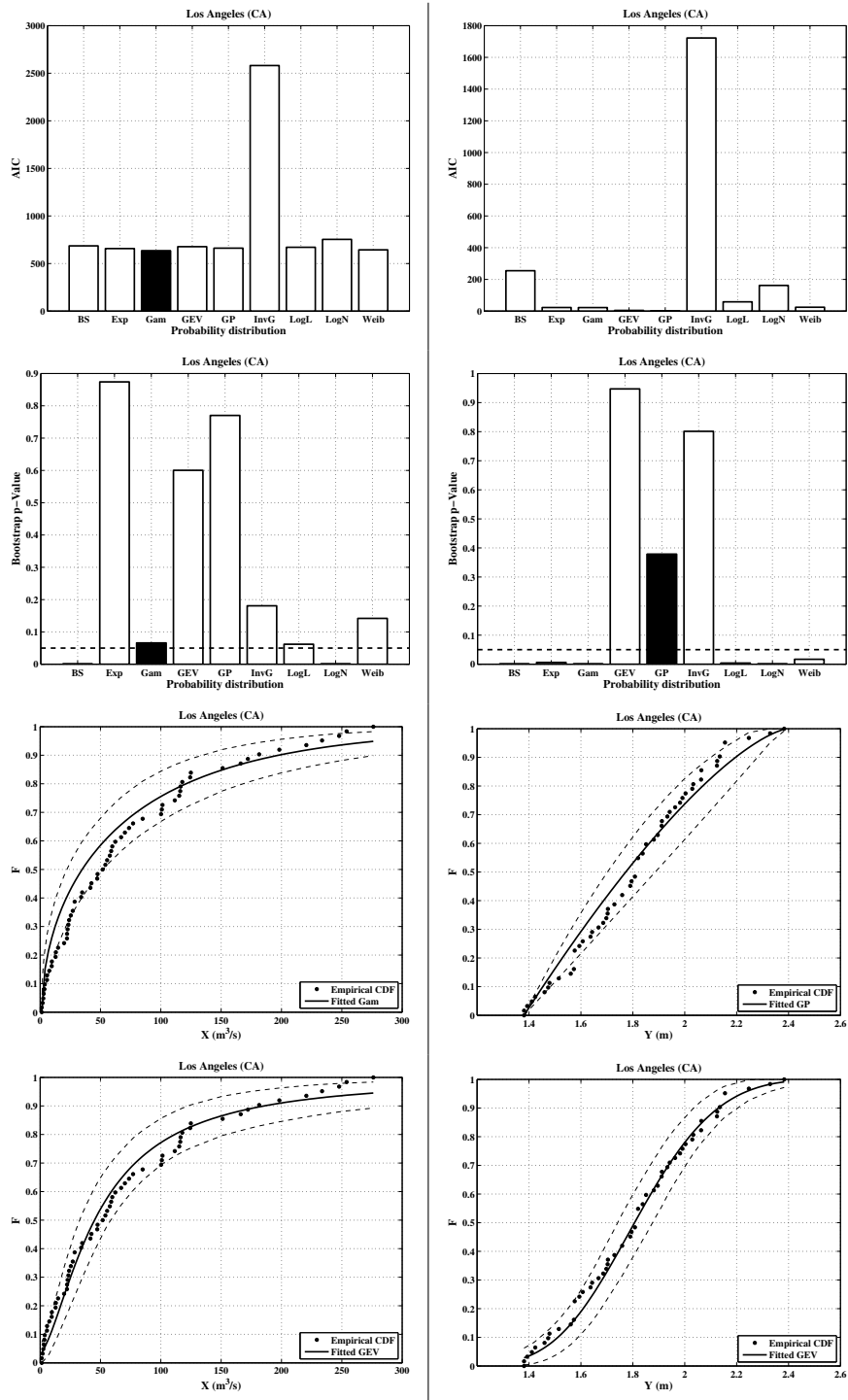


Figure SM.3: see text for explanation.

2.3 New York, NY

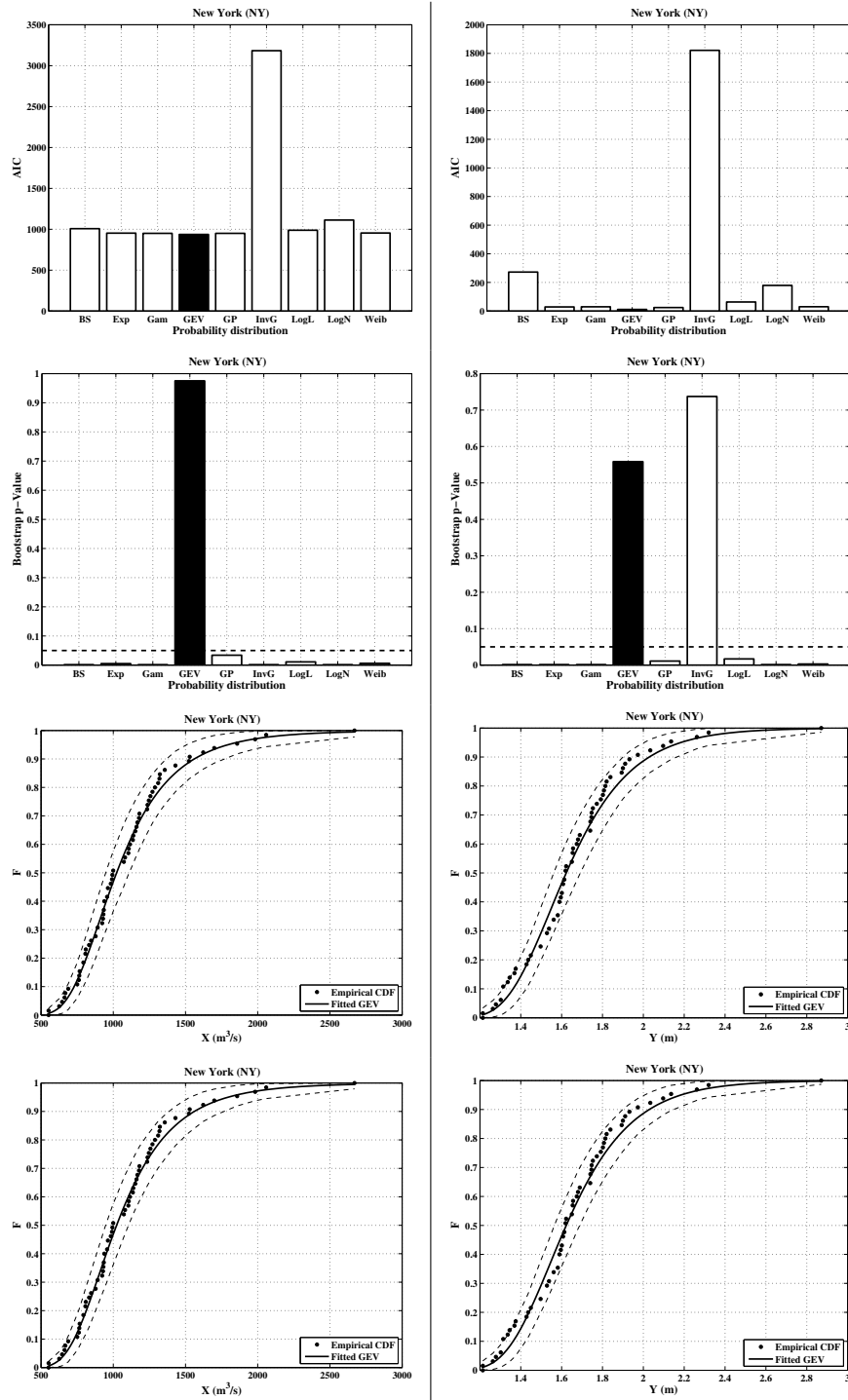


Figure SM.4: see text for explanation.

2.4 Norfolk, VA

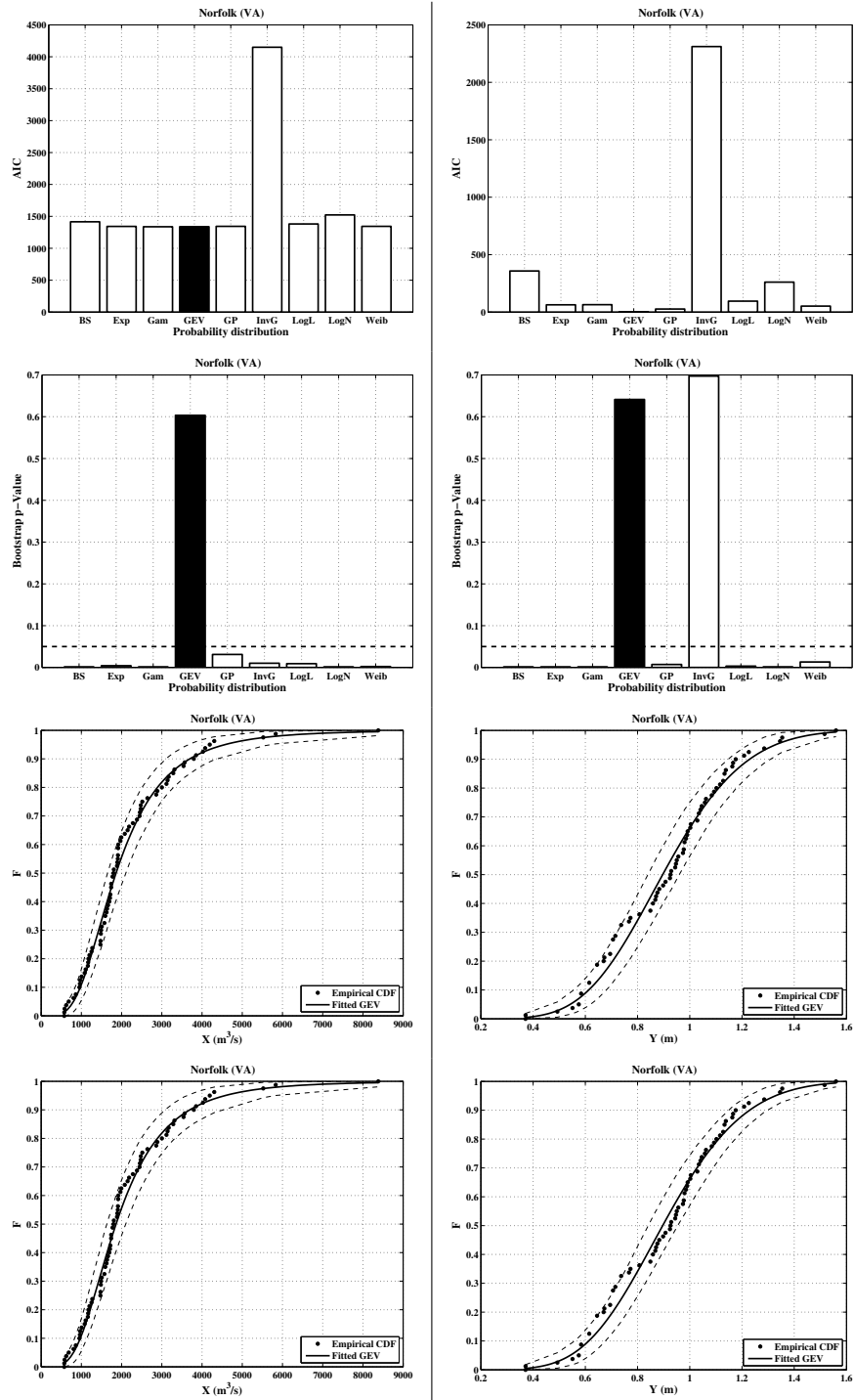


Figure SM.5: see text for explanation.

2.5 Philadelphia, PA

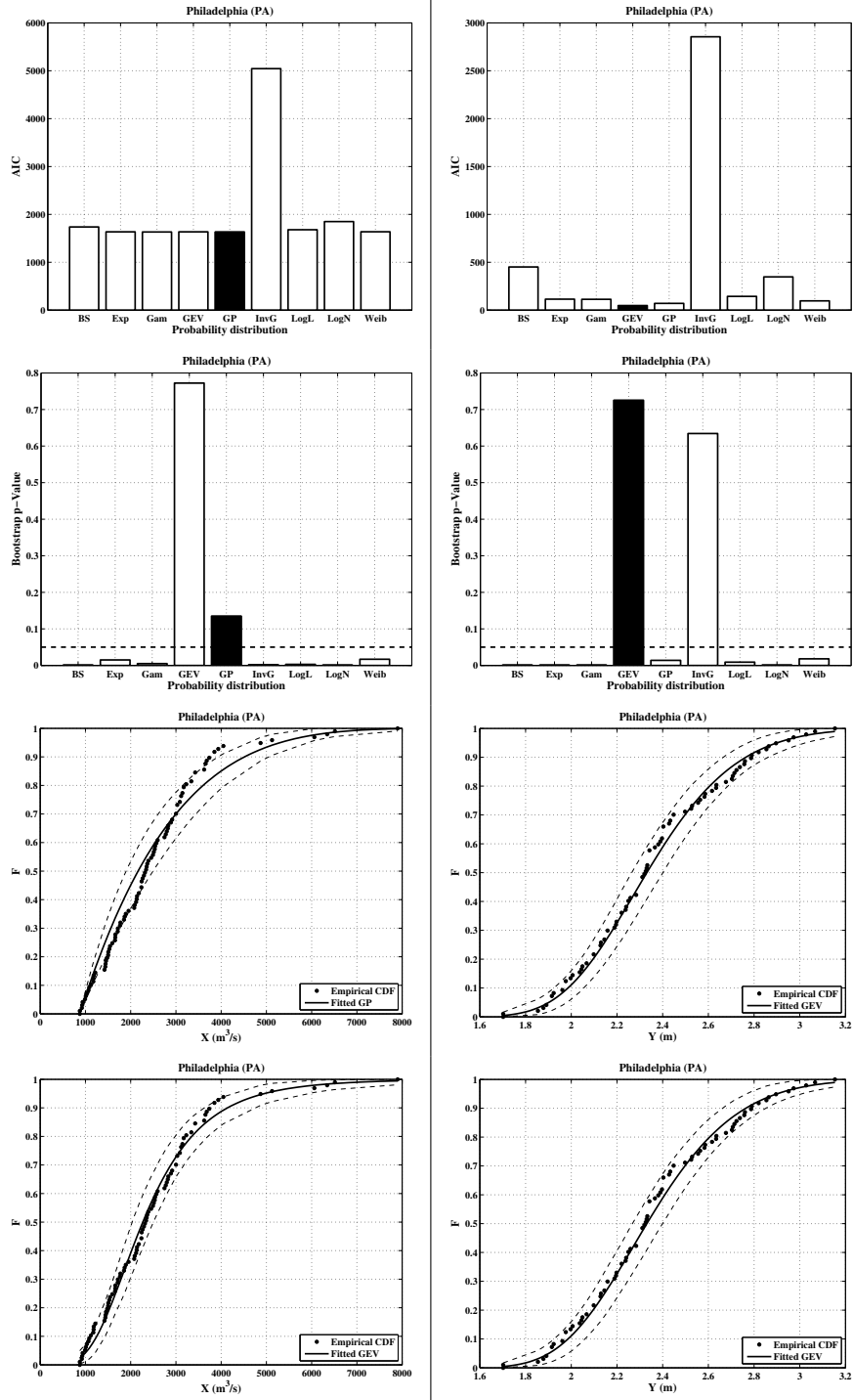


Figure SM.6: see text for explanation.

2.6 Portland, OR

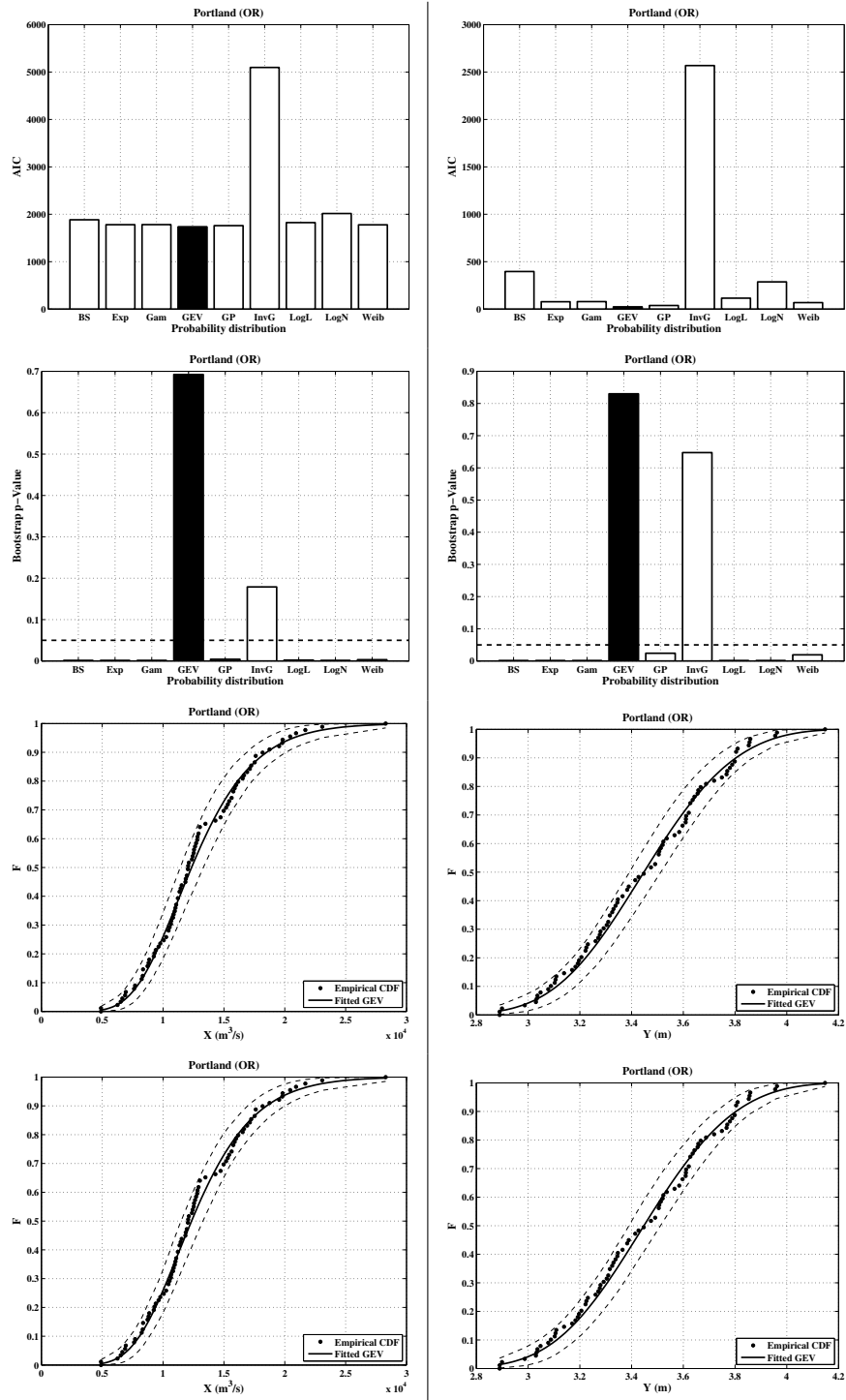


Figure SM.7: see text for explanation.

2.7 San Francisco, CA

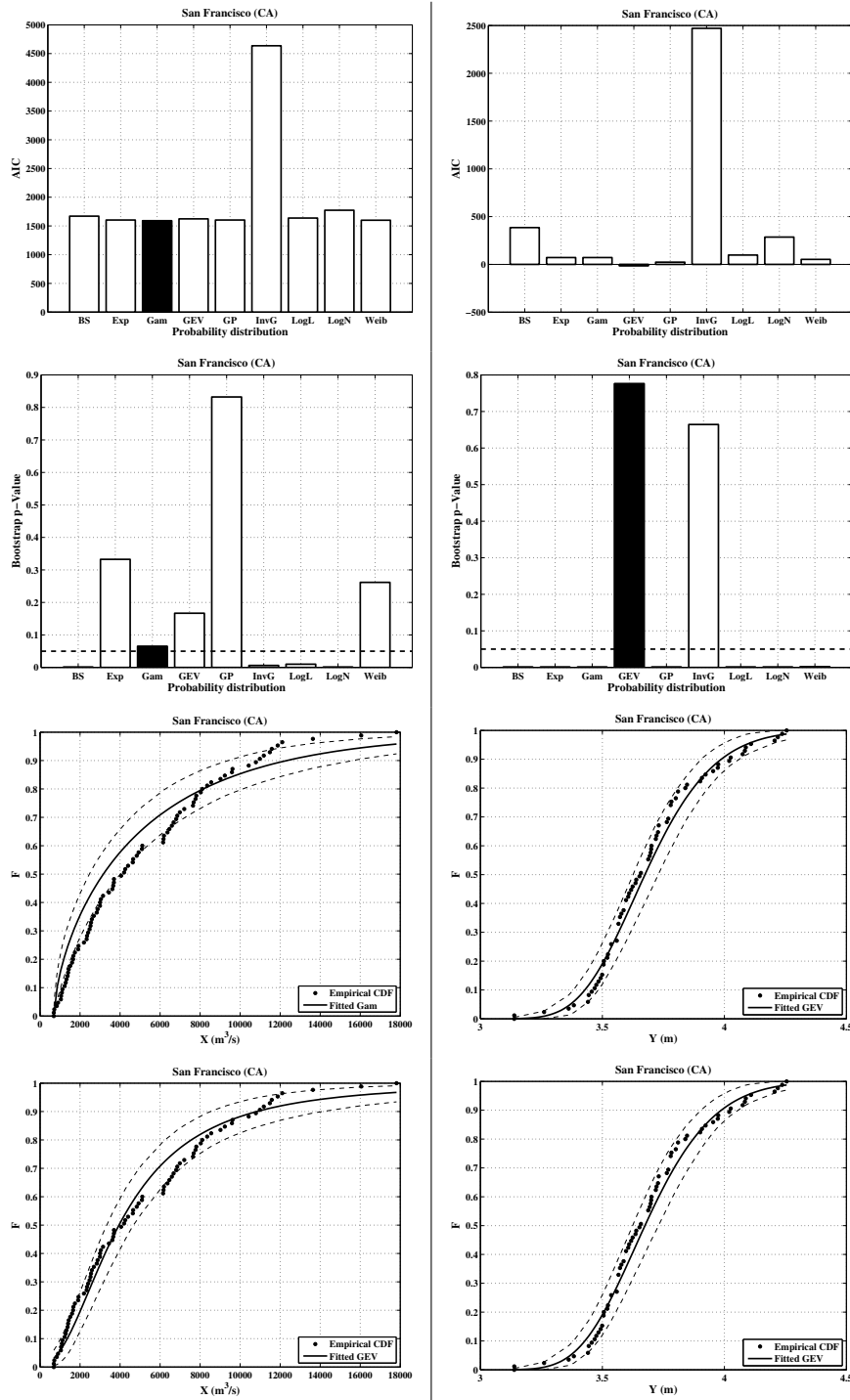


Figure SM.8: see text for explanation.

2.8 Washington, DC

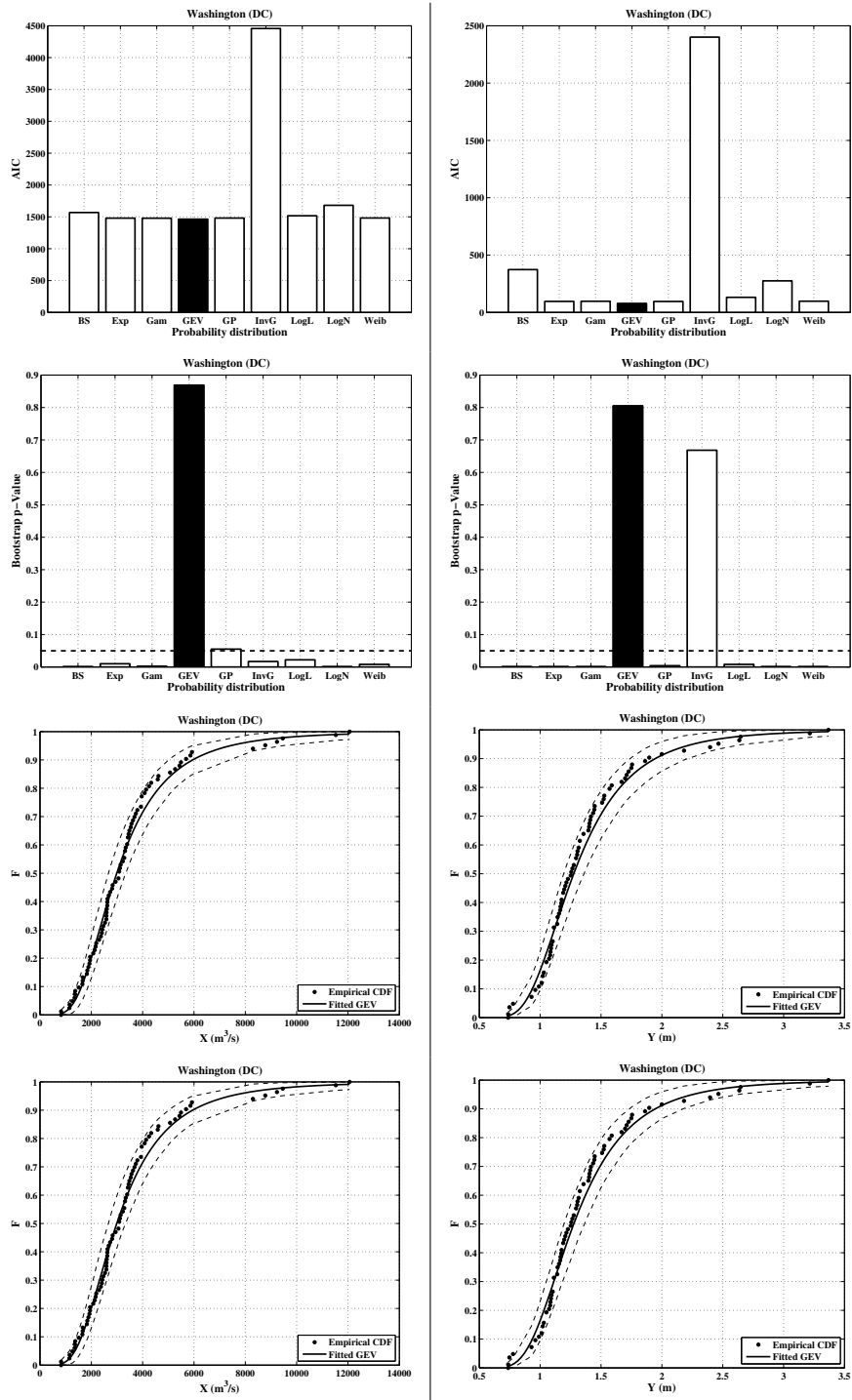


Figure SM.9: see text for explanation.

3 Bivariate Analysis: Kendall τ & Spearman ρ

The estimates of the Kendall τ and the Spearman ρ rank correlation coefficients [Lehman et al., 2005] are computed for the eight sites considered: namely, Houston, Los Angeles, New York, Norfolk, Philadelphia, Portland, San Francisco, and Washington — in the plots, these are abbreviated as Hou, LA, NY, Nfk, Phi, Por, SF, and Wsh. Also shown are the p -Values of the corresponding independence tests: values larger than 5% indicate that (at a 5% level) the null assumption that X and Y are independent cannot be rejected — the 5% level is indicated by a *dashed* line. Apparently, Philadelphia, San Francisco, and Washington data show some statistically significant dependence.

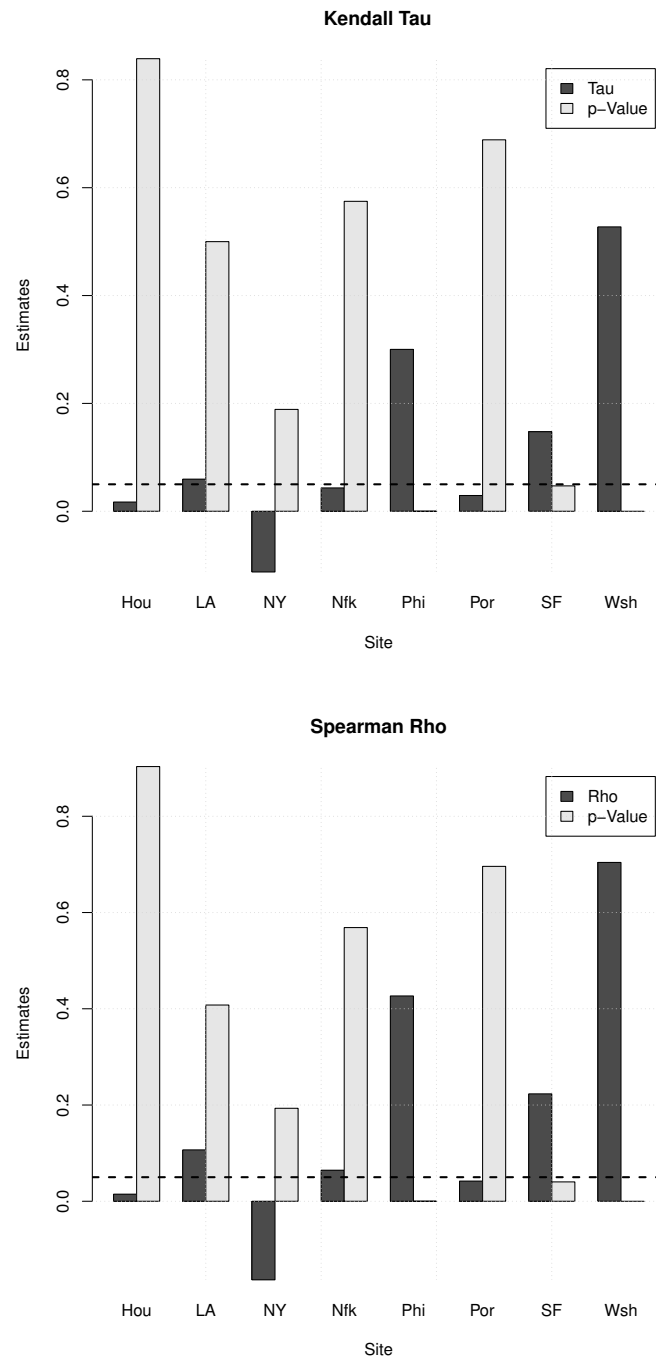


Figure SM.10: see text for explanation.

4 Bivariate Analysis: fits

As a result of the univariate analyses, the Generalized Extreme Value (GEV) distribution turns out to adequately fit the marginal distributions of the two variables of interest here. Indeed, the corresponding approximate bootstrap p -Values are always larger than 5% (see the statistical results shown in Section 2 in this Supplementary Materials, and Figures SM.2–SM.9).

Concerning the bivariate analysis, suitable non-parametric independence tests (i.e., the Kendall and the Spearman ones shown in Section 3) indicate that only for three, out of the eight stations considered, the independence assumption can be rejected: viz., Philadelphia, San Francisco, and Washington. In these cases, several bivariate copulas (12), as well as the corresponding survival copulas (for a total of 24 copulas), are fitted to the available data. The survival copulas are denoted by a “s”-prefix before the names/abbreviations of the dependence structures of interest.

The families of copulas considered here are as follows.

Archimedean: Ali-Mikhail-Haq, Clayton, Frank, Gumbel, Joe — in the plots, these are abbreviated as A, Cl, Fr, Gb, J.

Elliptical: Normal, t-Student — in the plots, these are abbreviated as N, t.

Extreme Value: Galambos, Husler-Reiss, Tawn [the Gumbel and t-Student Extreme Value copulas have already been considered] — in the plots, these are abbreviated as Gs, HR, Tw.

Farlie-Gumbel-Morgenstern: Farlie-Gumbel-Morgenstern — in the plots, it is abbreviated as M.

Plackett: Plackett — in the plots, it is abbreviated as P.

Using the R-package “copula” [Hofert et al., 2016], all these 24 copulas were tested, and those who passed suitable non-parametric Goodness-of-Fit tests (available in the package) were compared via a standard Akaike criterion, in order to select the “best” model among the ones considered. In turn, the following families are chosen: Tawn (Philadelphia), Survival Ali-Mikhail-Haq (San Francisco), and Survival Clayton (Washington). For all the other stations, the assumption of independent discharge and water level cannot be rejected at a standard 5% level, and the copula $\Pi_2(u, v) = uv$ modeling independent variables is used.

According to the results of the Kendall τ and the Spearman ρ independence tests shown in Section 3, different figures are plotted. On the one hand, if X and Y are assumed to be independent, then only the data are plotted, as well as the pseudo-observations (i.e., the normalized ranks), the isolines of the Empirical Copula (viz., a non-parametric estimate of the copula at play), and the isolines of the copula Π_2 (labeled “Prod.” in the legends) corresponding to the case of independent variables. On the other hand, if X and Y show possible dependence, then the following plots are presented:

- the estimates of the AIC (Akaike Information Criterion) statistics for copula selection: the family associated with the smaller AIC value should be chosen;
- the estimates of the p -Values of a copula Cramér-von Mises Goodness-of-Fit test — the critical 5% level is indicated by a *dashed* line: copula families associated with p -Values smaller than the critical level should not be considered;
- the data;
- the pseudo-observations, the isolines of the Empirical Copula, and the isolines of the copula selected via the AIC.

4.1 Houston, TX

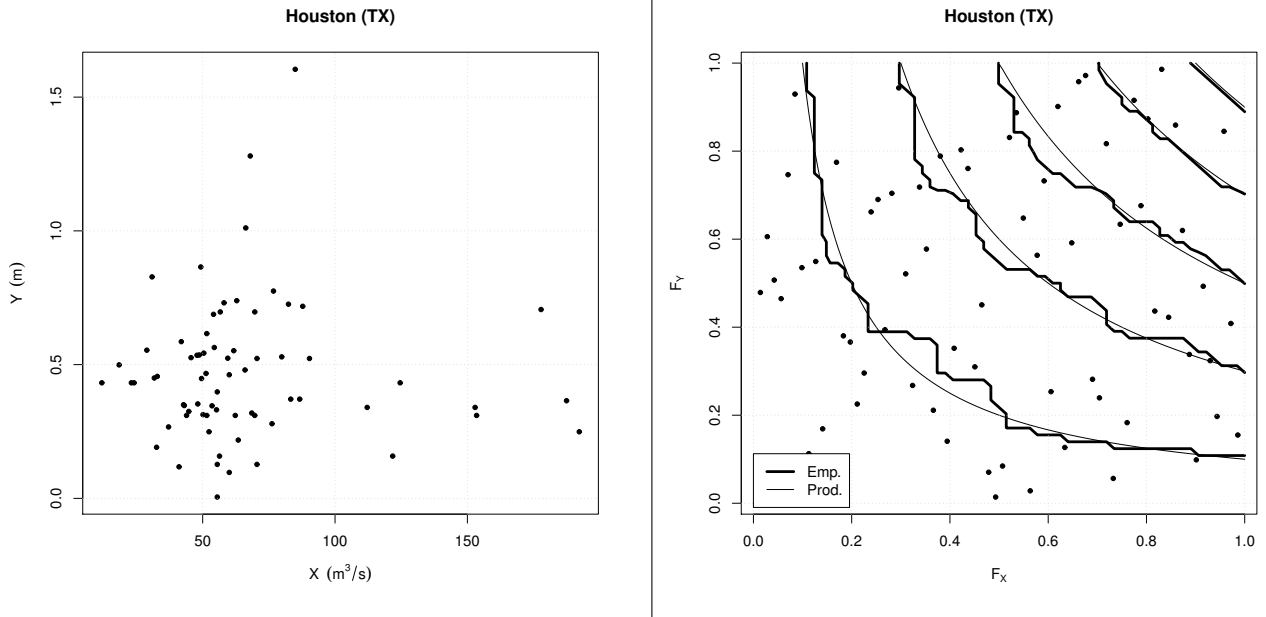


Figure SM.11: see text for explanation.

4.2 Los Angeles, CA

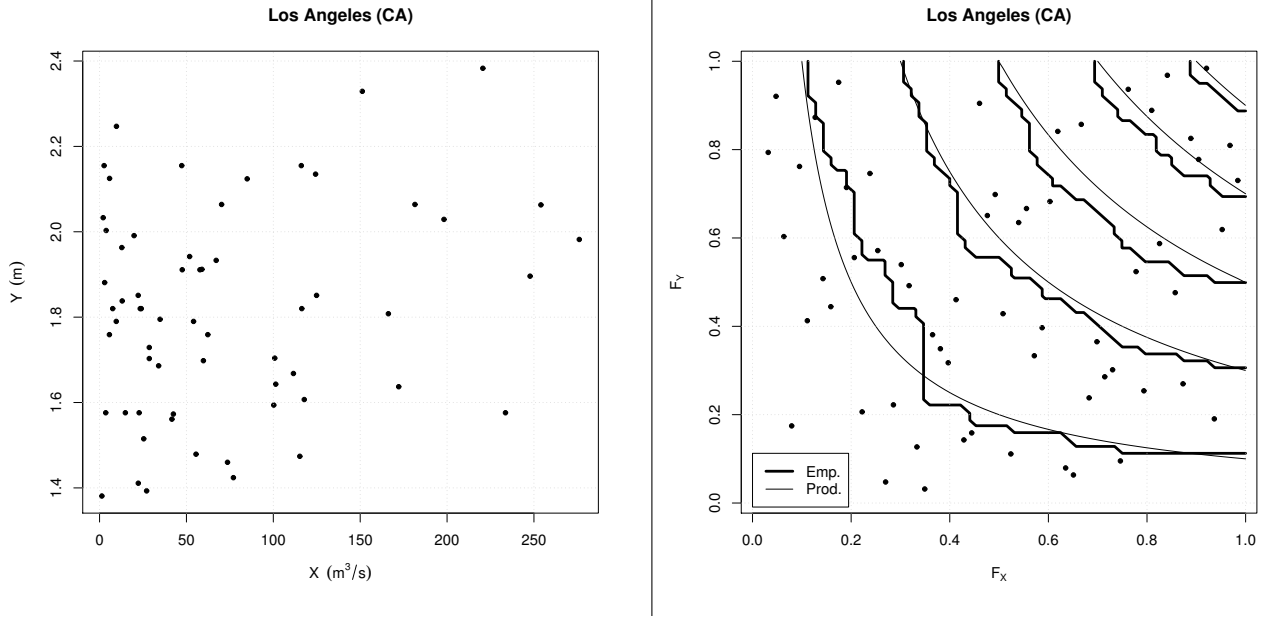


Figure SM.12: see text for explanation.

4.3 New York, NY

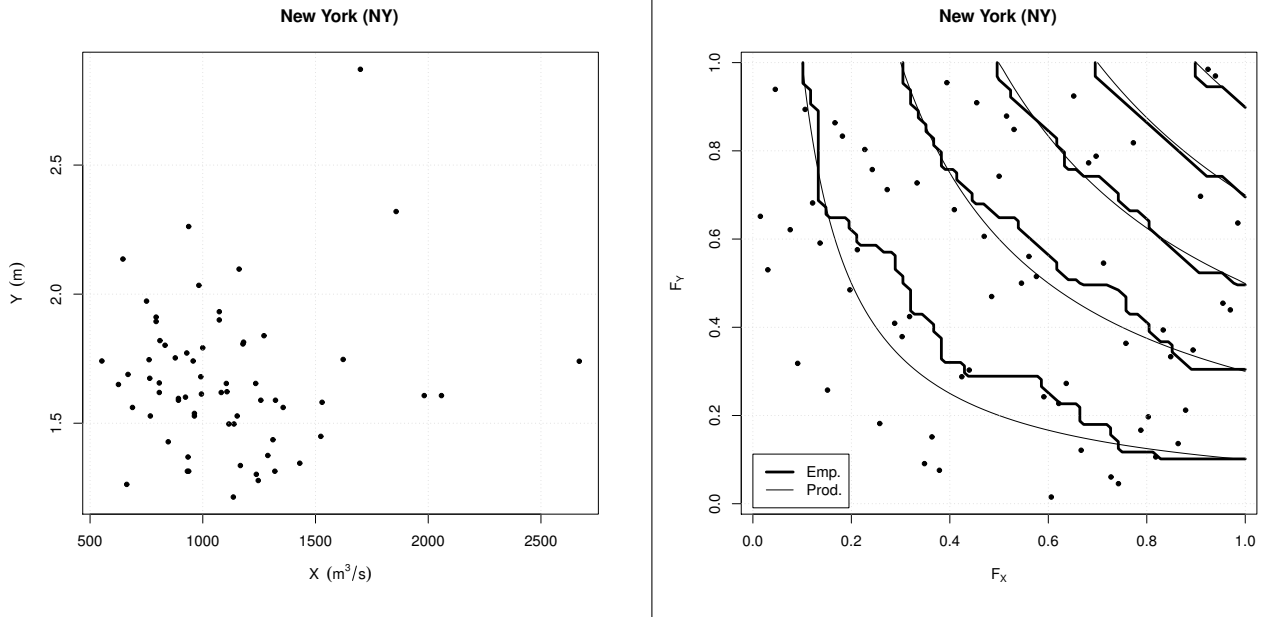


Figure SM.13: see text for explanation.

4.4 Norfolk, VA

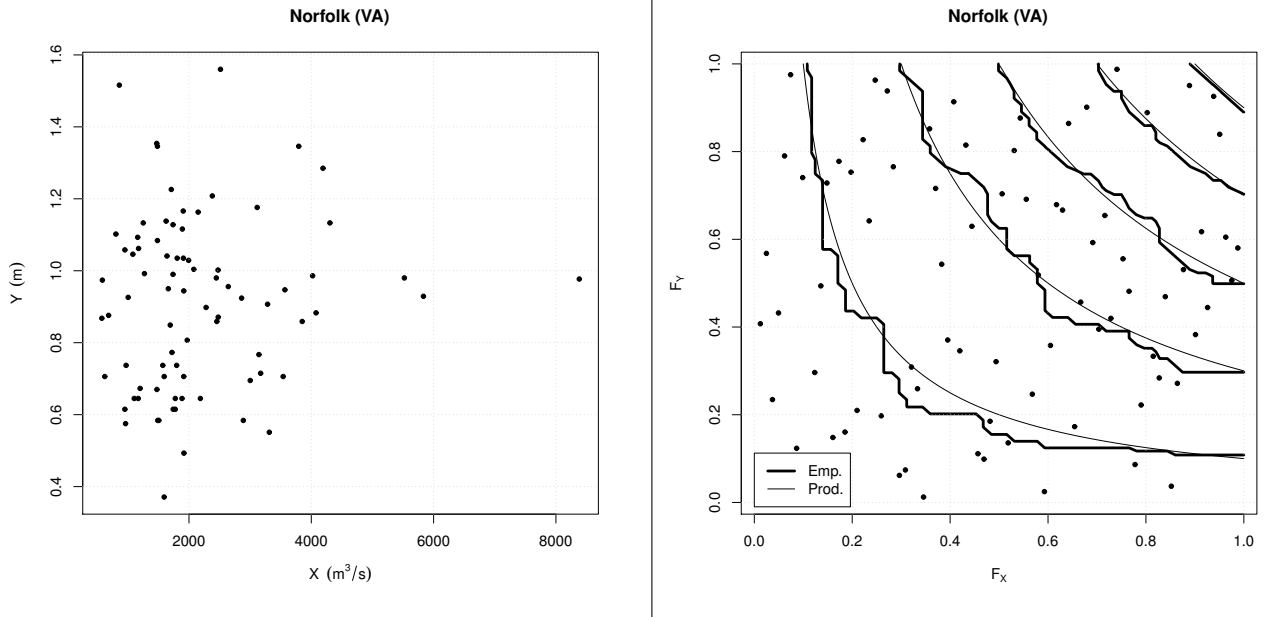


Figure SM.14: see text for explanation.

4.5 Philadelphia, PA

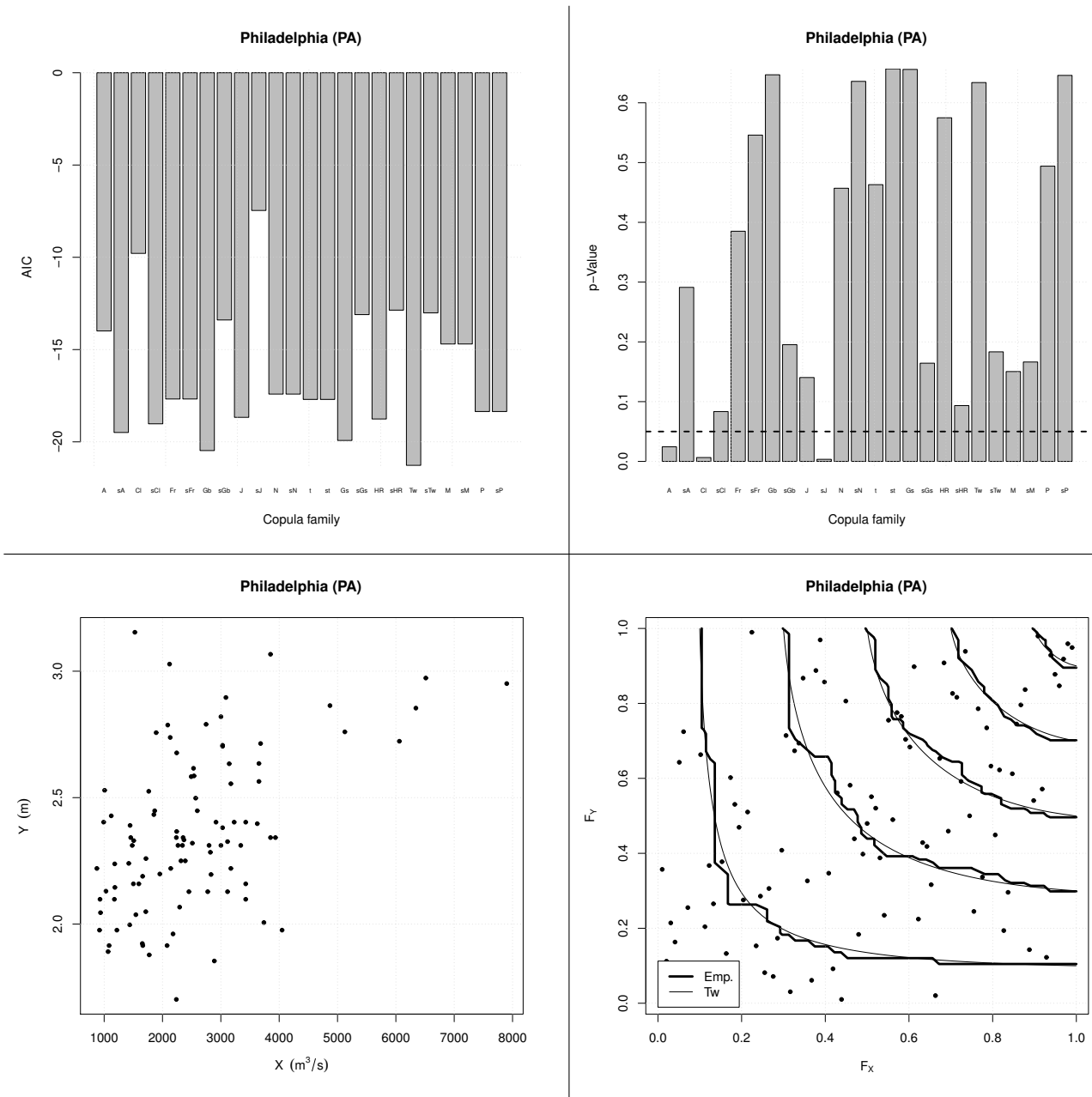


Figure SM.15: see text for explanation.

4.6 Portland, OR

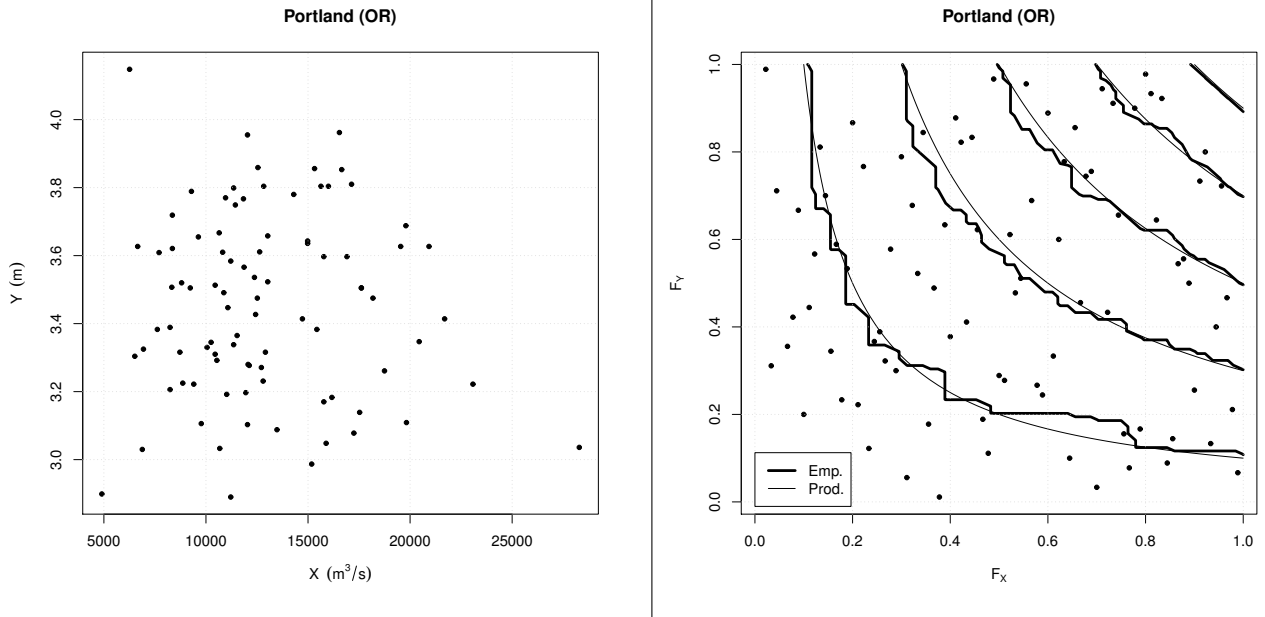


Figure SM.16: see text for explanation.

4.7 San Francisco, CA

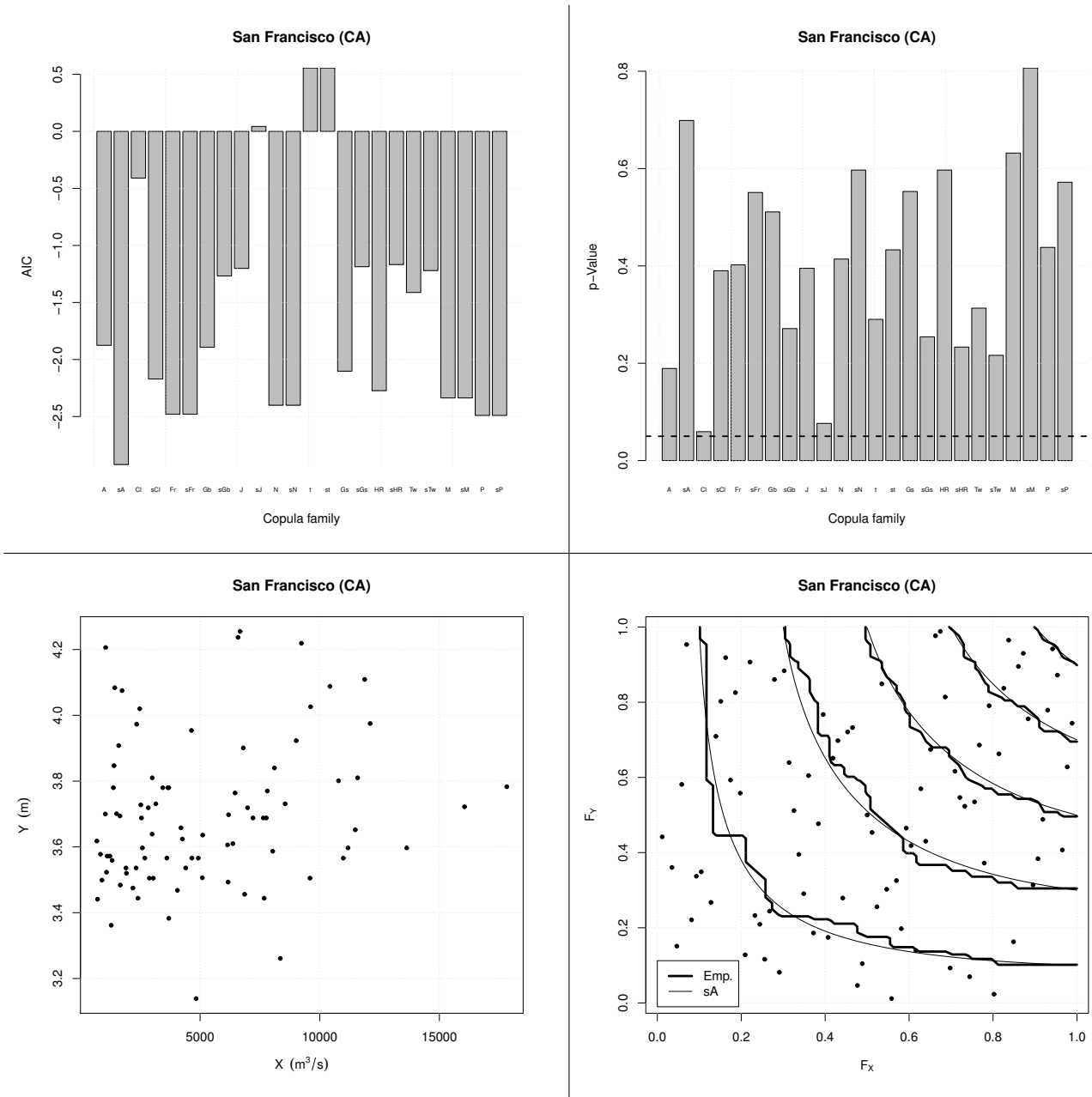


Figure SM.17: see text for explanation.

4.8 Washington, DC

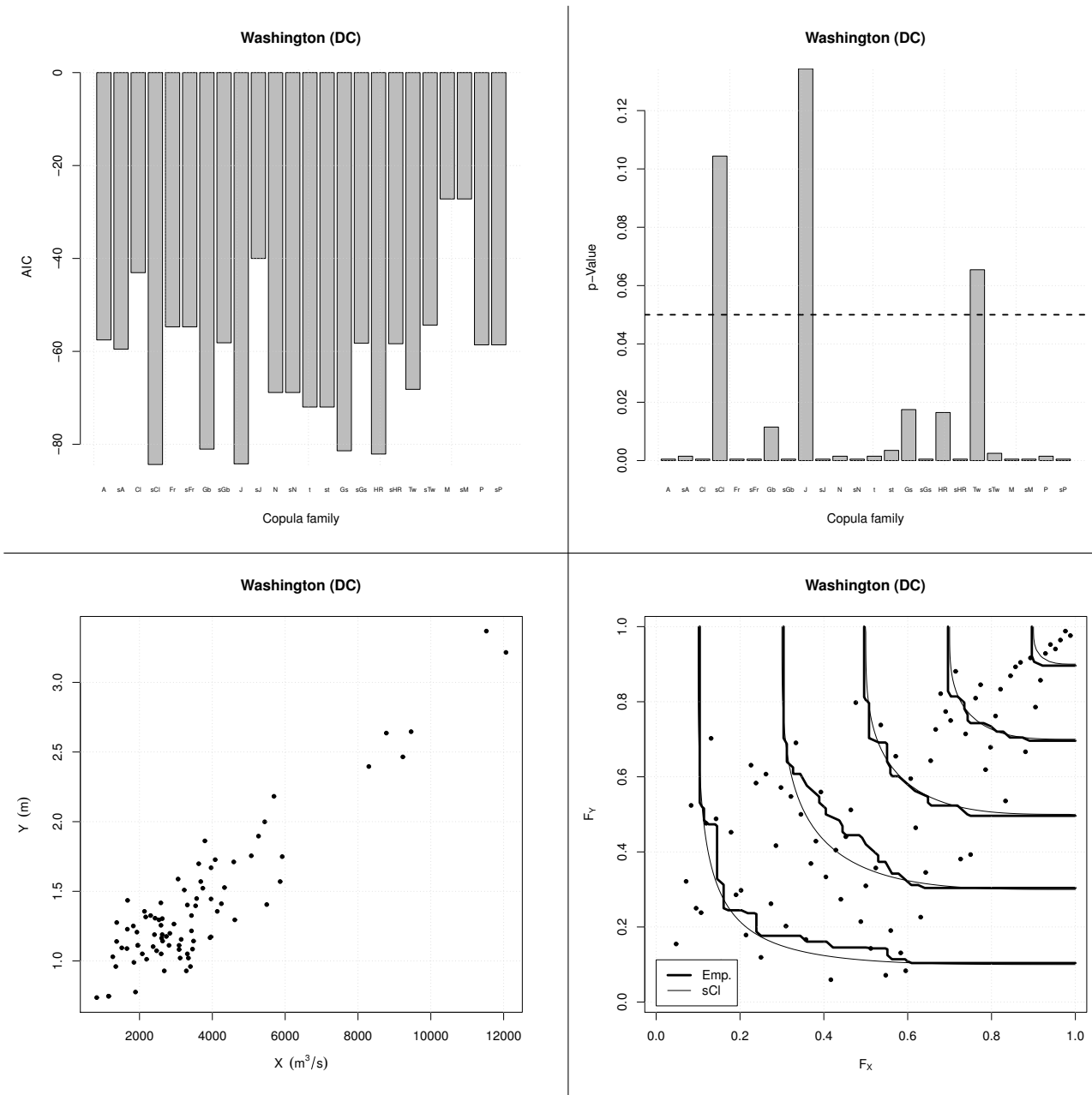


Figure SM.18: see text for explanation.

5 Bivariate Analysis: Return Period

For all the eight sites of interest (viz., Houston, Los Angeles, New York, Norfolk, Philadelphia, Portland, San Francisco, and Washington), four different Hazard Scenarios (HS) are considered (for further details see Salvadori et al. [2016]). Each scenario is identified via a pair of critical values (x^*, y^*) given by, respectively:

HS #1: a 80% percentile threshold is chosen, yielding

- x^* : quantile of order $p_X^* = 0.8$ of the distribution F_X fitted over the X data;
- y^* : quantile of order $p_Y^* = 0.8$ of the distribution F_Y fitted over the Y data.

HS #2: a 90% percentile threshold is chosen, yielding

- x^* : quantile of order $p_X^* = 0.9$ of the distribution F_X fitted over the X data;
- y^* : quantile of order $p_Y^* = 0.9$ of the distribution F_Y fitted over the Y data.

HS #3: a 95% percentile threshold is chosen, yielding

- x^* : quantile of order $p_X^* = 0.95$ of the distribution F_X fitted over the X data;
- y^* : quantile of order $p_Y^* = 0.95$ of the distribution F_Y fitted over the Y data.

HS #4: a 98% percentile threshold is chosen, yielding

- x^* : quantile of order $p_X^* = 0.98$ of the distribution F_X fitted over the X data;
- y^* : quantile of order $p_Y^* = 0.98$ of the distribution F_Y fitted over the Y data.

In Figure SM.19, the pair of critical values (x^*, y^*) is plotted as a red circle, and the corresponding univariate HS's for X and Y are indicated on, respectively, the horizontal and the vertical axes, by a green and a blue thick line.

The pair (x^*, y^*) also identifies an (inclusive) OR Hazard Scenario, plotted as a shaded region in Figure SM.19, given by the union of the three sub-regions A, B, and C: from a physical point of view, it is enough that one of the two variables be larger than the corresponding univariate critical threshold in order to get, say, a “dangerous” situation.

In the present annual framework, the general formula for calculating the RP T associated with a given HS is given by [Salvadori et al., 2011]

$$T = 1/\mathbf{P}(\text{HS}), \quad (1)$$

where $\mathbf{P}(\text{HS})$ is the probability of the HS of interest, viz. the probability that a realization of the phenomenon under investigation takes place in the given HS. In turn, in the univariate case, Eq. (1) reduces to the standard formulas

$$T_{X,x^*} = 1/(1 - F_X(x^*)) = 1/(1 - p_X^*)$$

and

$$T_{Y,y^*} = 1/(1 - F_Y(y^*)) = 1/(1 - p_Y^*),$$

while in the OR case the bivariate Return Period is given by

$$T_{OR,(x^*,y^*)} = 1/(1 - F_{XY}(x^*, y^*)) = 1/(1 - C_{XY}(F_X(x^*), F_Y(y^*))) = 1/(1 - C_{XY}(p_X^*, p_Y^*)),$$

where C_{XY} is the copula modeling the joint random behavior of the pair (X, Y) .

It is worth noting that, in the present annual framework, the chosen univariate quantiles correspond to, respectively, univariate Return Periods (RP) of 5, 10, 20, and 50 years for both the variables X (river flow) and Y (water level) of interest here, since $p_X^* = p_Y^*$. Furthermore, should the variables X and Y be independent, then $F_{XY} = F_X \cdot F_Y$. In turn,

$$T_{OR,(x^*,y^*)} = 1/(1 - F_X(x^*) \cdot F_Y(y^*)) = 1/(1 - p_X^* \cdot p_Y^*),$$

yielding both $T_{OR,(x^*,y^*)} \leq T_{X,x^*}$ and $T_{OR,(x^*,y^*)} \leq T_{Y,y^*}$, since a distribution function is always smaller than (or equal to) 1.

In this Section, the quantities plotted in the Figures are as follows.

Hazard Scenarios

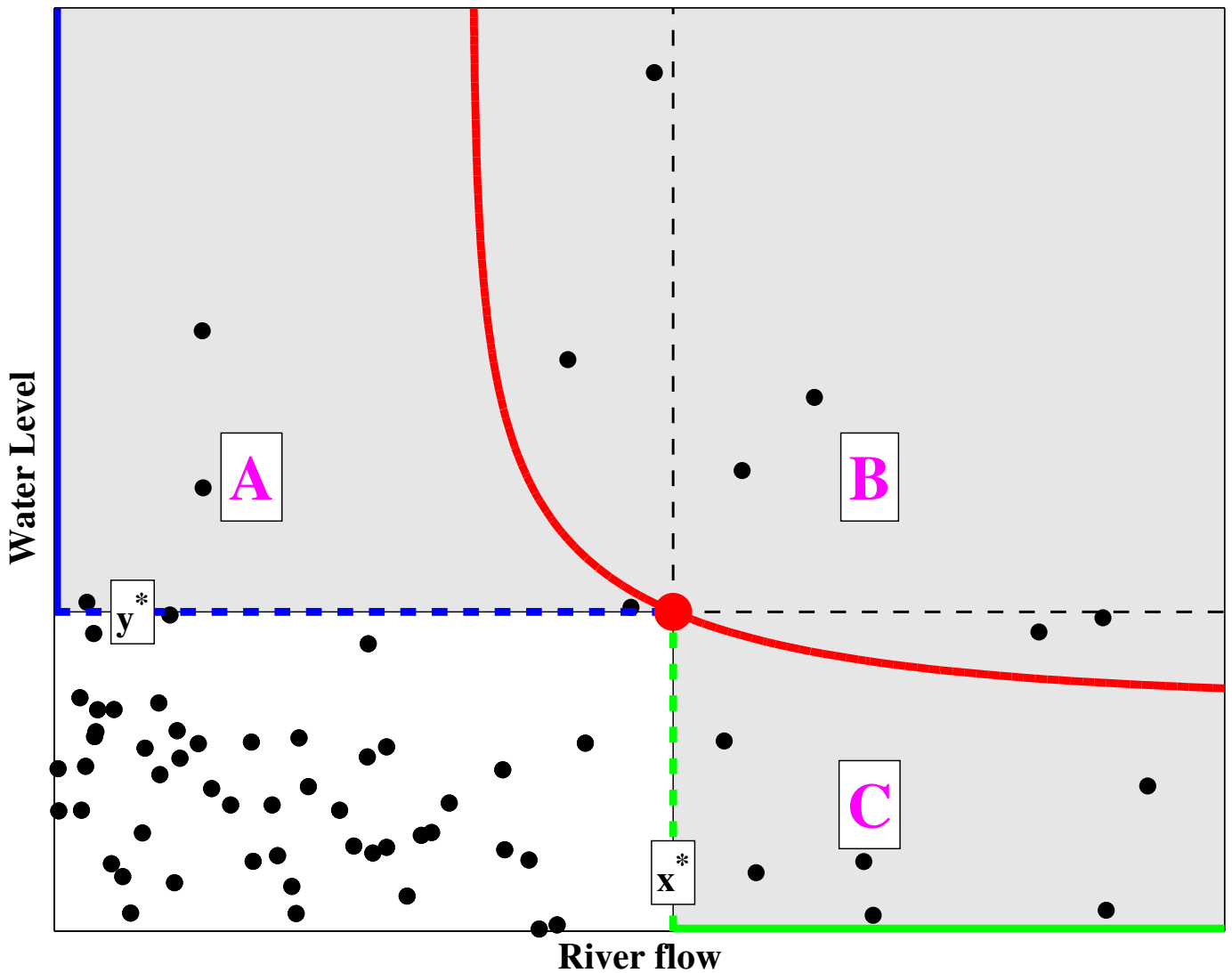


Figure SM.19

Black circles: the available data.

Red circle: the critical pair (x^*, y^*) corresponding to the univariate RP's reported in each figure title.

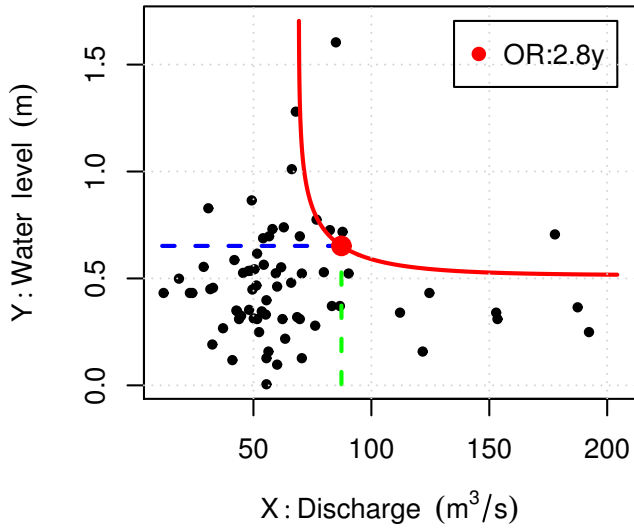
Red thick line: the isoline of the joint distribution F_{XY} crossing (x^*, y^*) .

The legend in each plot indicates the bivariate OR RP associated with (x^*, y^*) , to be compared with the univariate one reported in each figure title.

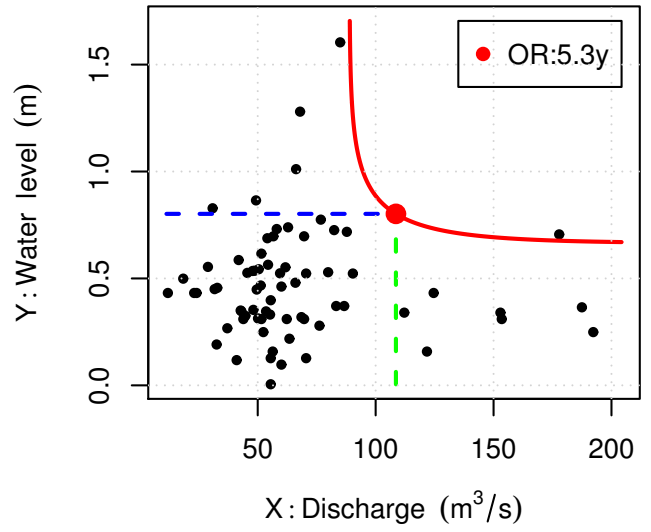
For the sake of comparison, if the variables are not independent, a **Black thick line** shows the isoline of the (wrong) Independence distribution $F_{XY} = F_X \cdot F_Y$ crossing (x^*, y^*) . The corresponding bivariate OR RP is reported in the legend, marked by a **Black cross**.

Houston (TX)

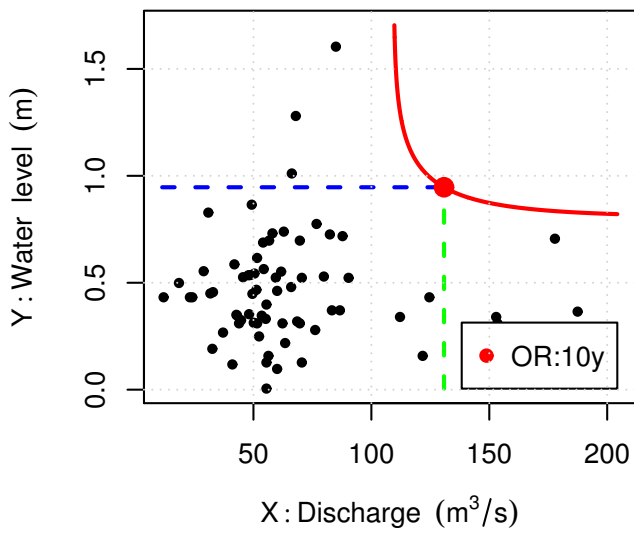
Univariate RP=5y



Univariate RP=10y



Univariate RP=20y



Univariate RP=50y

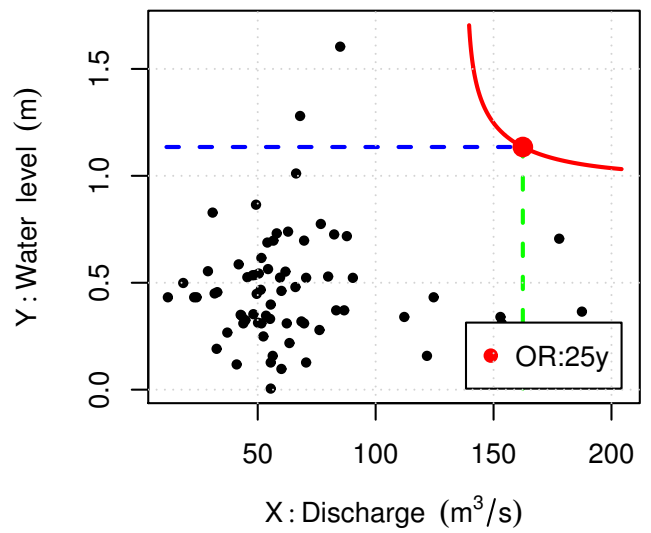
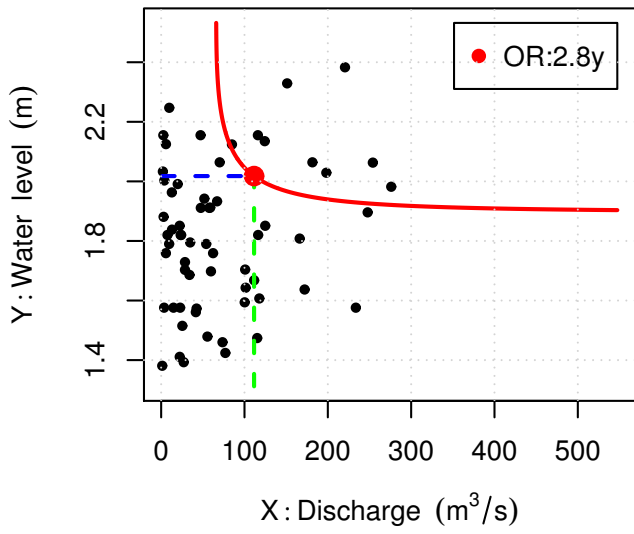


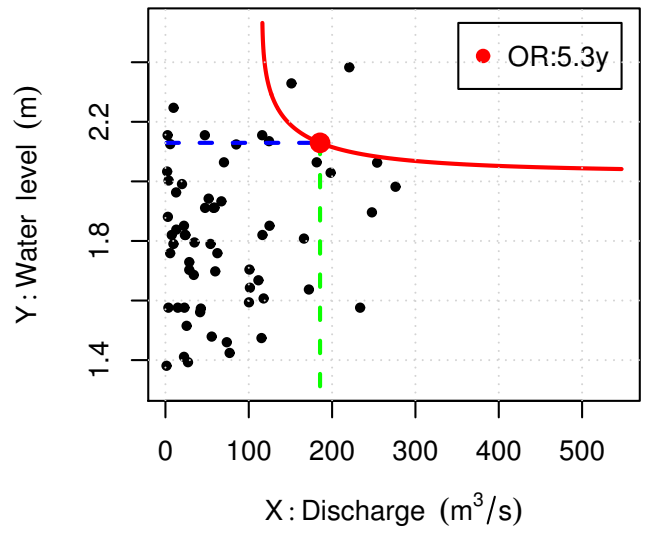
Figure SM.20: see text for explanation.

Los Angeles (CA)

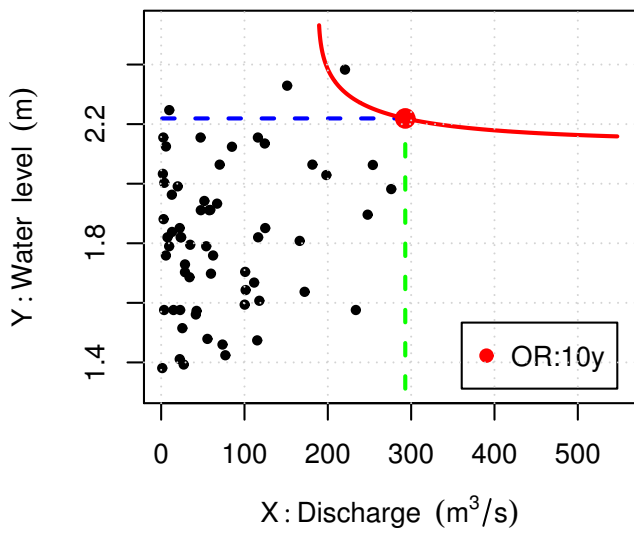
Univariate RP=5y



Univariate RP=10y



Univariate RP=20y



Univariate RP=50y

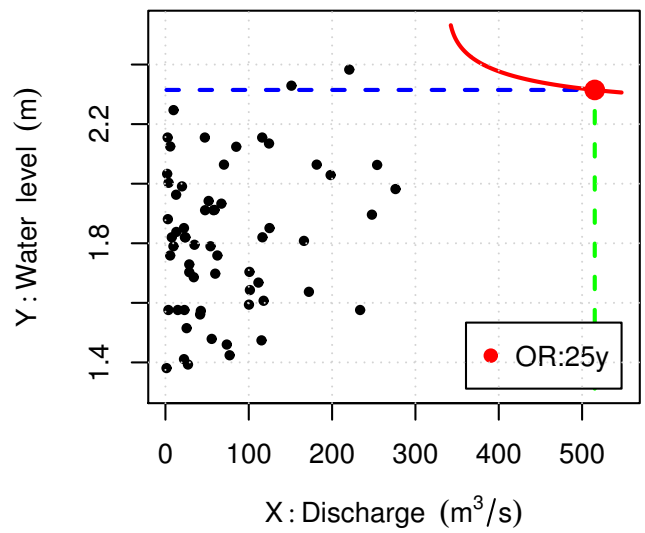
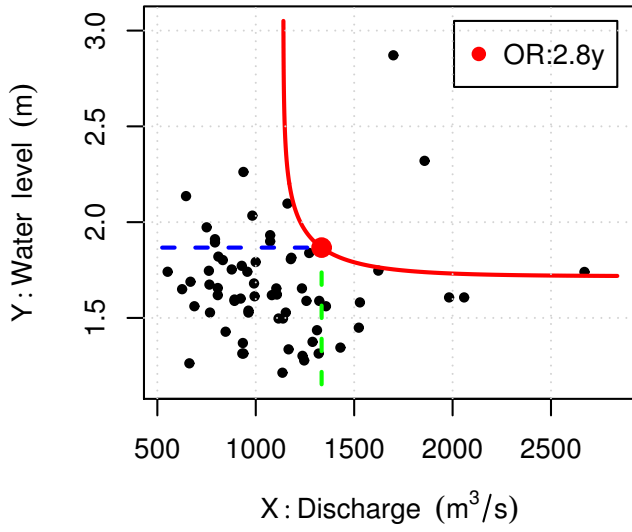


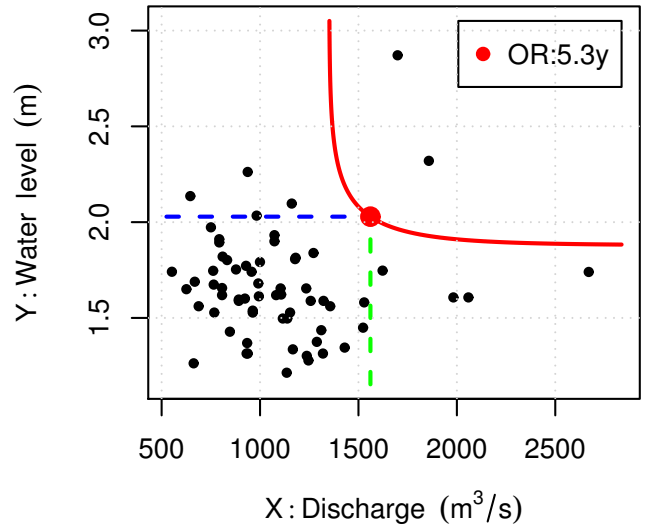
Figure SM.21: see text for explanation.

New York (NY)

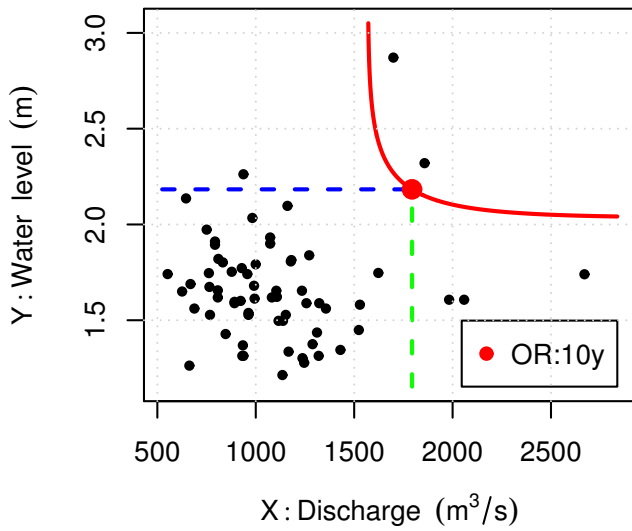
Univariate RP=5y



Univariate RP=10y



Univariate RP=20y



Univariate RP=50y

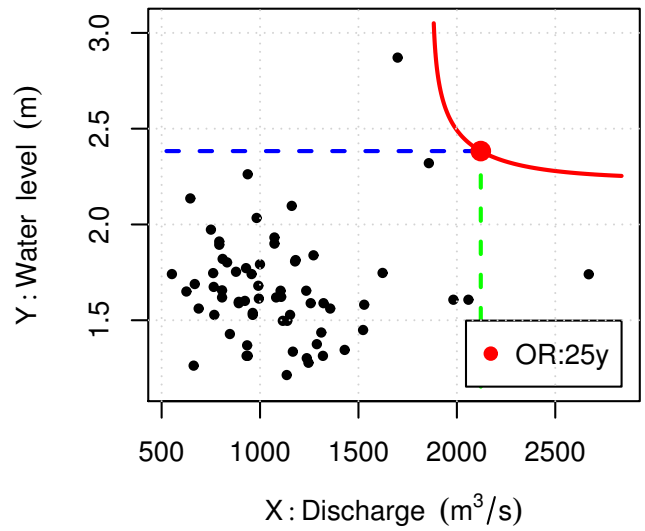
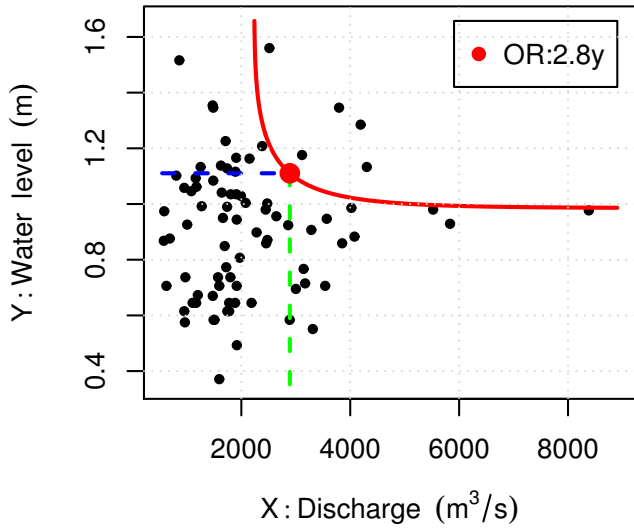


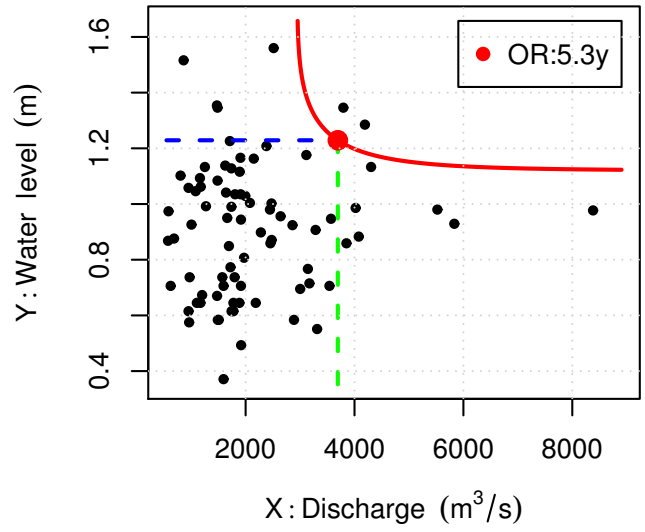
Figure SM.22: see text for explanation.

Norfolk (VA)

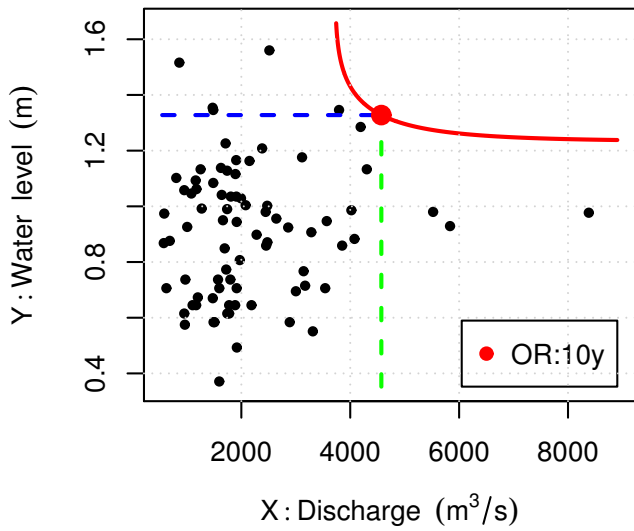
Univariate RP=5y



Univariate RP=10y



Univariate RP=20y



Univariate RP=50y

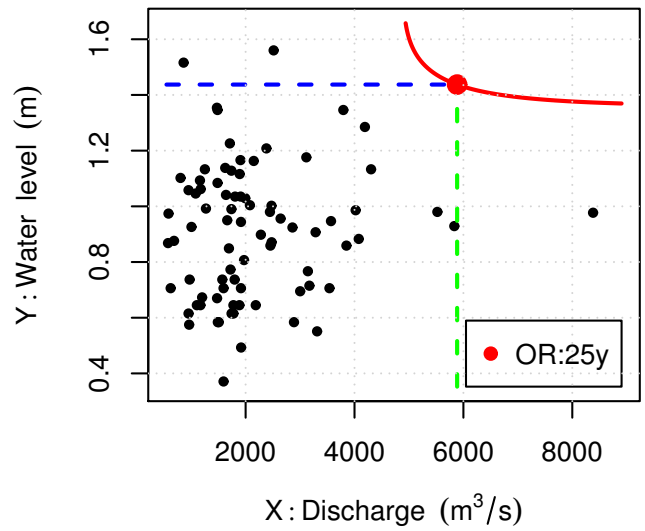
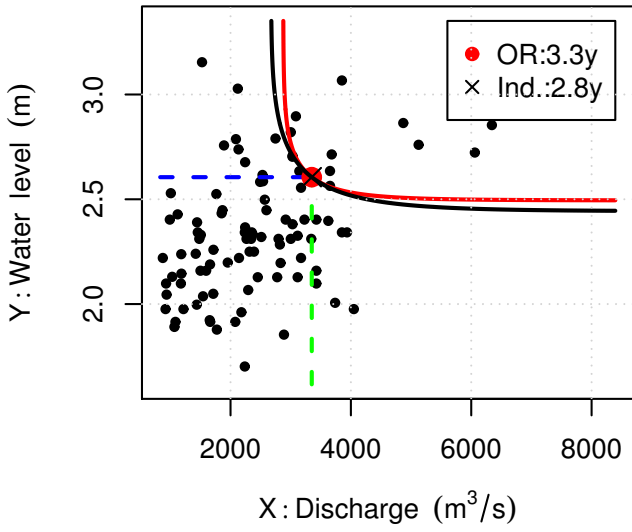


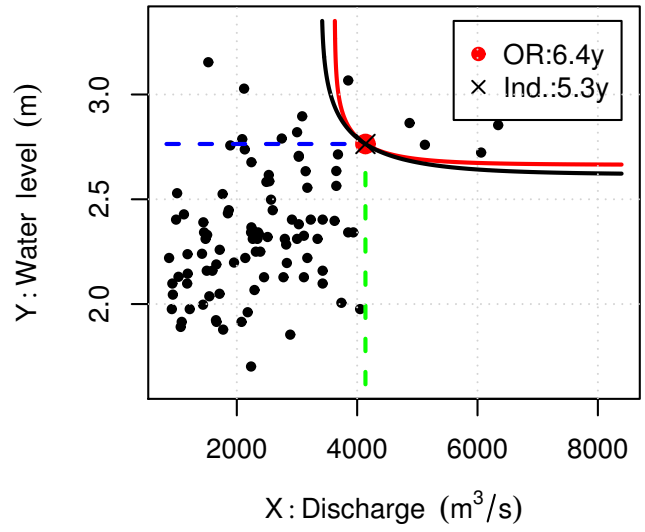
Figure SM.23: see text for explanation.

Philadelphia (PA)

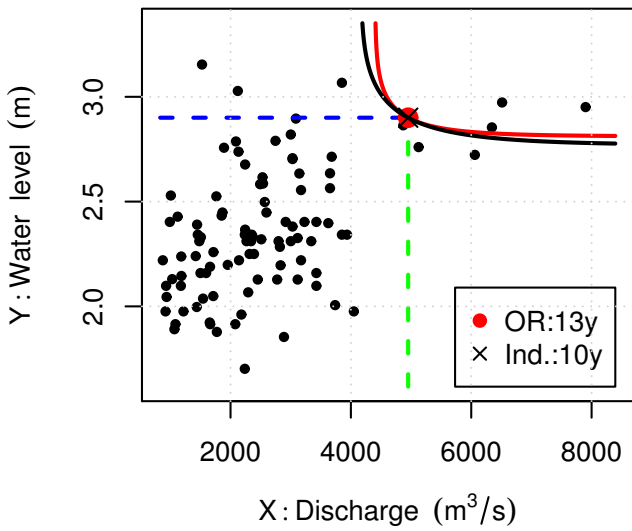
Univariate RP=5y



Univariate RP=10y



Univariate RP=20y



Univariate RP=50y

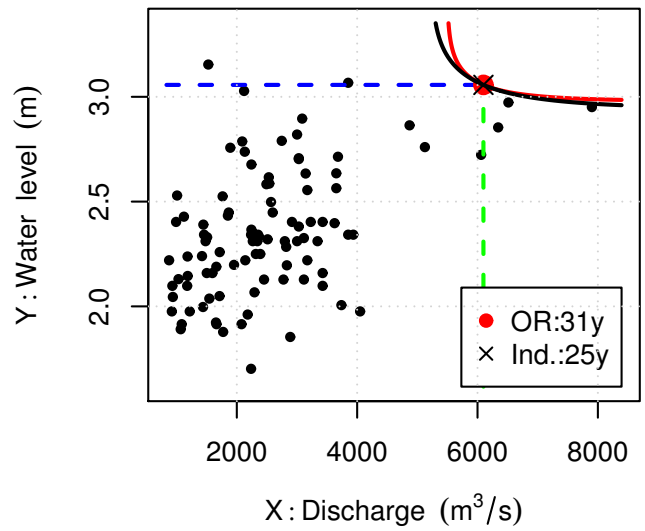
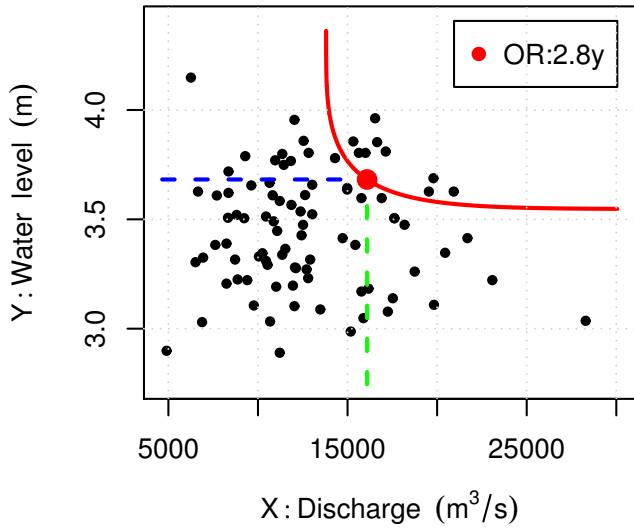


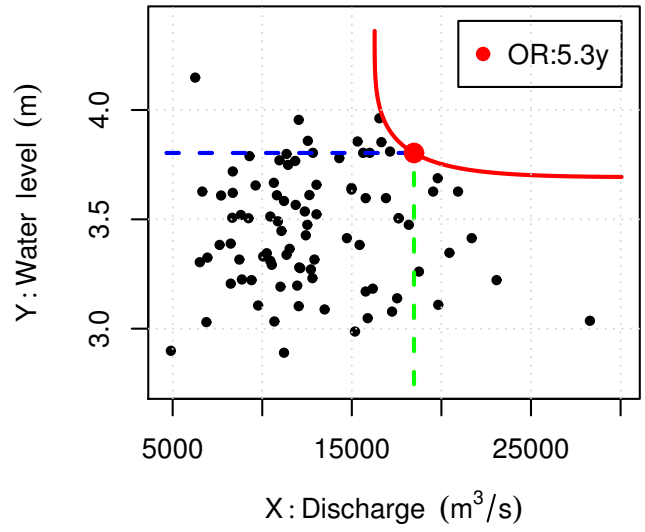
Figure SM.24: see text for explanation.

Portland (OR)

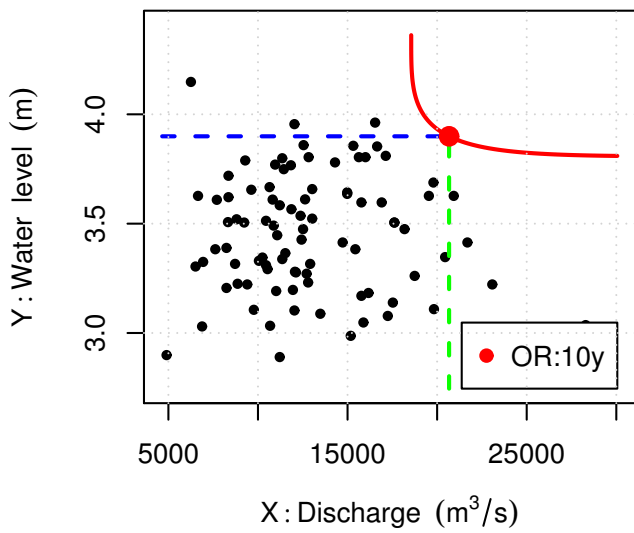
Univariate RP=5y



Univariate RP=10y



Univariate RP=20y



Univariate RP=50y

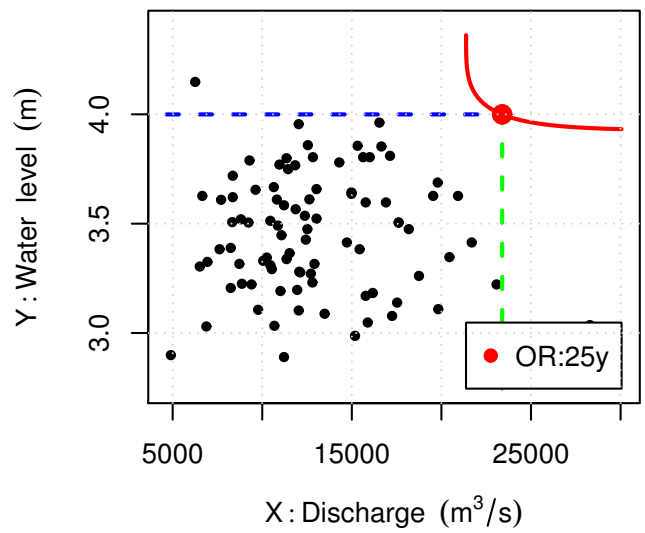
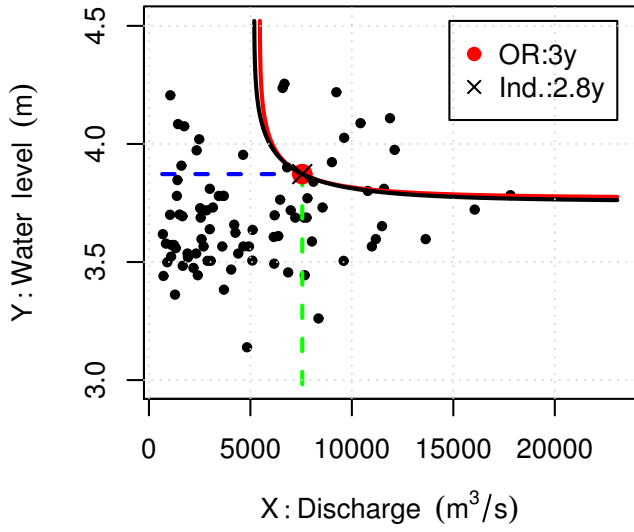


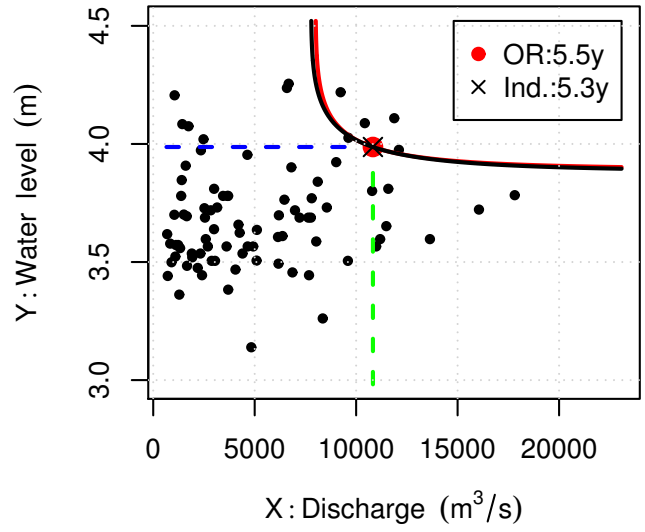
Figure SM.25: see text for explanation.

San Francisco (CA)

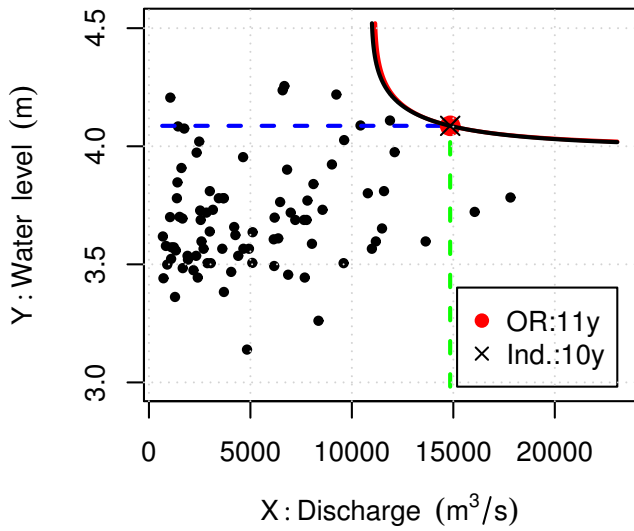
Univariate RP=5y



Univariate RP=10y



Univariate RP=20y



Univariate RP=50y

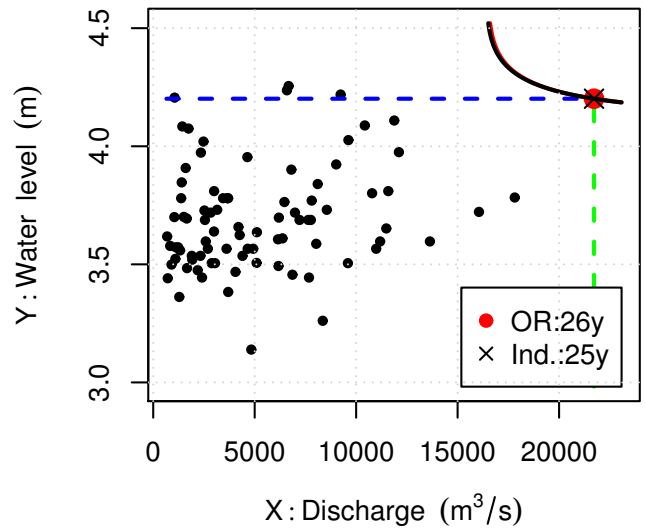
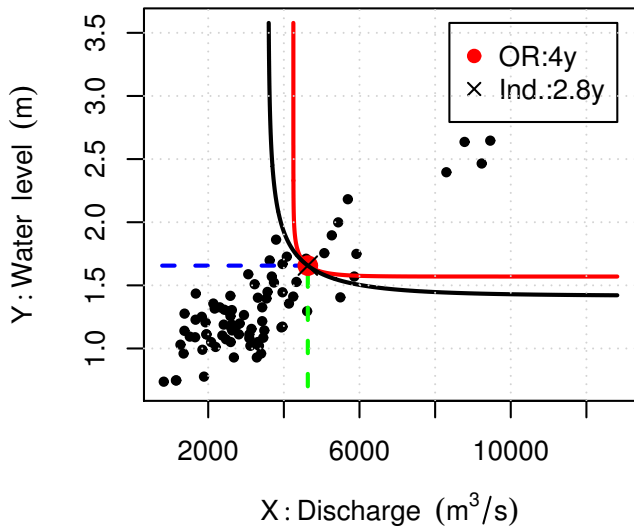


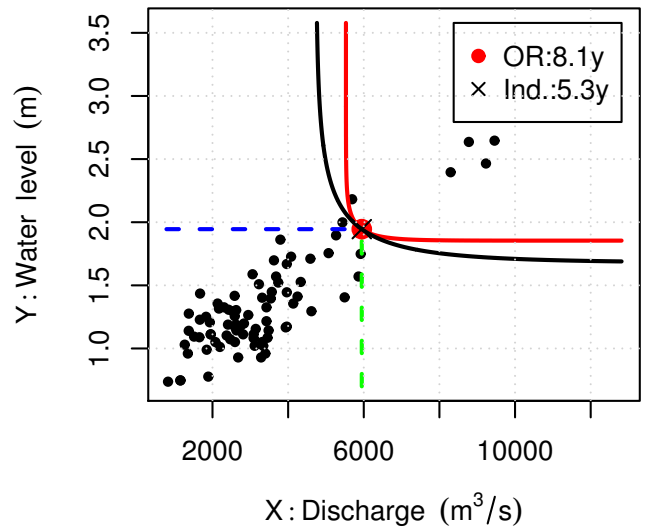
Figure SM.26: see text for explanation.

Washington (DC)

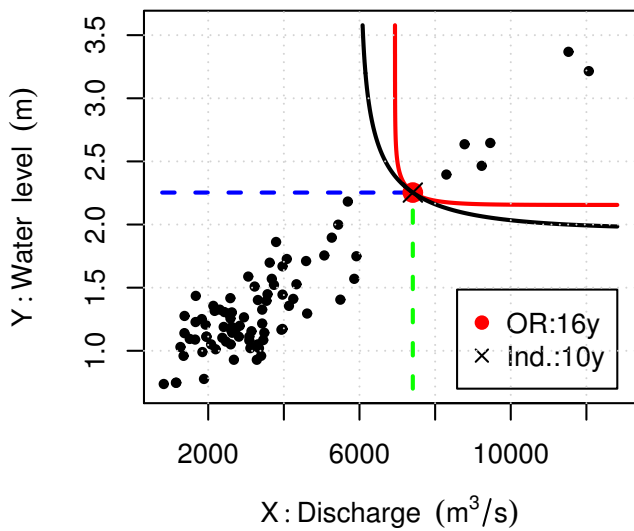
Univariate RP=5y



Univariate RP=10y



Univariate RP=20y



Univariate RP=50y

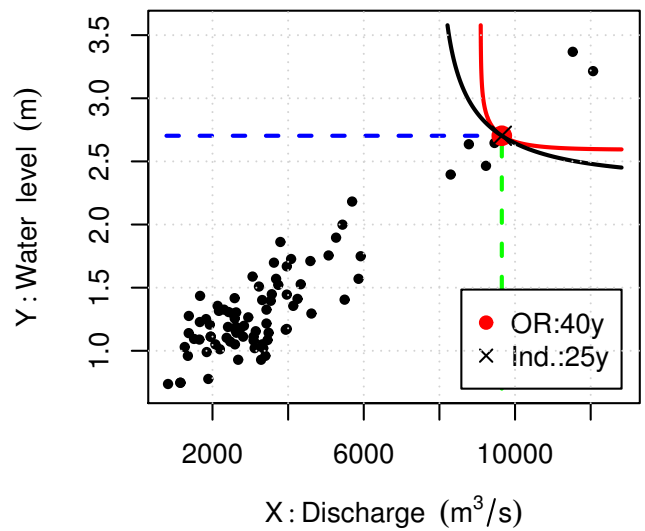


Figure SM.27: see text for explanation.

6 Bivariate Analysis: Failure Probabilities

For all the eight sites of interest (viz., Houston, Los Angeles, New York, Norfolk, Philadelphia, Portland, San Francisco, and Washington), the same four Hazard Scenarios (HS) used in Section 5 (concerning Return Periods) are considered.

In this study, we estimate the probability of coastal flooding under projected local rise in sea level (SLR) by 2030 and 2050 and Representative Concentration Pathways (RCP) 4.5 and 8.5, in order to quantify the effect of SLR on increased Failure Probability of coastal flood defenses in the mid-term future. A standard Monte Carlo analysis is used to estimate 95% bootstrap confidence bands of the Failure Probability (FP) over a 30-year temporal horizon, under different sea level rise scenarios. Here, 1000 independent bootstrap iterations are used, each involving huge simulated samples of size 10^6 to evaluate the uncertainties: for further details see Salvadori et al. [2016].

Four different SLR future projection are considered: viz., (RCP=4.5, Year=2030), (RCP=8.5, Year=2030), (RCP=4.5, Year=2050), and (RCP=8.5, Year=2050) — these are indicated in the main figure titles. Remember that the FP is simply the probability that (at least) an occurrence of the phenomenon under investigation takes place in the HS of interest during the given Lifetime: in turn, the notion of FP can be used both for univariate and bivariate HS's, once these have been well defined (as done in the present work).

Plotted are the following quantities, for each of the four Hazard Scenarios considered: these latter are indicated in the sub-plot titles by showing the pair of critical values (x^*, y^*) used to generate the HS of interest according to the corresponding univariate RP's (e.g., $(X_{5\text{years}}, Y_{5\text{years}})$, etc. . .).

Top panel. The probability distribution F_{SLR} of the SLR is given in a discrete form by providing, for each of the eight sites of interest, $n_{\text{SLR}} = 7$ increasing quantiles q_i 's of orders, respectively,

$$p_i = 0.005, 0.05, 0.17, 0.5, 0.83, 0.95, 0.995$$

with $i = 1, \dots, n_{\text{SLR}}$. A continuous version of F_{SLR} is constructed via a linear interpolation: this latter procedure corresponds to a (non-parametric) least-informative strategy, since it does not require additional parameters as in Kernel or Spline approximations. Practically, the SLR variates is assumed to be Uniform in any interval (q_i, q_{i+1}) , where the density is constant, and the corresponding CDF is simply a continuous sequence of line segments. In order to construct a full distribution, also the lower quantile q_0 (for $p = 0$), and the upper quantile $q_{n_{\text{SLR}}+1}$ (for $p = 1$) must be specified. These are empirically calculated by, first, computing the average μ_q of the differences $q_{i+1} - q_i$, and then by taking $q_0 = q_1 - \mu_q$ and $q_{n_{\text{SLR}}+1} = q_{n_{\text{SLR}}} + \mu_q$. In the Figures, the linear interpolation of F_{SLR} is plotted as a **Black solid line**, while the empirical distribution function of the SLR values (simulated from F_{SLR} via the Probability Integral Transform) are plotted as a **Black marked line**. Note that only positive SLRs are considered, being interested in more “dangerous” conditions.

Bottom panel. Estimated Failure Probabilities, plotted considering a 30-years temporal horizon.

Black line: univariate FP's, both for X and Y (the two are equal, since the univariate X - and Y -HS's have the same probability).

Red line: Bivariate OR FP's.

Purple thick line: Bivariate OR FP's accounting for random SLR's extracted from F_{SLR} .

Purple thin dotted lines: Monte Carlo 95% confidence band for the bivariate OR FP's accounting for random SLR's extracted from F_{SLR} .

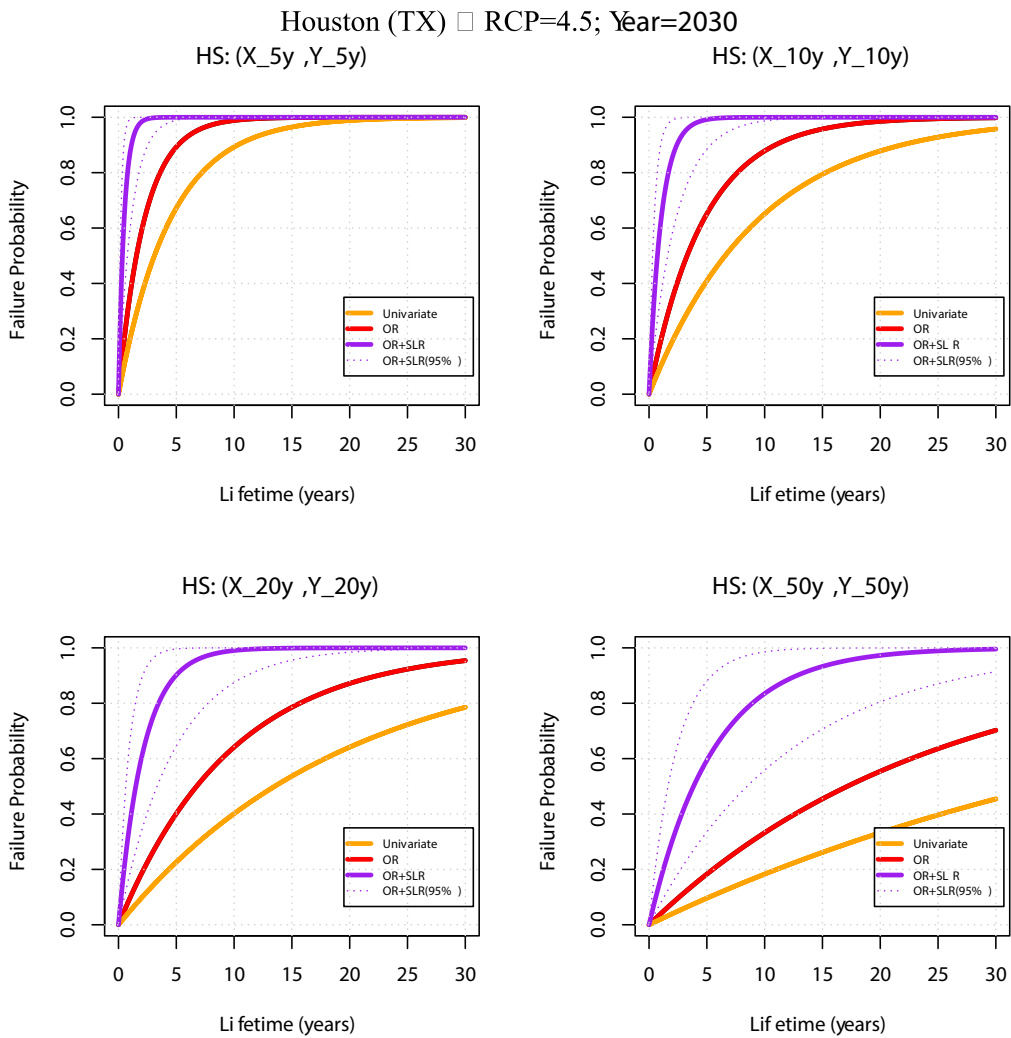
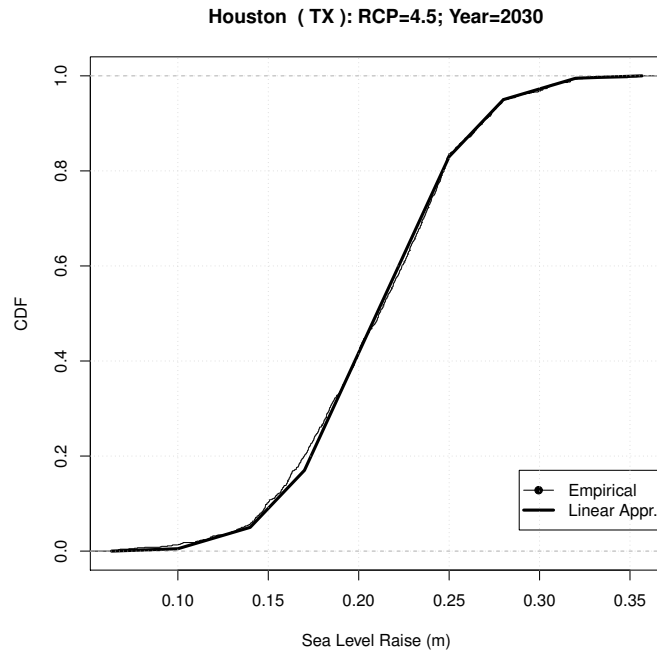


Figure SM.28: see text for explanation.

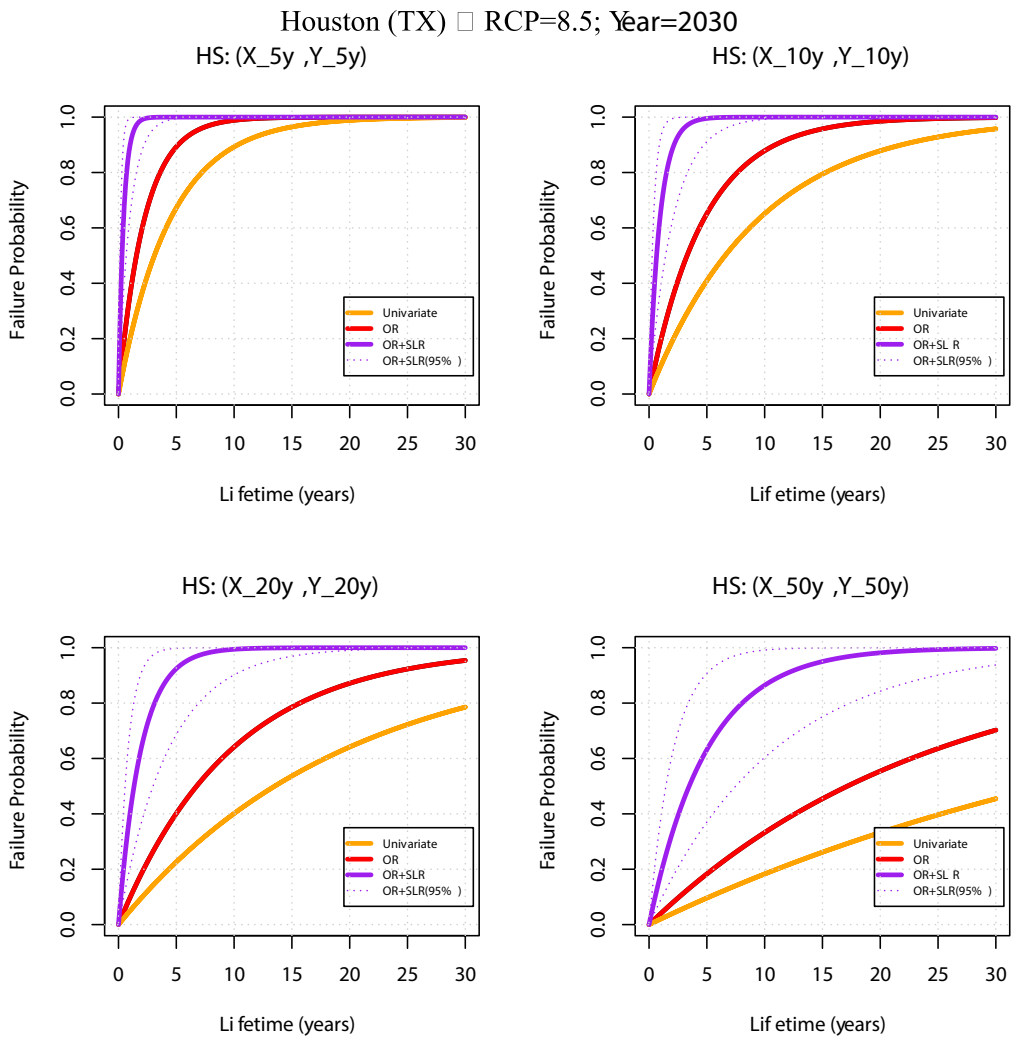
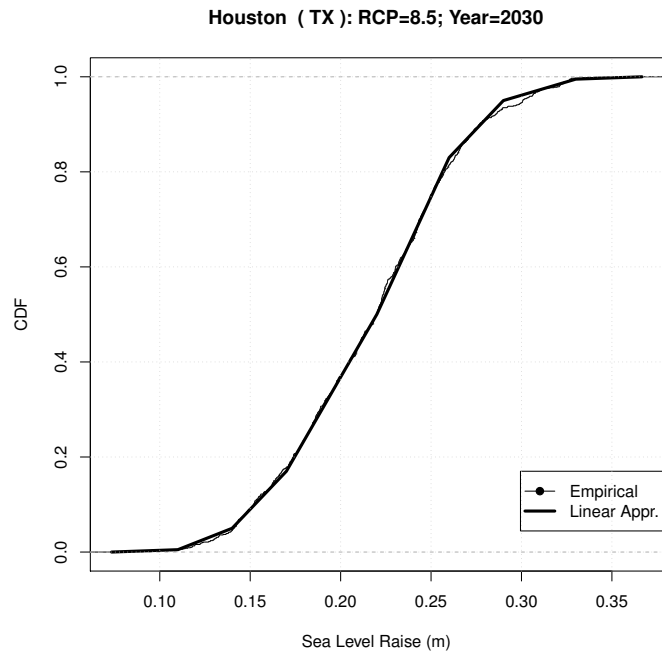


Figure SM.29: see text for explanation.

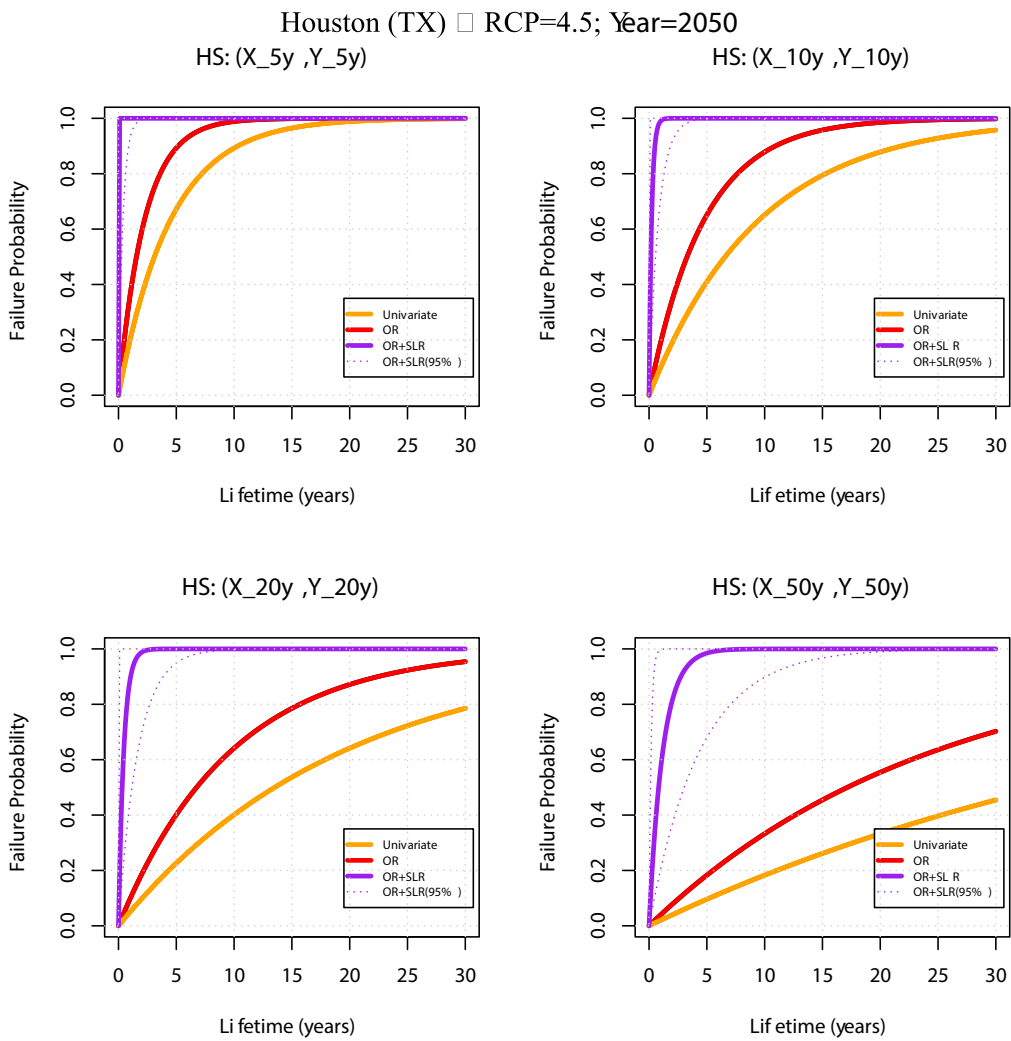
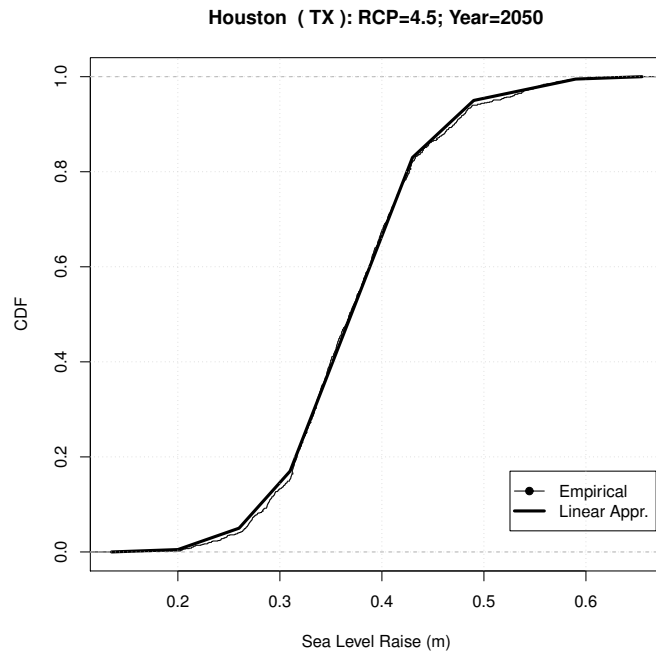
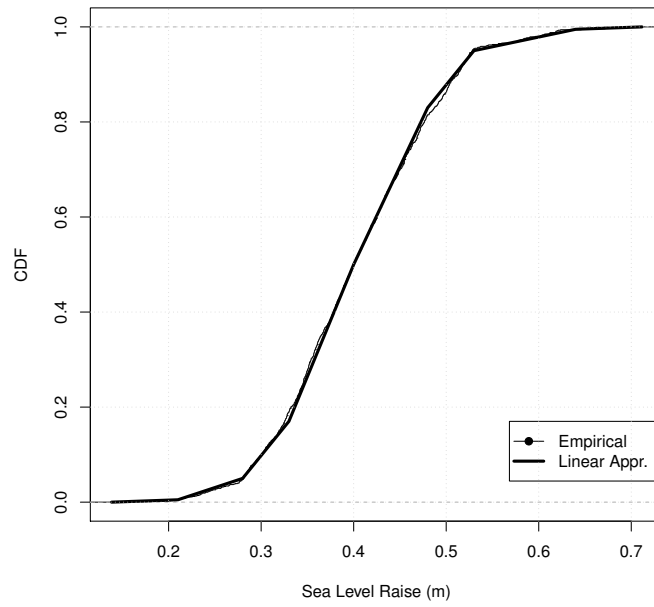
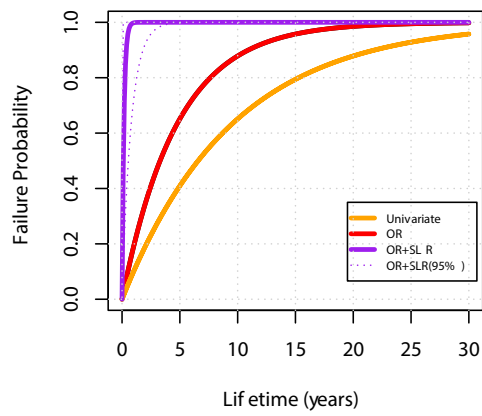
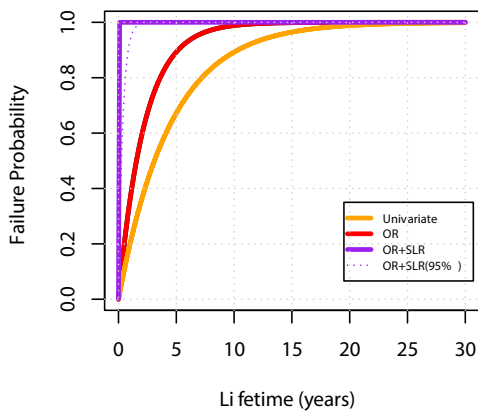


Figure SM.30: see text for explanation.

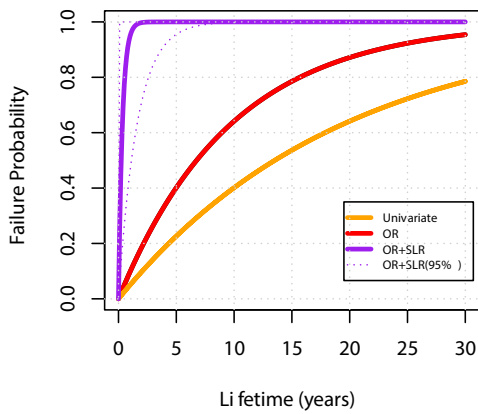
Houston (TX): RCP=8.5; Year=2050



Houston (TX) □ RCP=8.5; Year=2050
 HS: (X_{5y} ,Y_{5y}) HS: (X_{10y} ,Y_{10y})



HS: (X_{20y} ,Y_{20y})



HS: (X_{50y} ,Y_{50y})

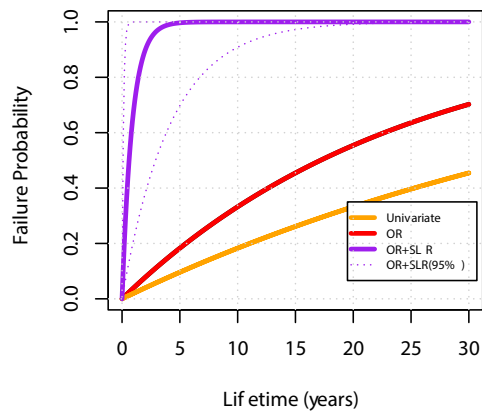
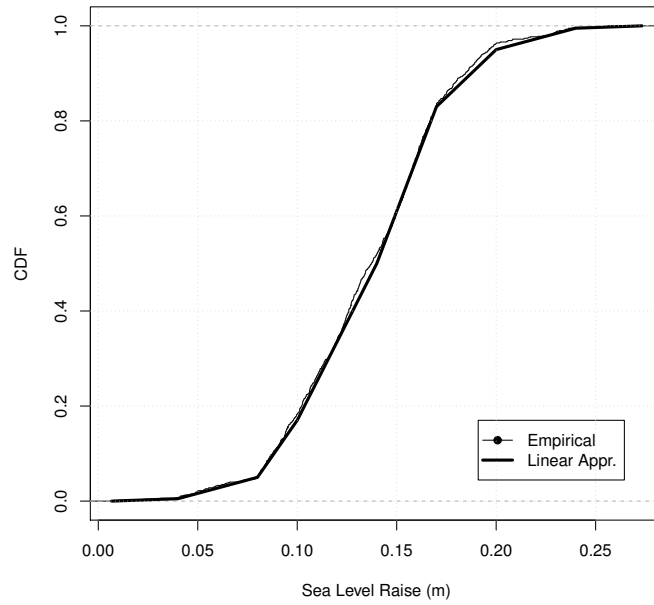


Figure SM.31: see text for explanation.

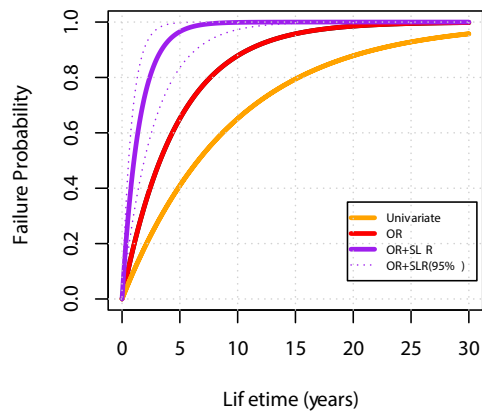
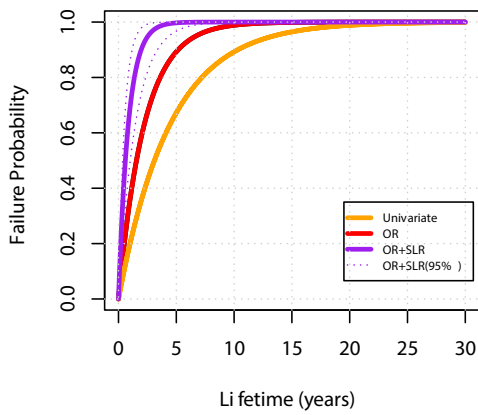
Los Angeles (CA): RCP=4.5; Year=2030



Los Angeles (CA) □ RCP=4.5; Year=2030

HS: (X_{5y} ,Y_{5y})

HS: (X_{10y} ,Y_{10y})



HS: (X_{20y} ,Y_{20y})

HS: (X_{50y} ,Y_{50y})

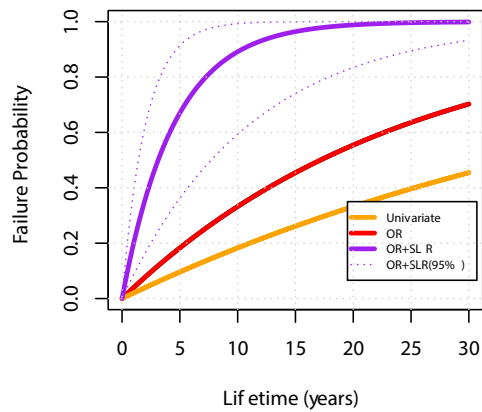
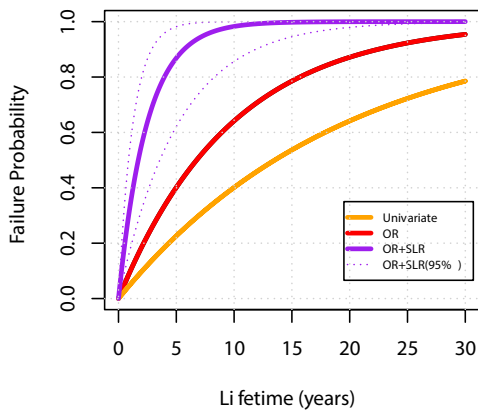
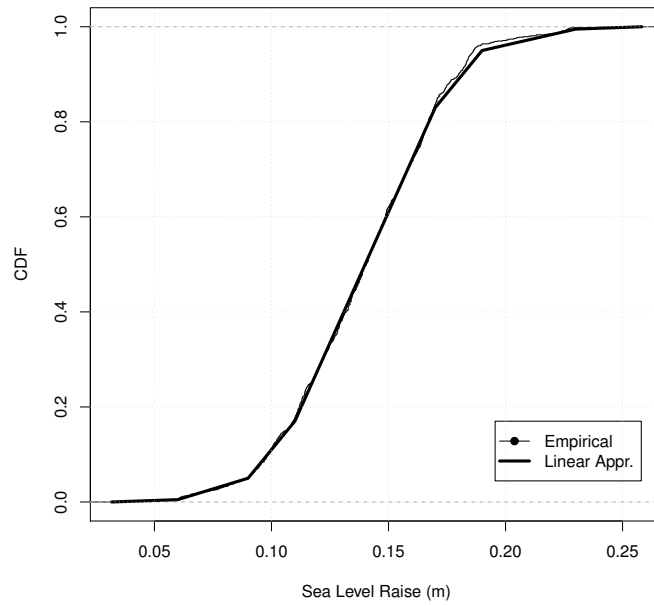


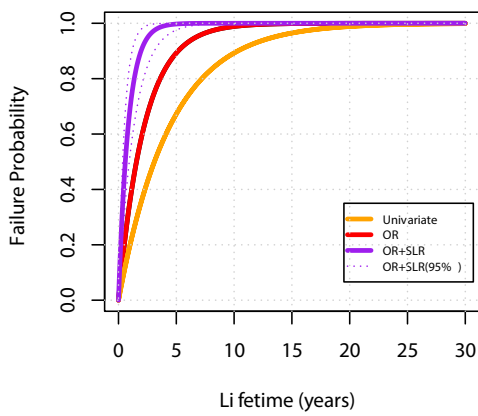
Figure SM.32: see text for explanation.

Los Angeles (CA): RCP=8.5; Year=2030

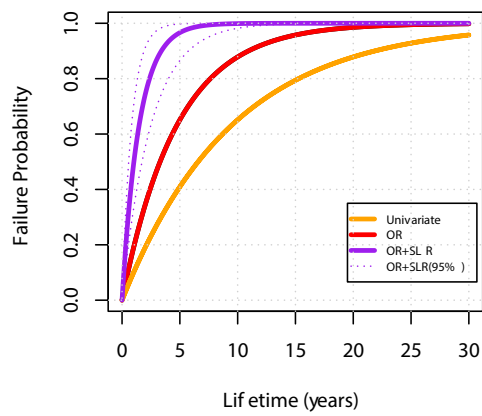


Los Angeles (CA) □ RCP=8.5; Year=2030

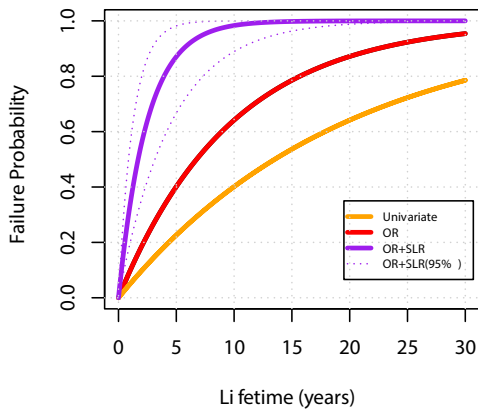
HS: (X_{5y}, Y_{5y})



HS: (X_{10y}, Y_{10y})



HS: (X_{20y}, Y_{20y})



HS: (X_{50y}, Y_{50y})

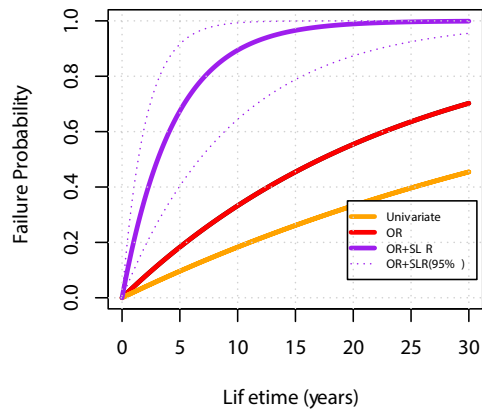
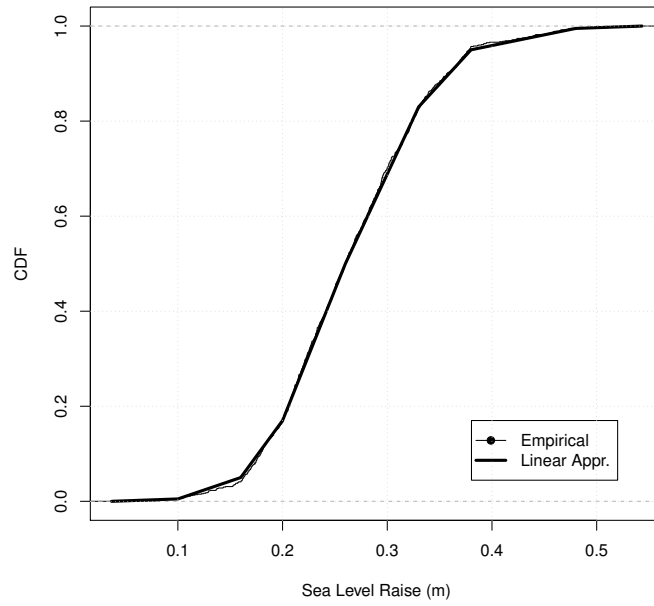


Figure SM.33: see text for explanation.

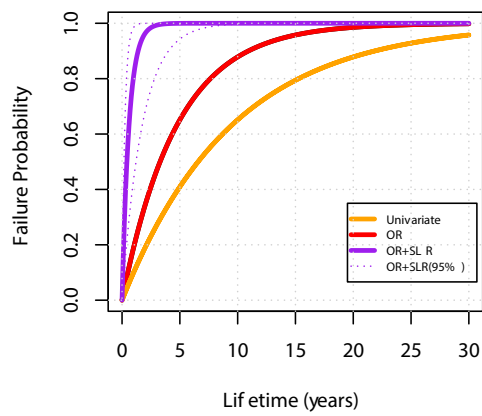
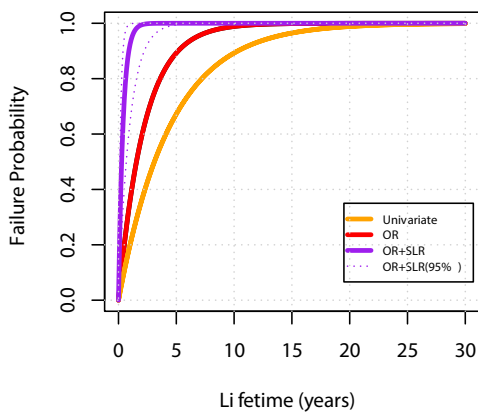
Los Angeles (CA): RCP=4.5; Year=2050



Los Angeles (CA) □ RCP=4.5; Year=2050

HS: (X_{5y} ,Y_{5y})

HS: (X_{10y} ,Y_{10y})



HS: (X_{20y} ,Y_{20y})

HS: (X_{50y} ,Y_{50y})

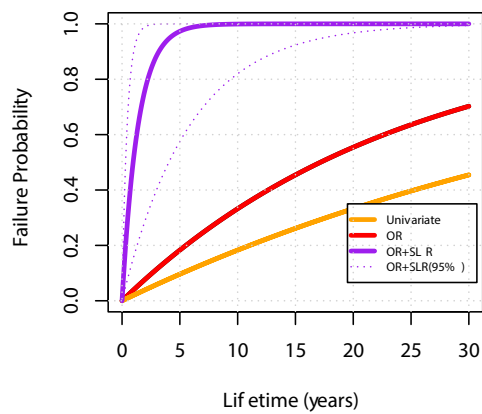
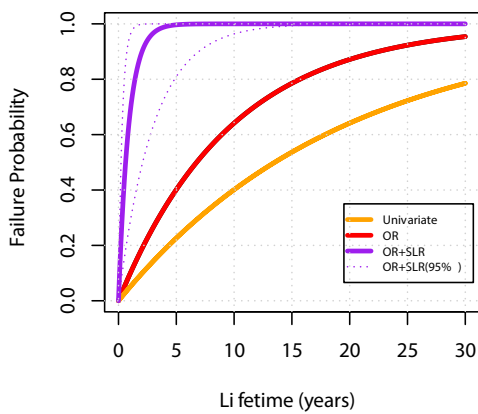
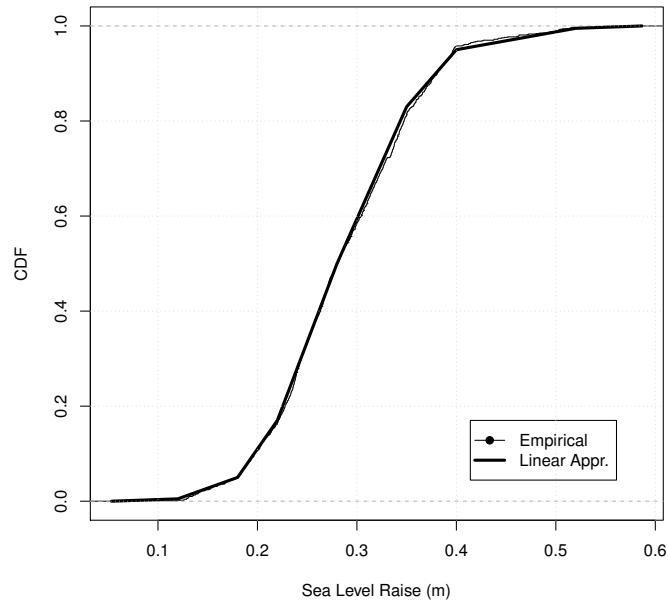


Figure SM.34: see text for explanation.

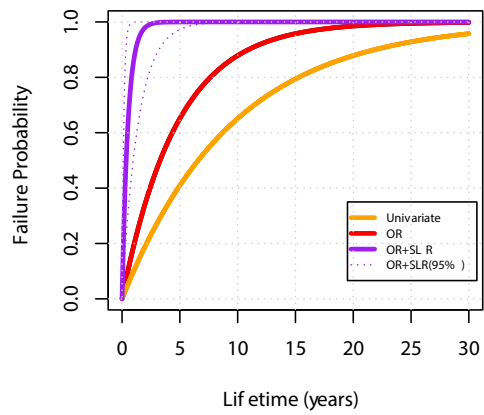
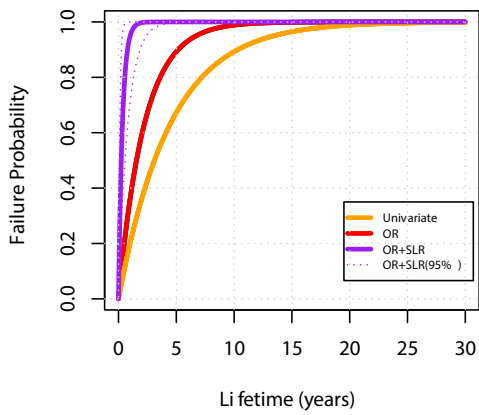
Los Angeles (CA): RCP=8.5; Year=2050



Los Angeles (CA) □ RCP=8.5; Year=2050

HS: (X_{5y} ,Y_{5y})

HS: (X_{10y} ,Y_{10y})



HS: (X_{20y} ,Y_{20y})

HS: (X_{50y} ,Y_{50y})

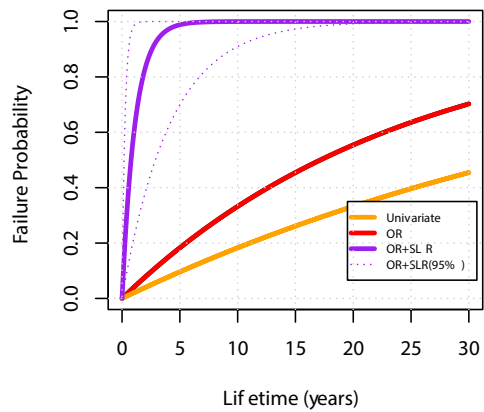
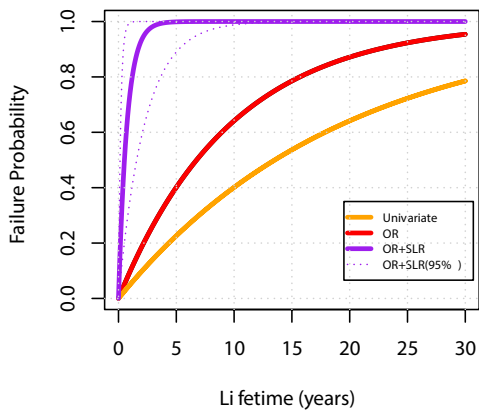
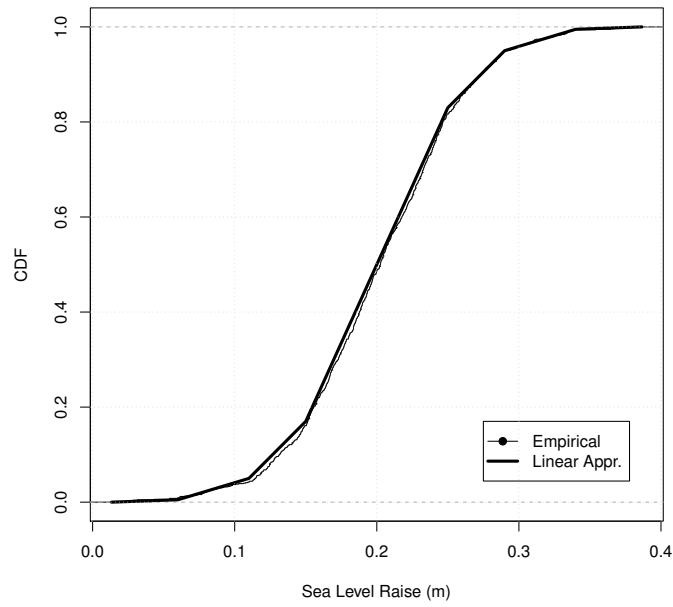


Figure SM.35: see text for explanation.

New York (NY): RCP=4.5; Year=2030



New York (NY) □ RCP=4.5; Year=2030
 HS: (X_{5y}, Y_{5y}) HS: (X_{10y}, Y_{10y})

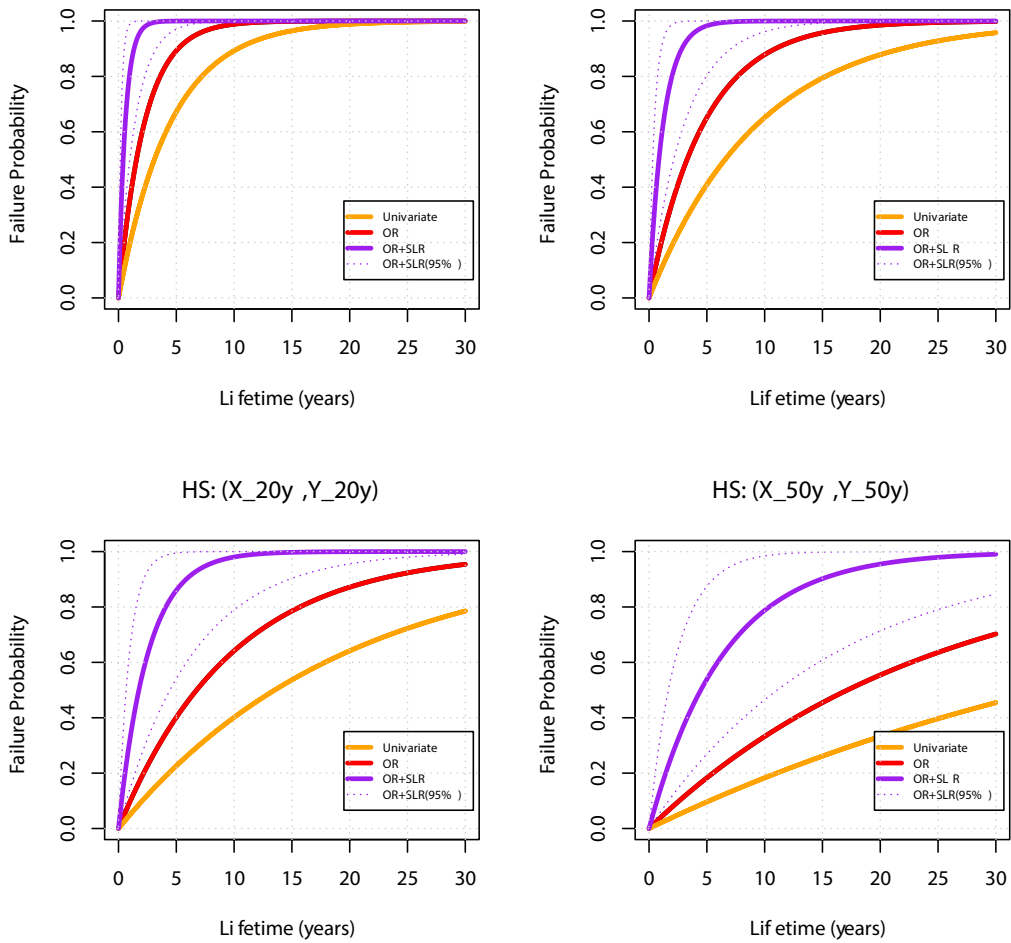


Figure SM.36: see text for explanation.

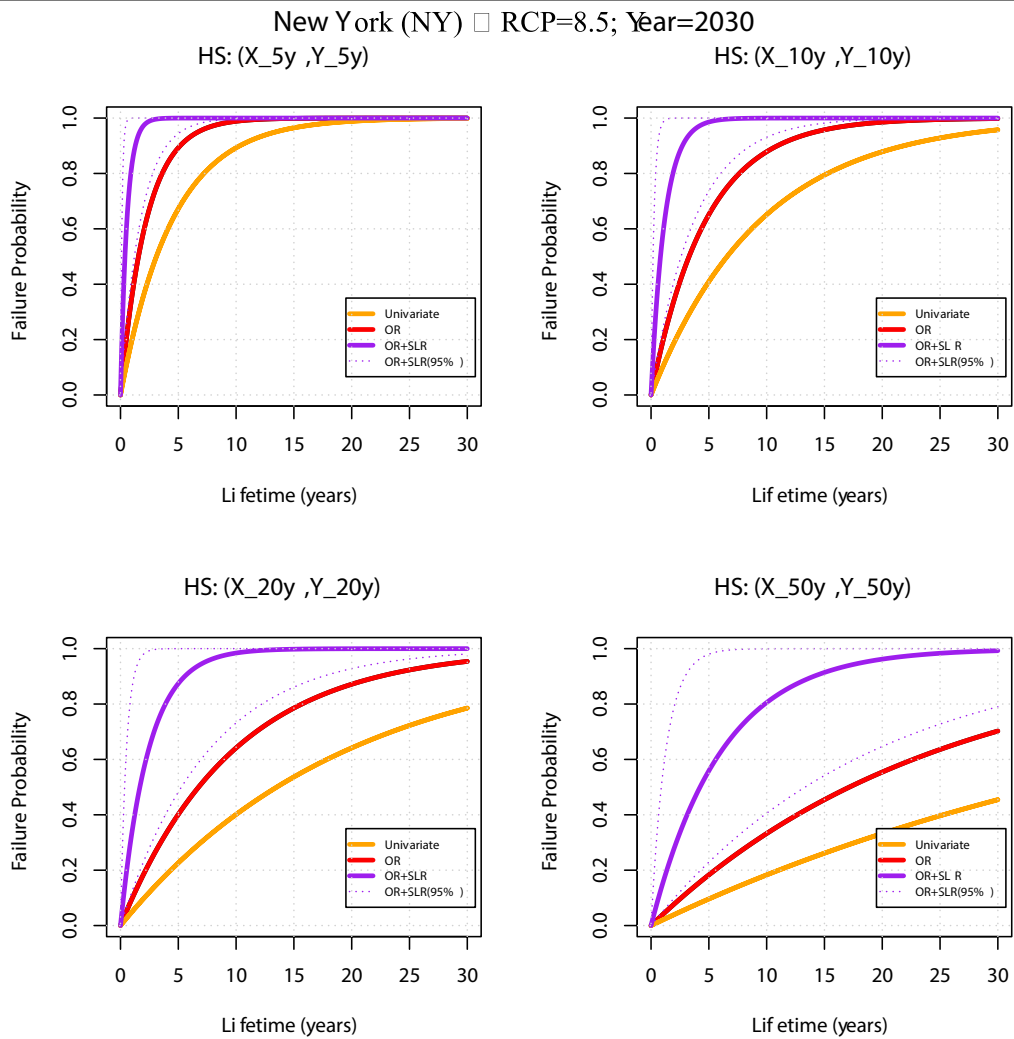
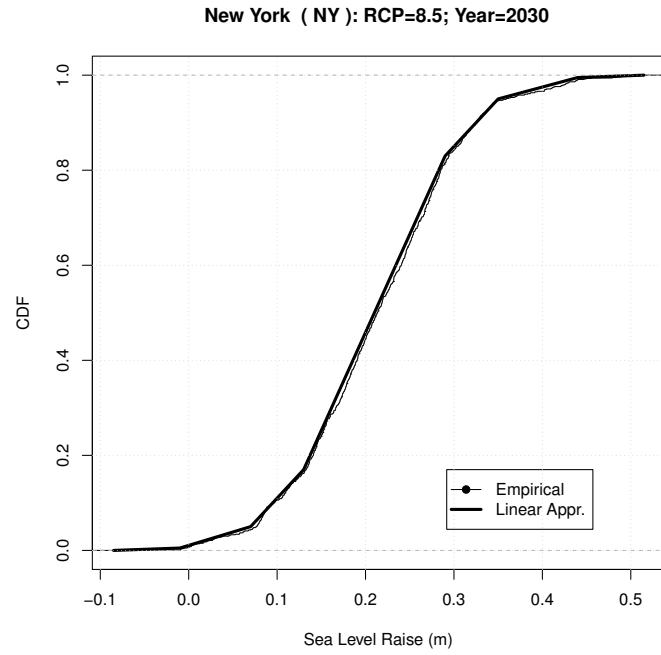


Figure SM.37: see text for explanation.

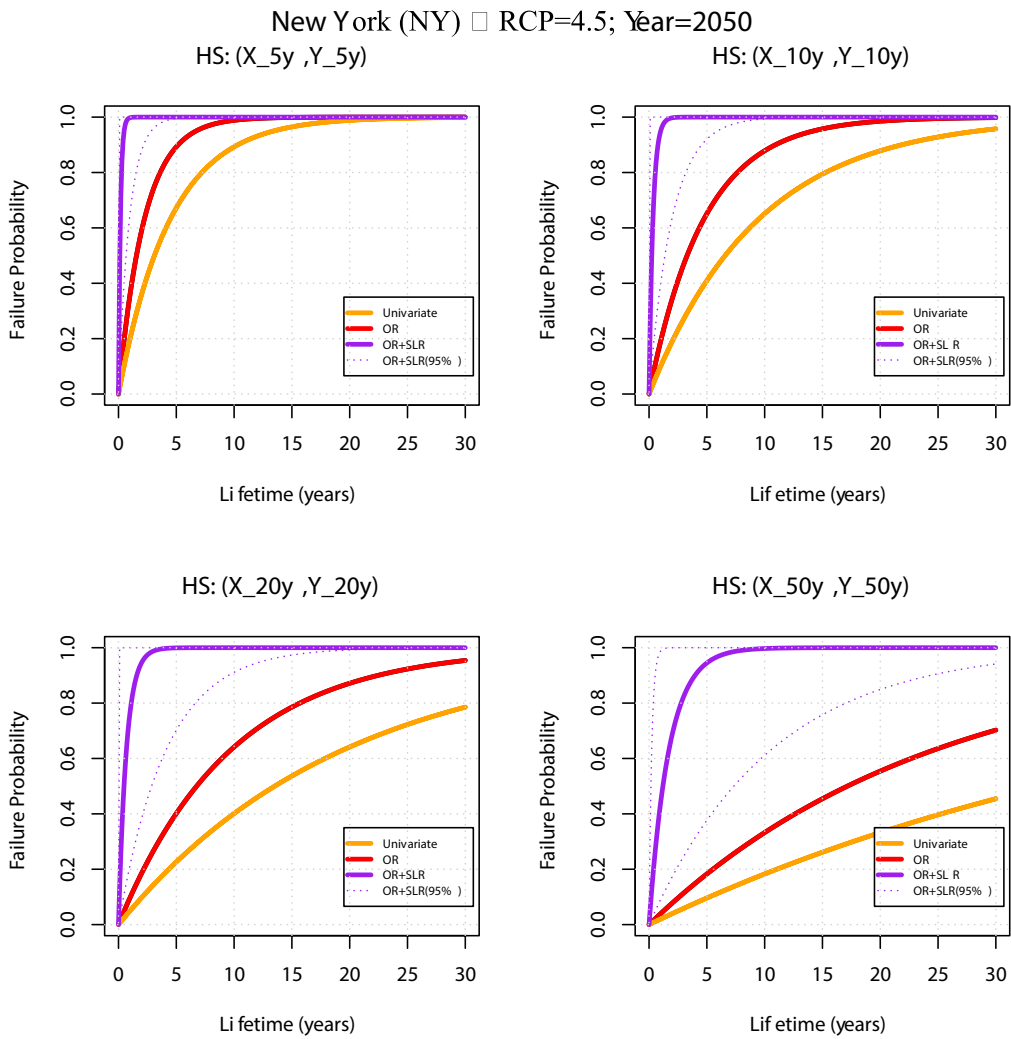
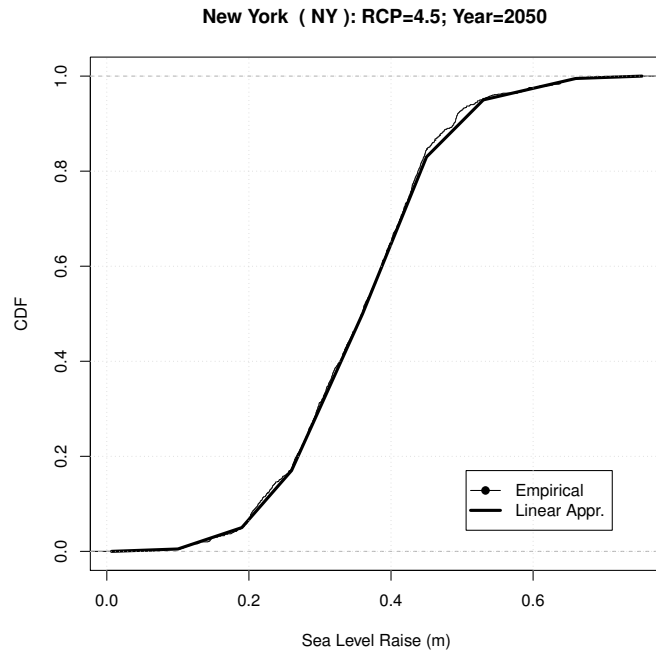


Figure SM.38: see text for explanation.

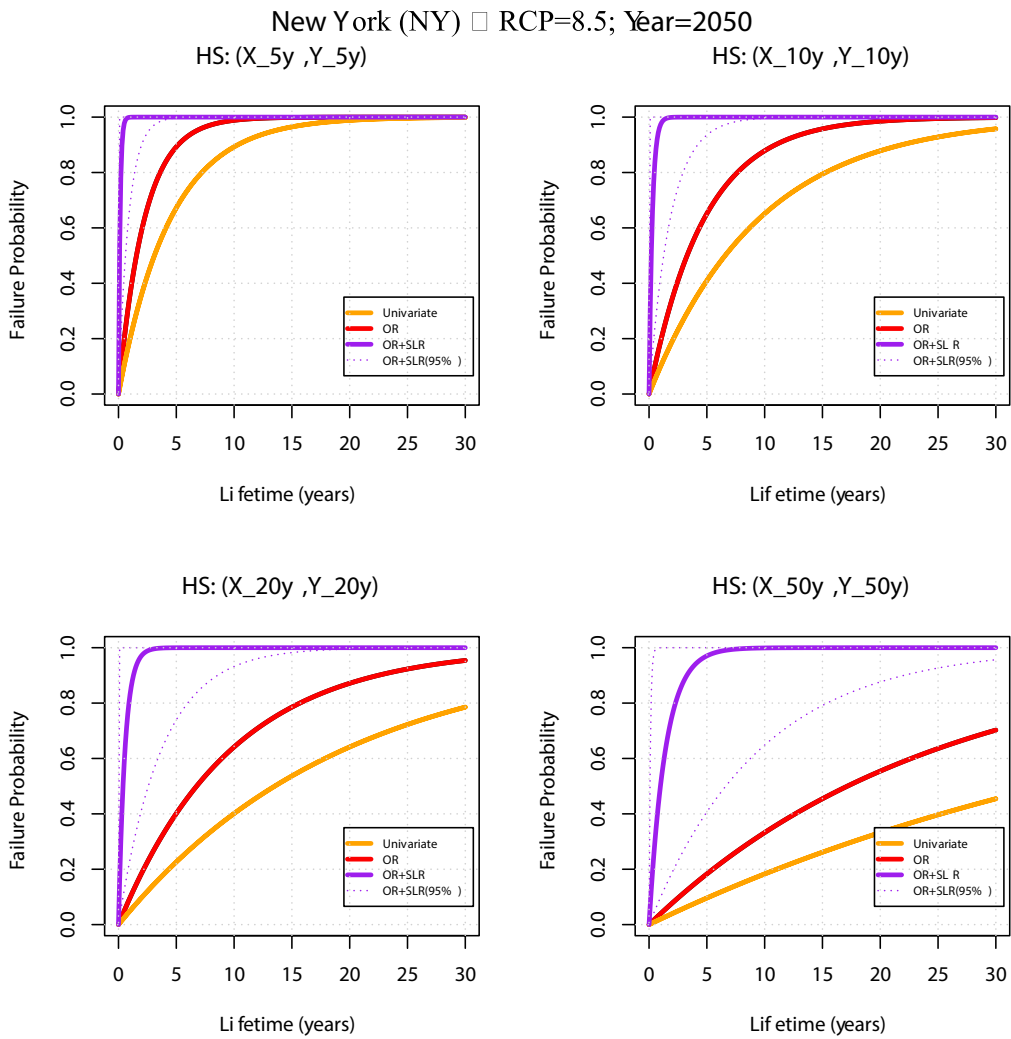
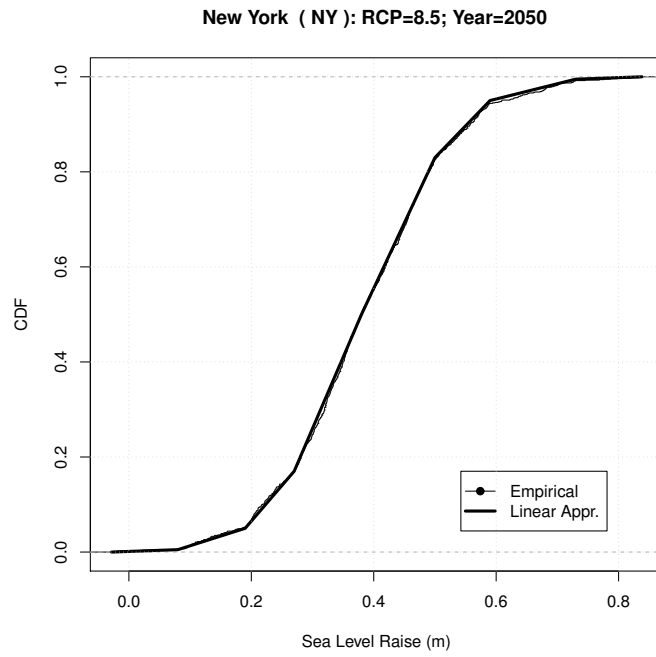
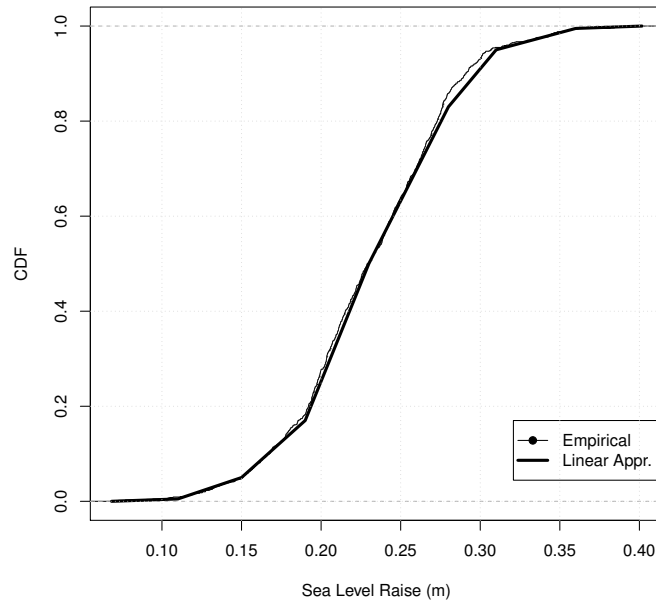


Figure SM.39: see text for explanation.

Norfolk (VA): RCP=4.5; Year=2030



Norfolk (VA) □ RCP=4.5; Year=2030
 HS: (X_{5y}, Y_{5y}) HS: (X_{10y}, Y_{10y})

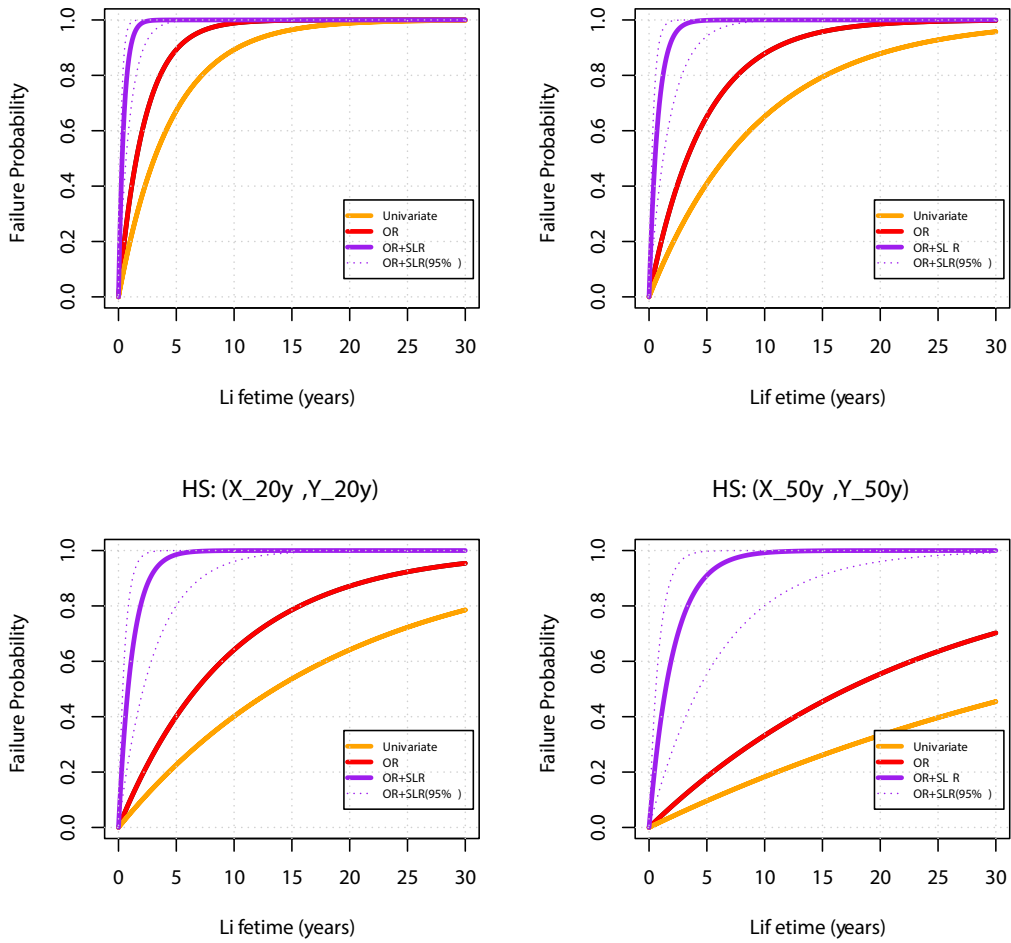
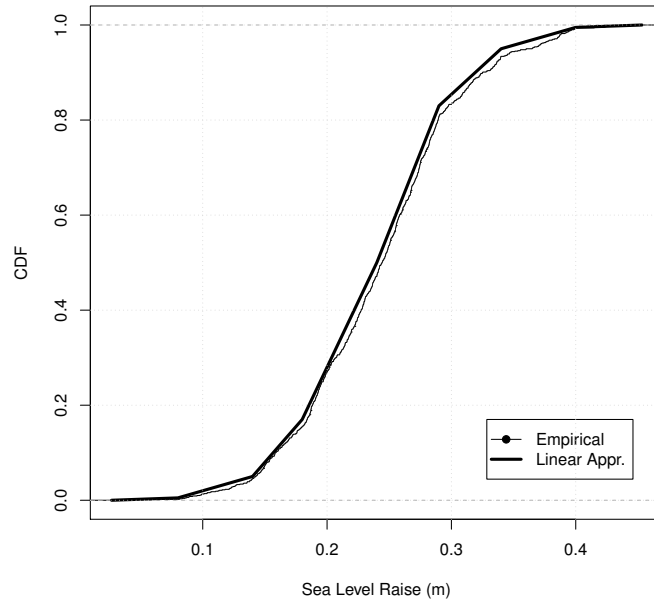


Figure SM.40: see text for explanation.

Norfolk (VA): RCP=8.5; Year=2030



Norfolk (VA) □ RCP=8.5; Year=2030
 HS: (X_{5y}, Y_{5y}) HS: (X_{10y}, Y_{10y})

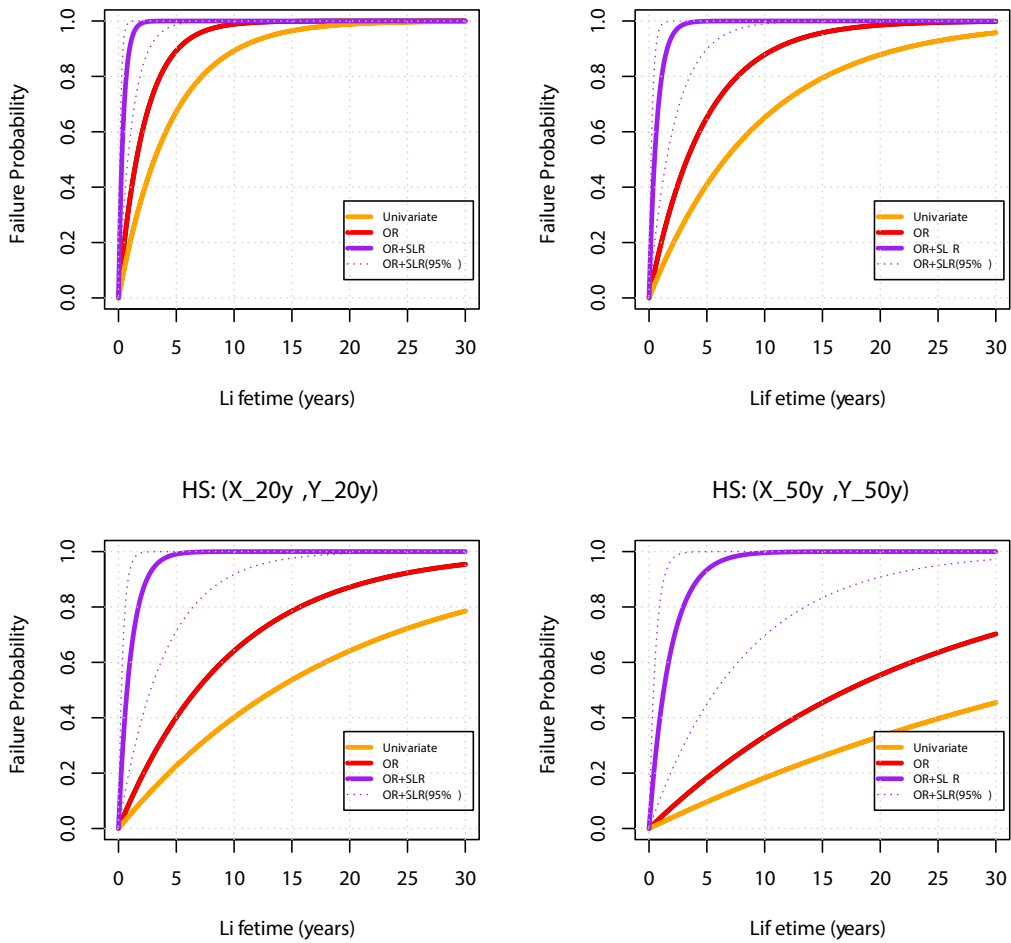
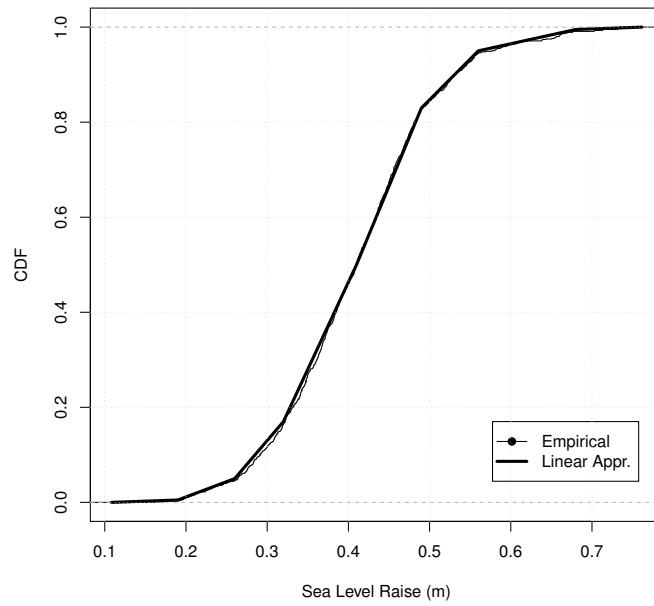


Figure SM.41: see text for explanation.

Norfolk (VA): RCP=4.5; Year=2050



Norfolk (VA) □ RCP=4.5; Year=2050
 HS: (X_{5y}, Y_{5y}) HS: (X_{10y}, Y_{10y})

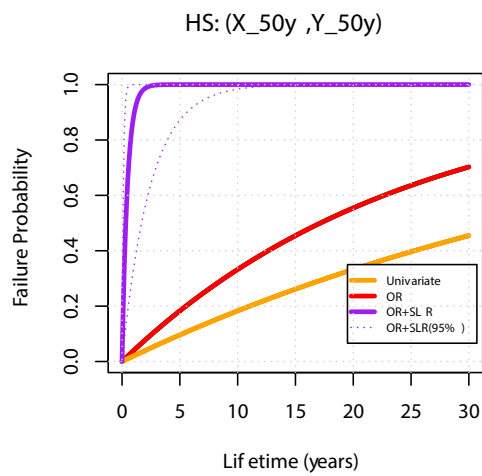
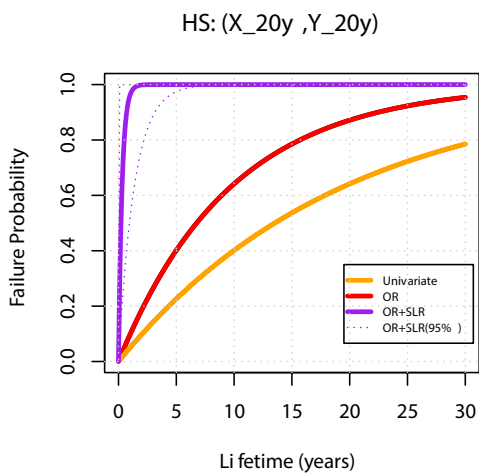
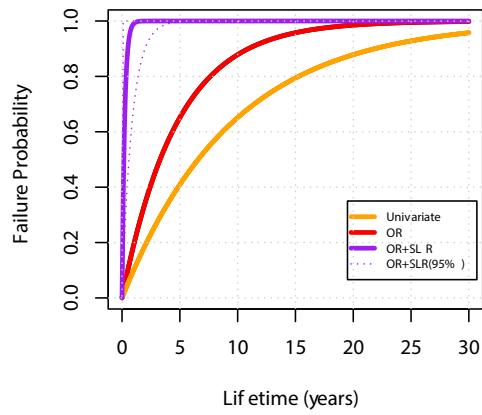
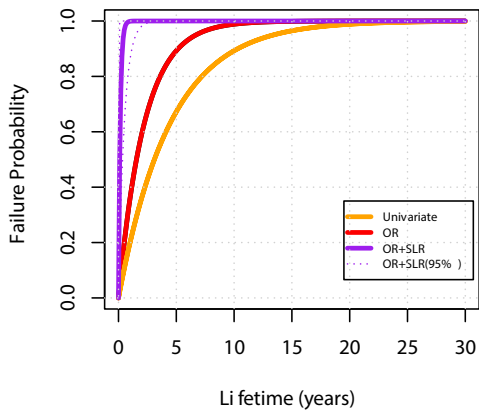
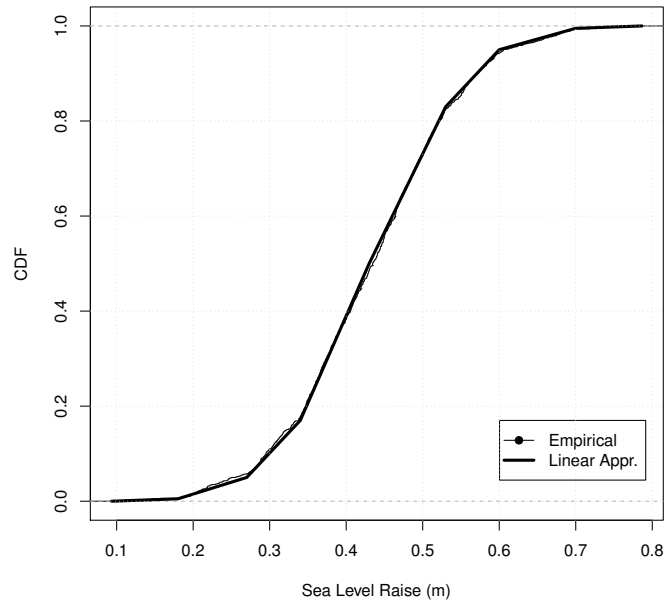
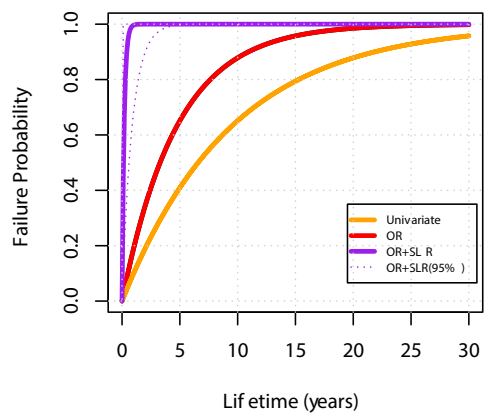
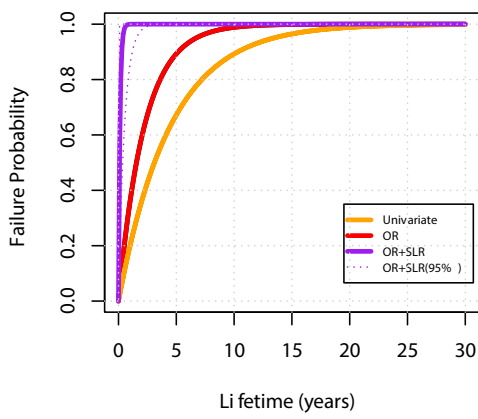


Figure SM.42: see text for explanation.

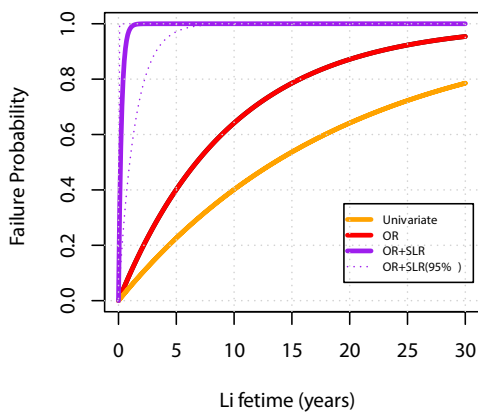
Norfolk (VA): RCP=8.5; Year=2050



Norfolk (VA) □ RCP=8.5; Year=2050
 HS: (X_{5y}, Y_{5y}) HS: (X_{10y}, Y_{10y})



HS: (X_{20y}, Y_{20y})



HS: (X_{50y}, Y_{50y})

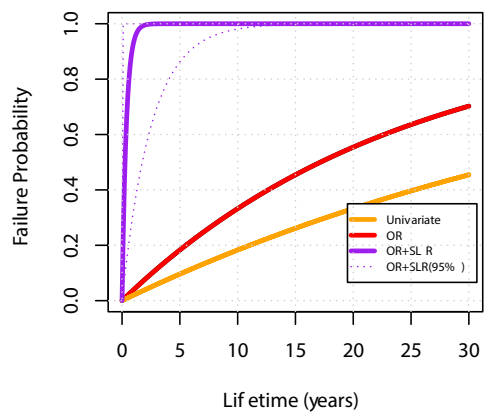
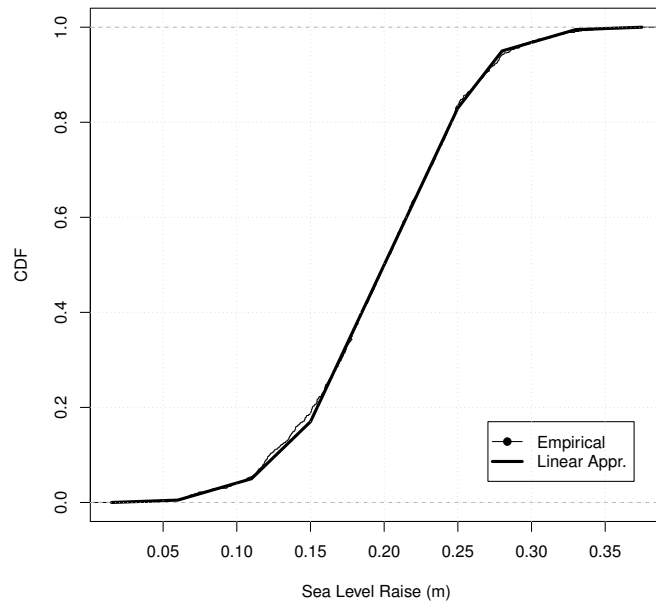


Figure SM.43: see text for explanation.

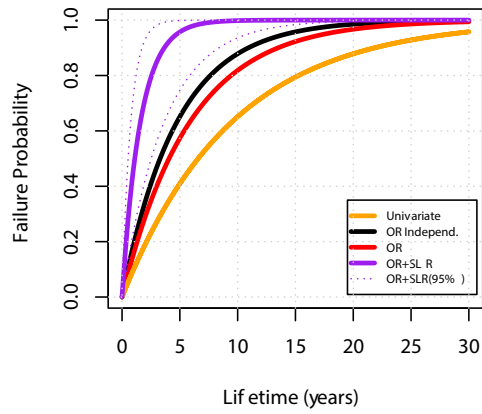
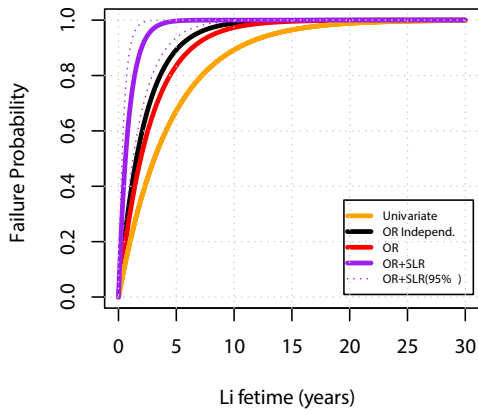
Philadelphia (PA): RCP=4.5; Year=2030



Philadelphia (PA) □ RCP=4.5; Year=2030

HS: (X_{5y} ,Y_{5y})

HS: (X_{10y} ,Y_{10y})



HS: (X_{20y} ,Y_{20y})

HS: (X_{50y} ,Y_{50y})

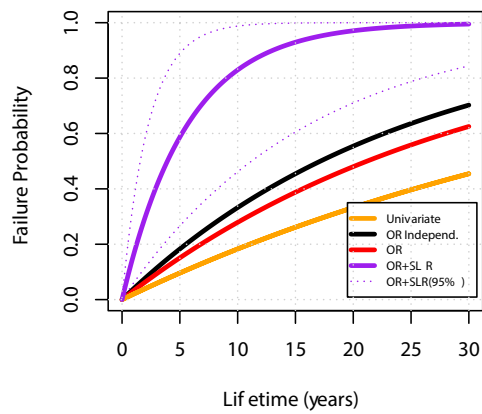
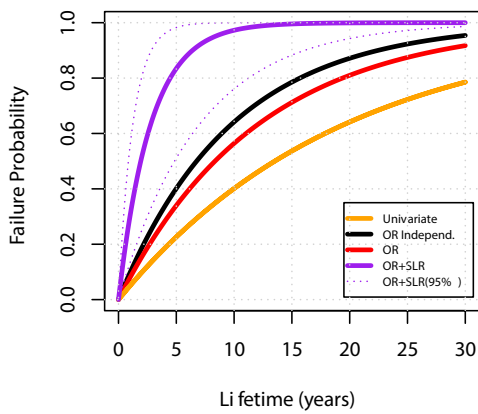
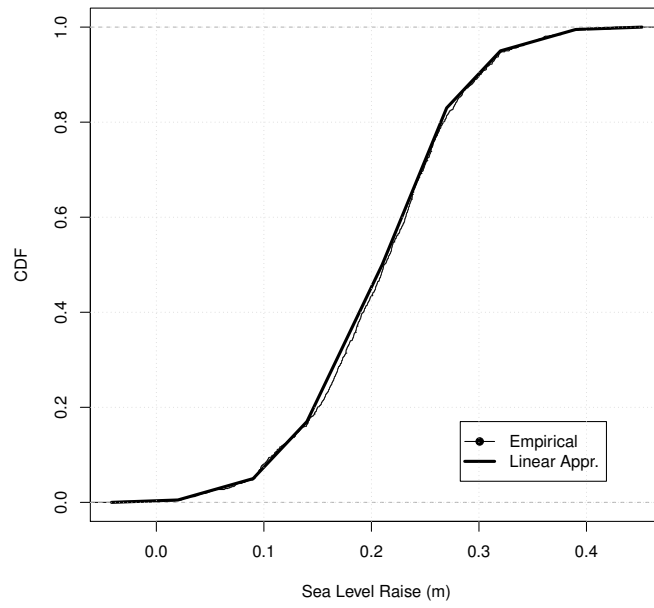


Figure SM.44: see text for explanation.

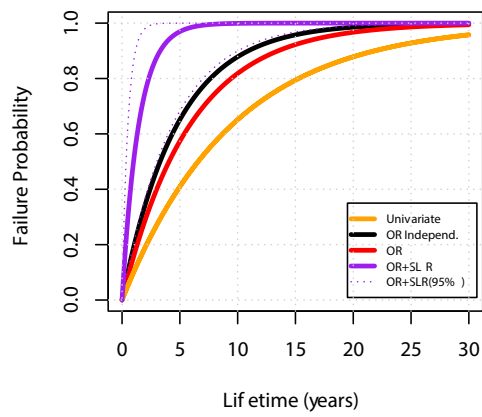
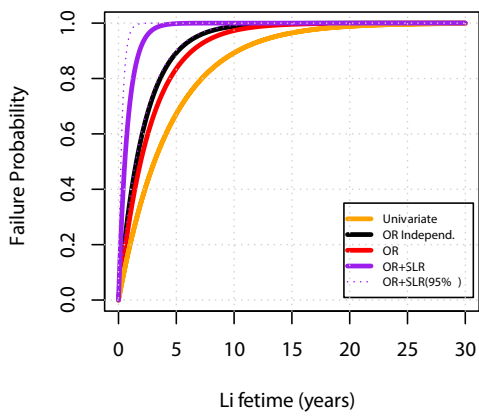
Philadelphia (PA): RCP=8.5; Year=2030



Philadelphia (PA) □ RCP=8.5; Year=2030

HS: (X_{5y} ,Y_{5y})

HS: (X_{10y} ,Y_{10y})



HS: (X_{20y} ,Y_{20y})

HS: (X_{50y} ,Y_{50y})

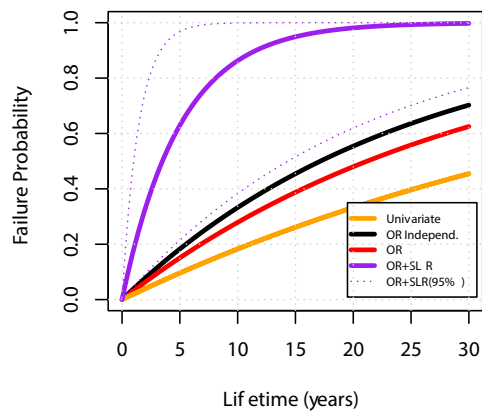
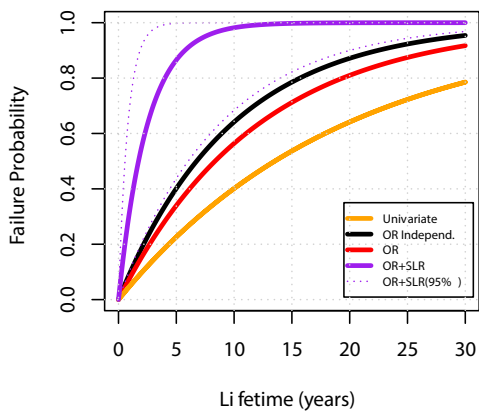
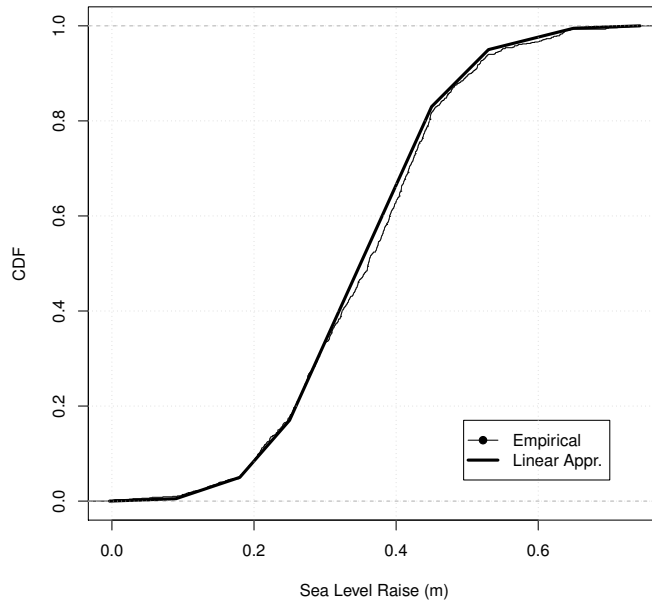


Figure SM.45: see text for explanation.

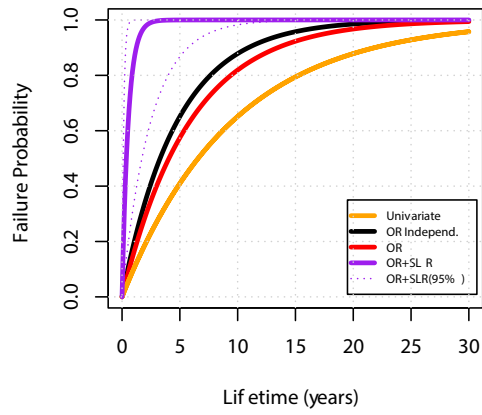
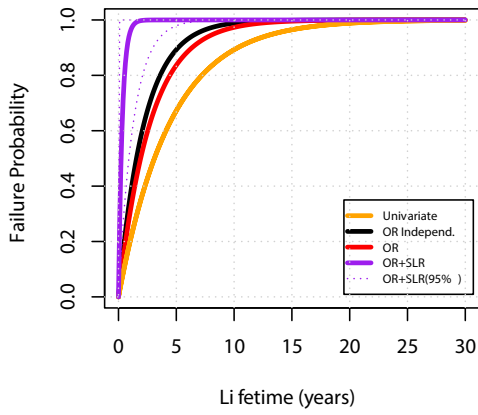
Philadelphia (PA): RCP=4.5; Year=2050



Philadelphia (PA) □ RCP=4.5; Year=2050

HS: (X_{5y}, Y_{5y})

HS: (X_{10y}, Y_{10y})



HS: (X_{20y}, Y_{20y})

HS: (X_{50y}, Y_{50y})

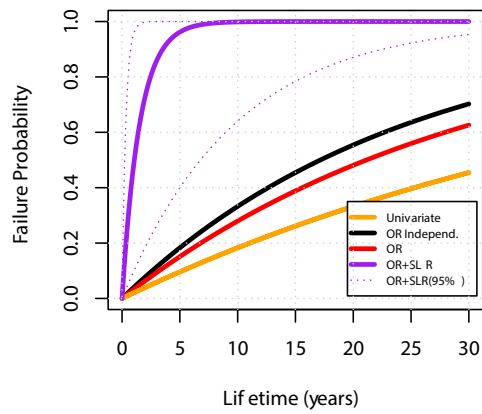
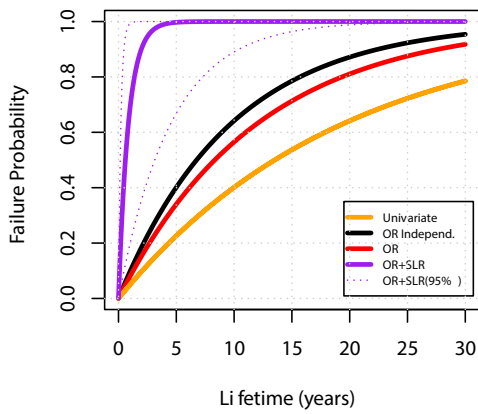
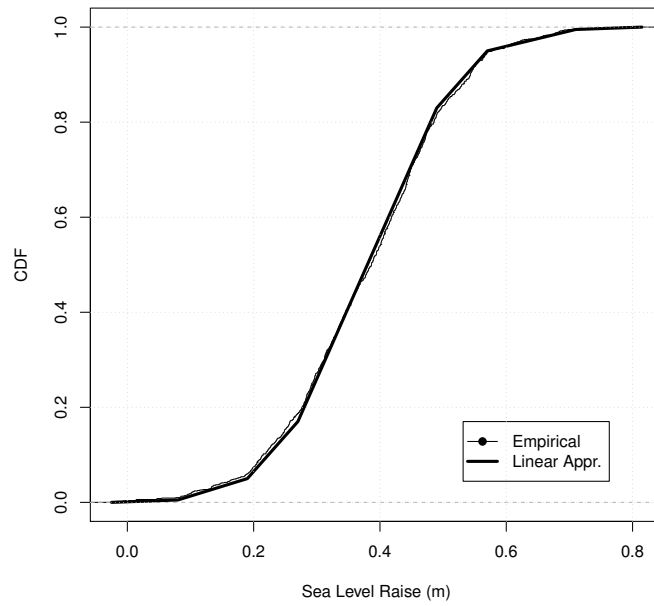


Figure SM.46: see text for explanation.

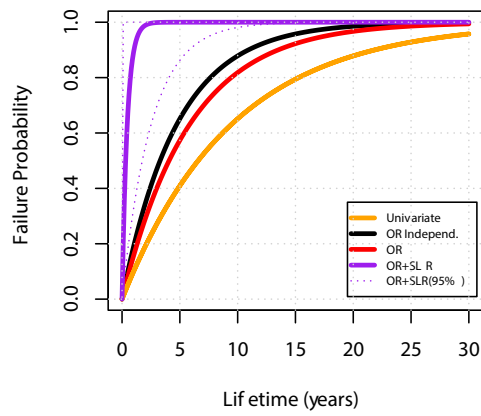
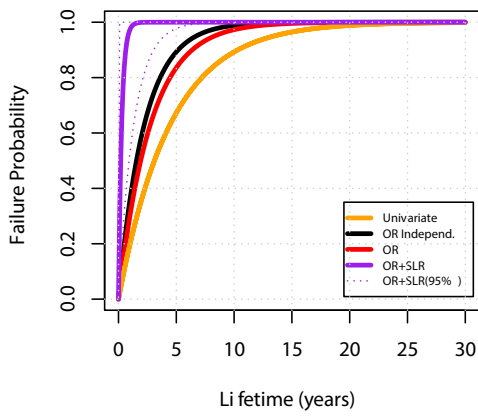
Philadelphia (PA): RCP=8.5; Year=2050



Philadelphia (PA) □ RCP=8.5; Year=2050

HS: (X_{5y} ,Y_{5y})

HS: (X_{10y} ,Y_{10y})



HS: (X_{20y} ,Y_{20y})

HS: (X_{50y} ,Y_{50y})

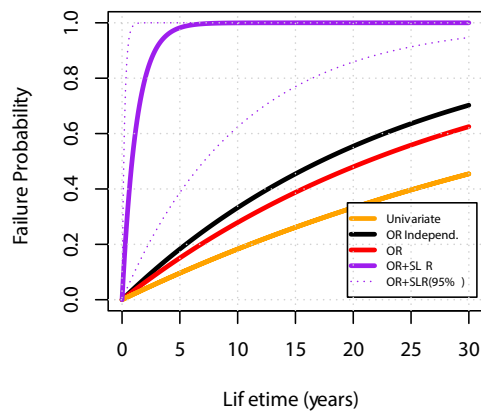
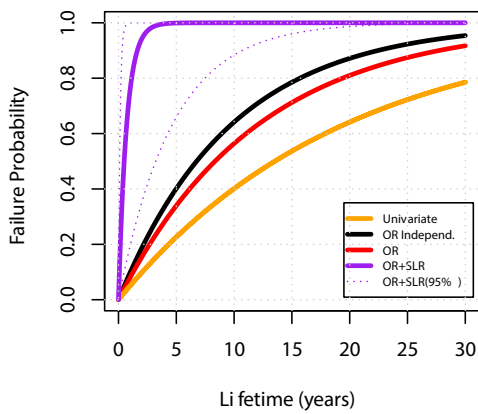
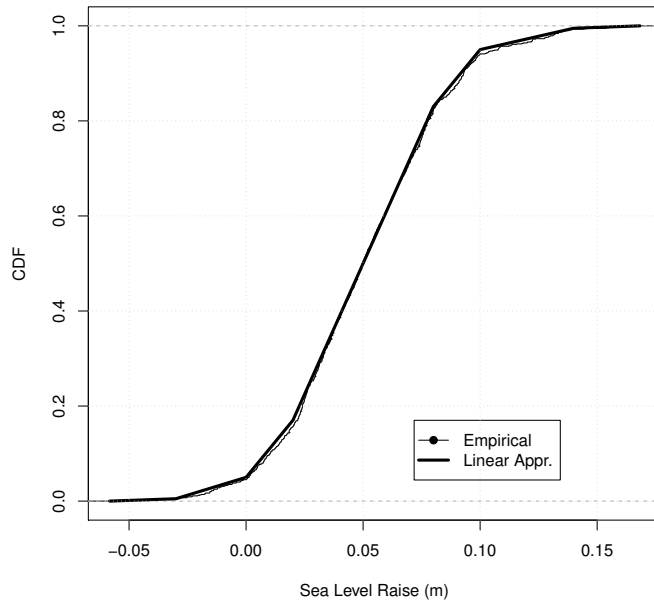
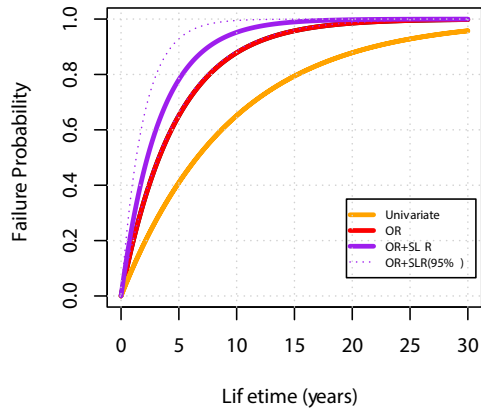
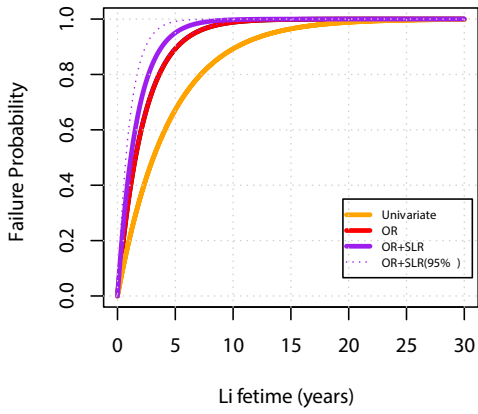


Figure SM.47: see text for explanation.

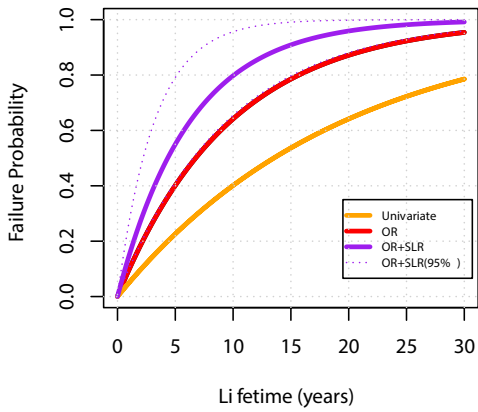
Portland (OR): RCP=4.5; Year=2030



Portland (OR) □ RCP=4.5; Year=2030
 HS: (X_{5y} ,Y_{5y}) HS: (X_{10y} ,Y_{10y})



HS: (X_{20y} ,Y_{20y})



HS: (X_{50y} ,Y_{50y})

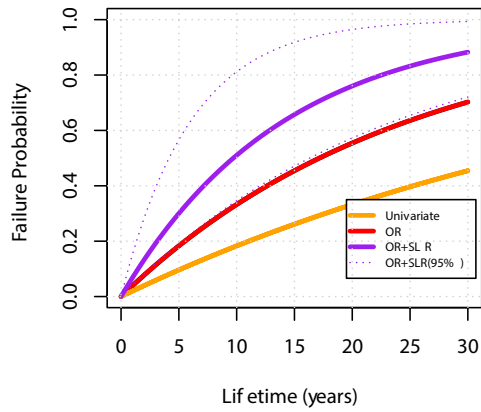
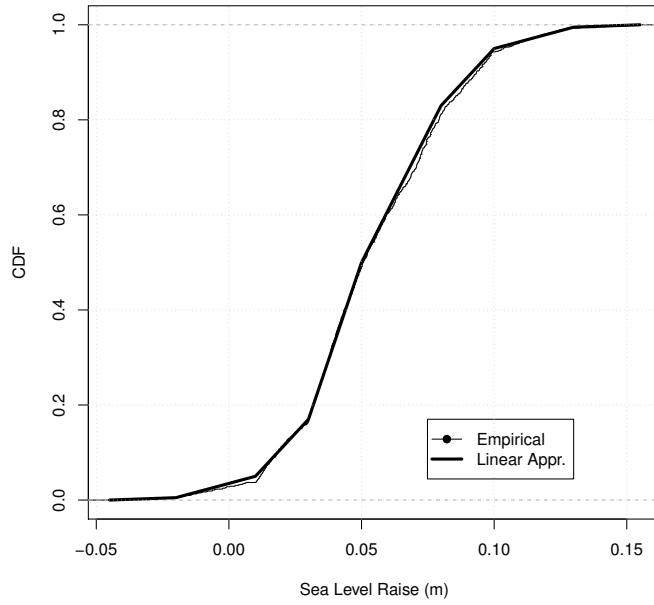
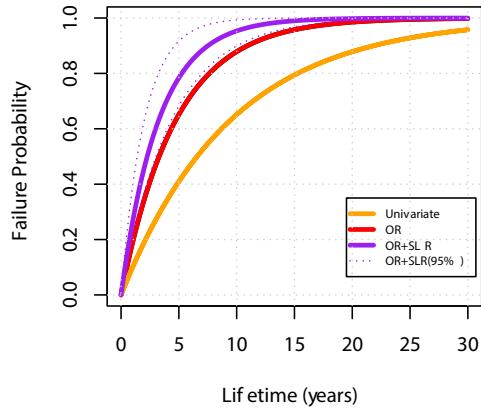
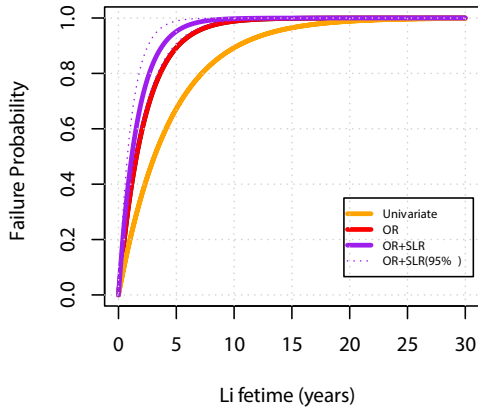


Figure SM.48: see text for explanation.

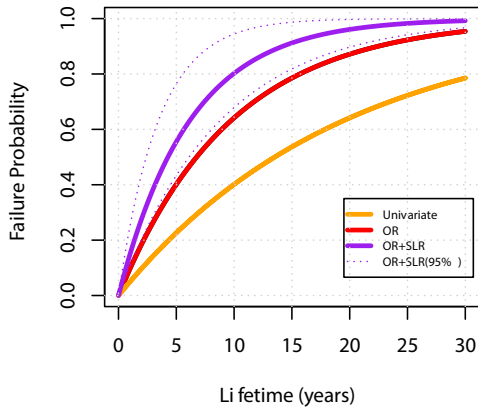
Portland (OR): RCP=8.5; Year=2030



Portland (OR) □ RCP=8.5; Year=2030
 HS: (X_{5y}, Y_{5y}) HS: (X_{10y}, Y_{10y})



HS: (X_{20y}, Y_{20y})



HS: (X_{50y}, Y_{50y})

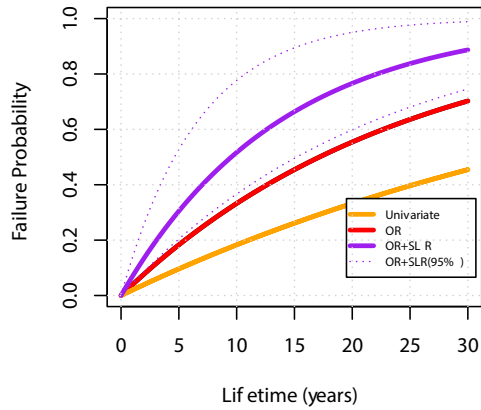
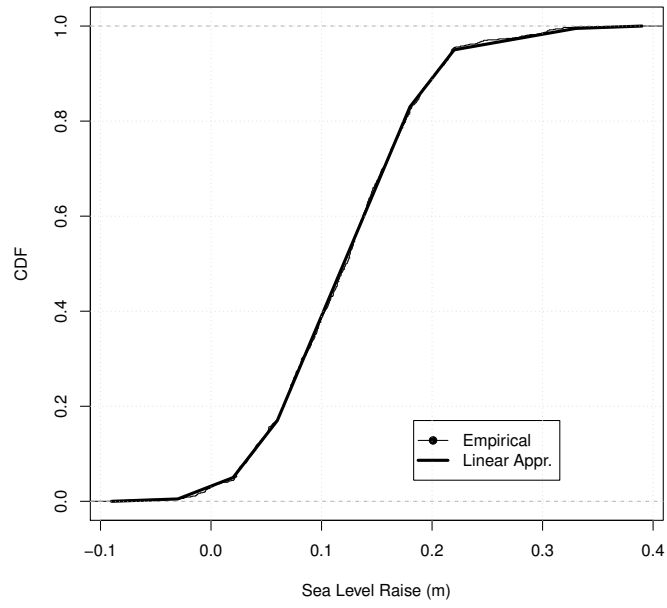


Figure SM.49: see text for explanation.

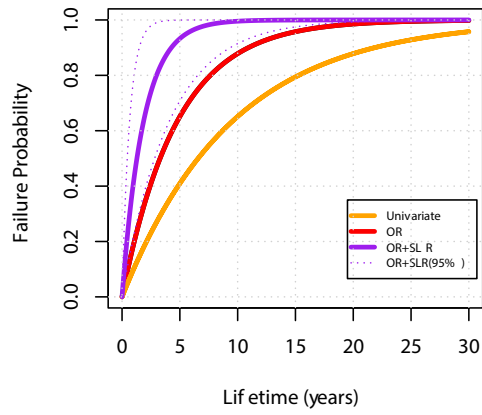
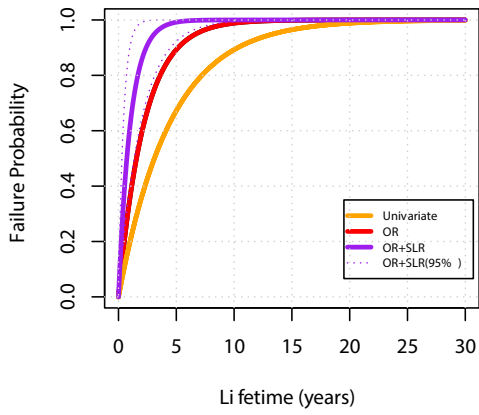
Portland (OR): RCP=4.5; Year=2050



Portland (OR) □ RCP=4.5; Year=2050

HS: (X_{5y}, Y_{5y})

HS: (X_{10y}, Y_{10y})



HS: (X_{20y}, Y_{20y})

HS: (X_{50y}, Y_{50y})

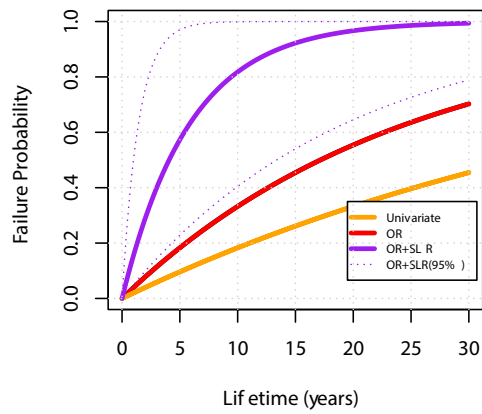
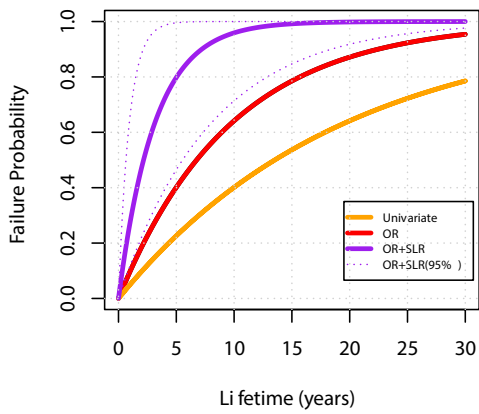
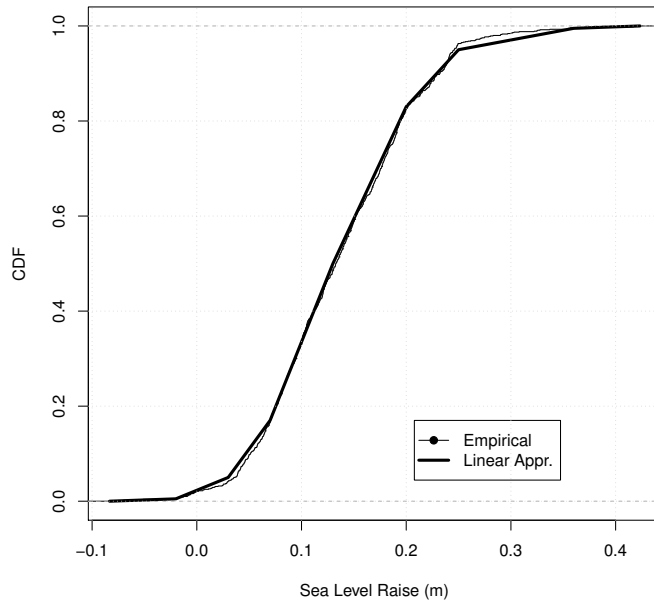


Figure SM.50: see text for explanation.

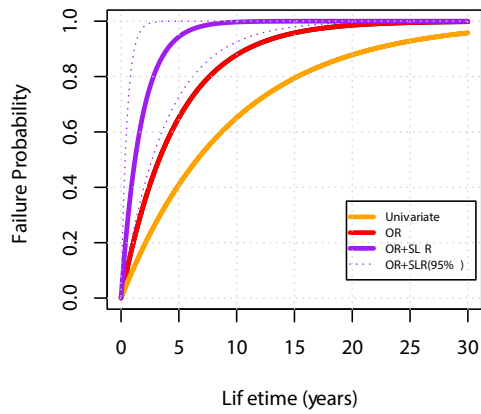
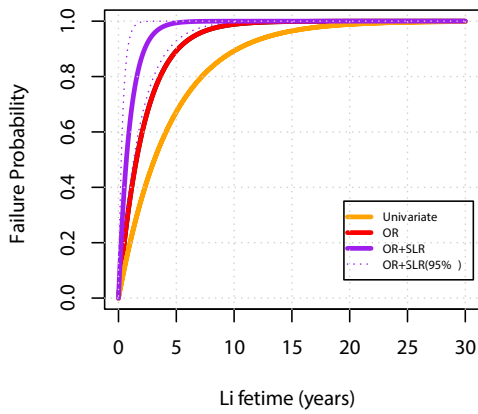
Portland (OR): RCP=8.5; Year=2050



Portland (OR) □ RCP=8.5; Year=2050

HS: (X_{5y}, Y_{5y})

HS: (X_{10y}, Y_{10y})



HS: (X_{20y}, Y_{20y})

HS: (X_{50y}, Y_{50y})

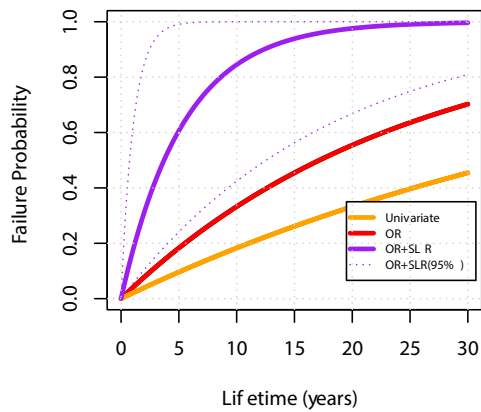
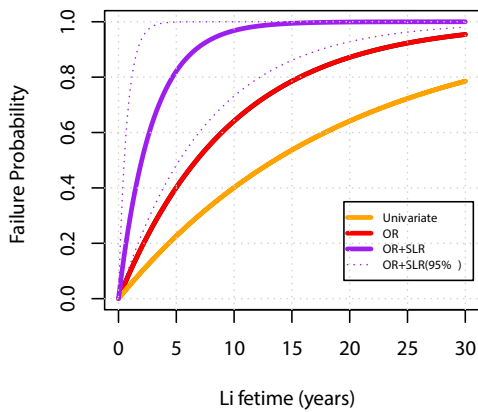
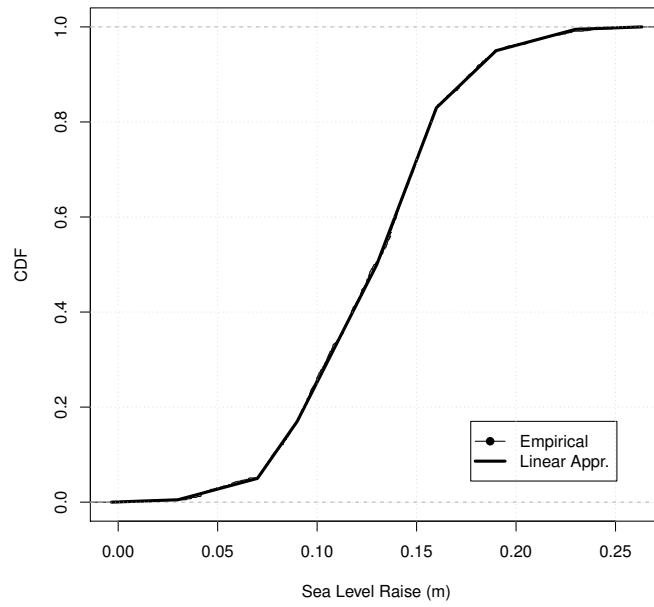


Figure SM.51: see text for explanation.

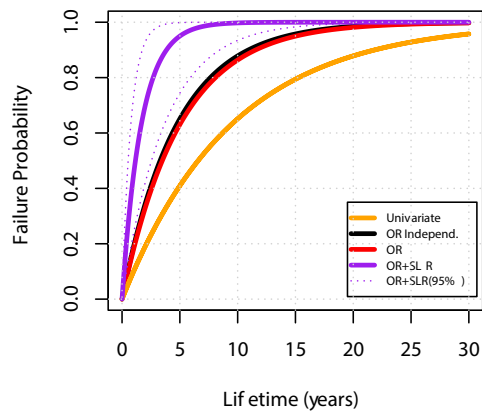
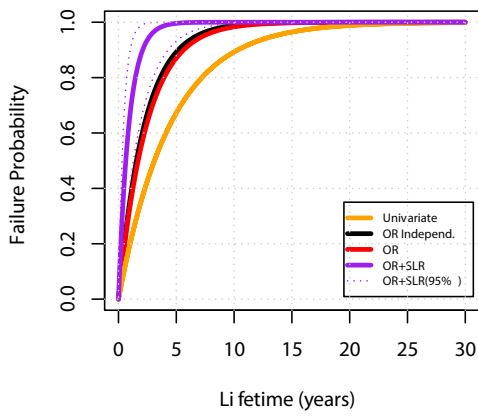
San Francisco (CA): RCP=4.5; Year=2030



San Francisco (CA) □ RCP=4.5; Year=2030

HS: (X_{5y}, Y_{5y})

HS: (X_{10y}, Y_{10y})



HS: (X_{20y}, Y_{20y})

HS: (X_{50y}, Y_{50y})

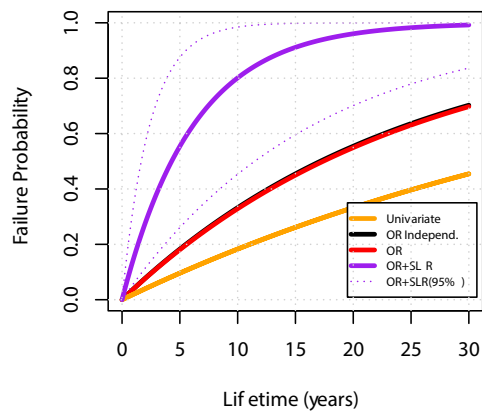
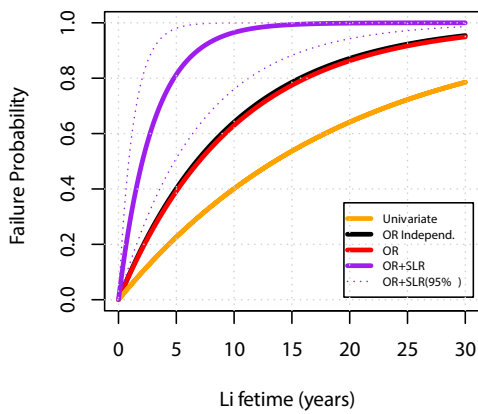
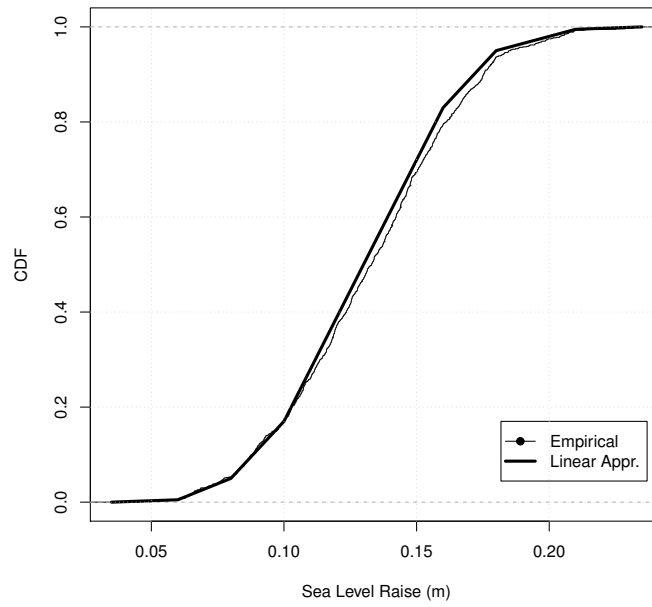


Figure SM.52: see text for explanation.

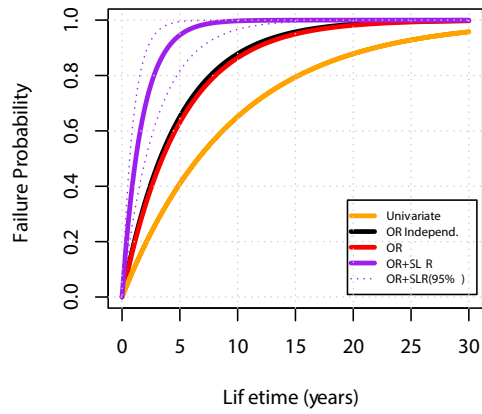
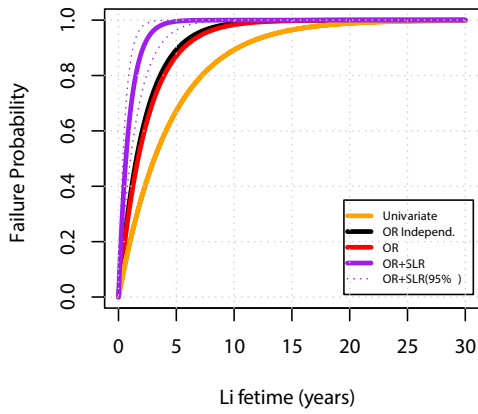
San Francisco (CA): RCP=8.5; Year=2030



San Francisco (CA) □ RCP=8.5; Year=2030

HS: (X_{5y} ,Y_{5y})

HS: (X_{10y} ,Y_{10y})



HS: (X_{20y} ,Y_{20y})

HS: (X_{50y} ,Y_{50y})

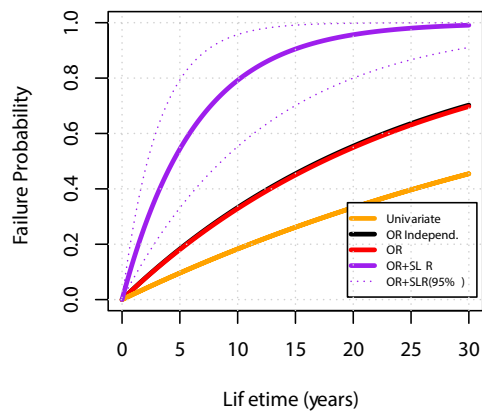
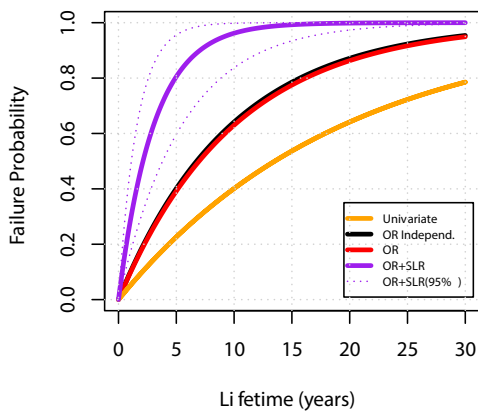
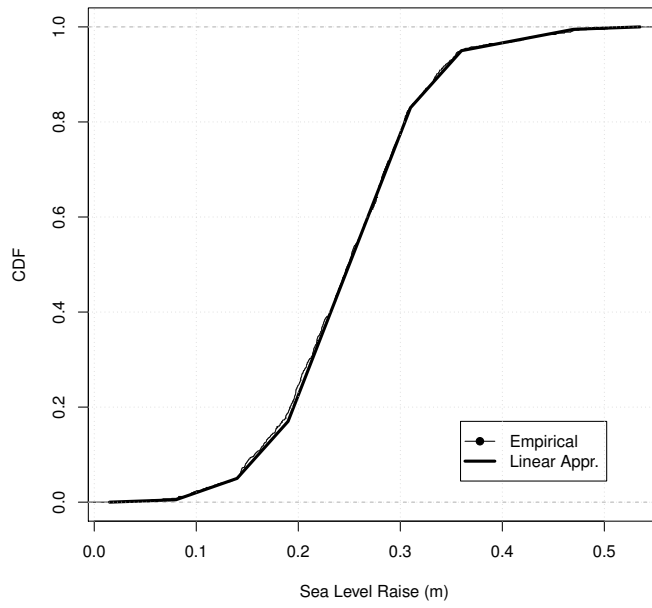


Figure SM.53: see text for explanation.

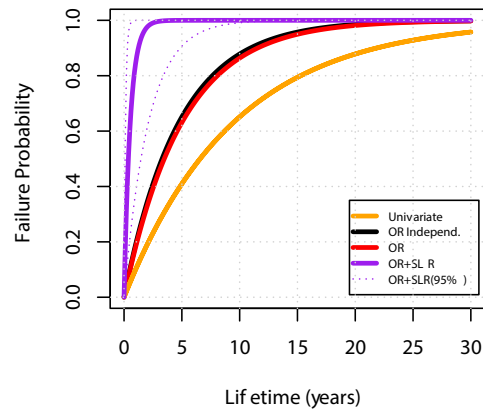
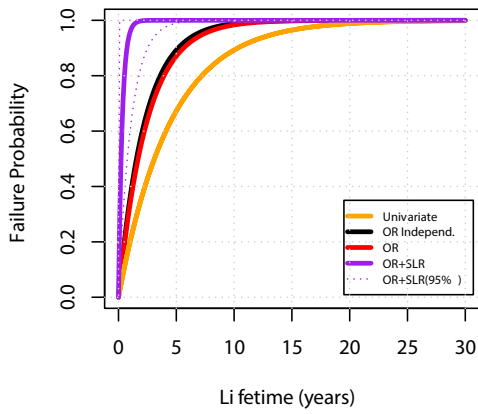
San Francisco (CA): RCP=4.5; Year=2050



San Francisco (CA) □ RCP=4.5; Year=2050

HS: (X_{5y} ,Y_{5y})

HS: (X_{10y} ,Y_{10y})



HS: (X_{20y} ,Y_{20y})

HS: (X_{50y} ,Y_{50y})

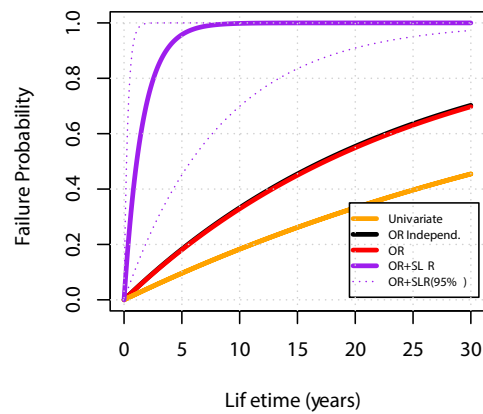
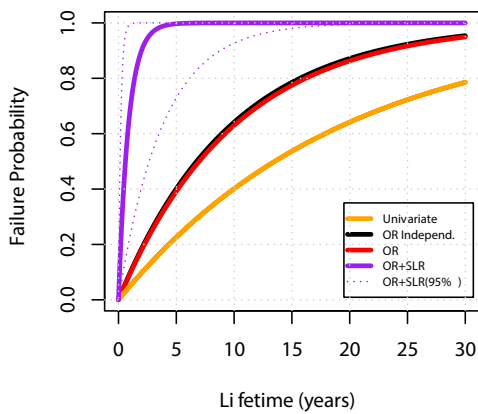
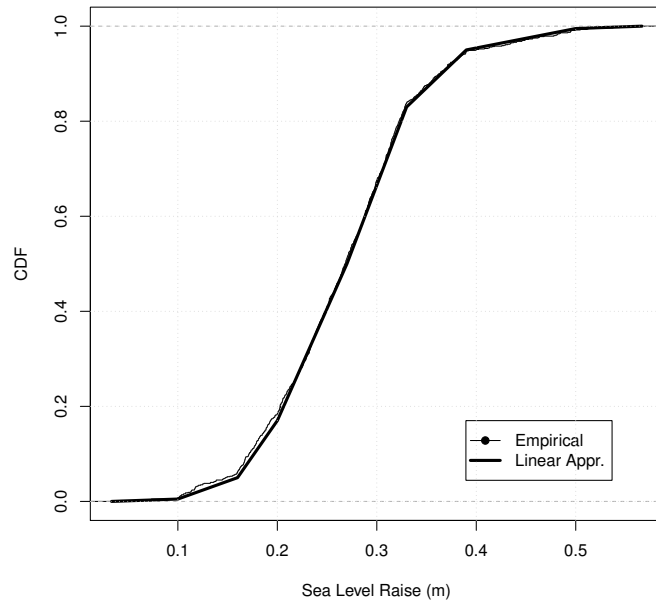


Figure SM.54: see text for explanation.

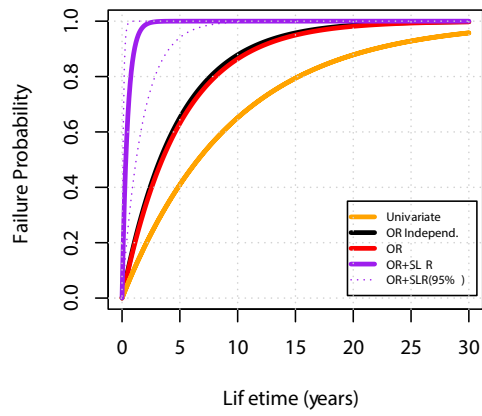
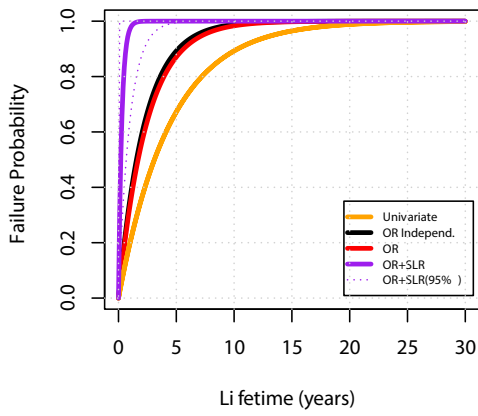
San Francisco (CA): RCP=8.5; Year=2050



San Francisco (CA) □ RCP=8.5; Year=2050

HS: (X_{5y} ,Y_{5y})

HS: (X_{10y} ,Y_{10y})



HS: (X_{20y} ,Y_{20y})

HS: (X_{50y} ,Y_{50y})

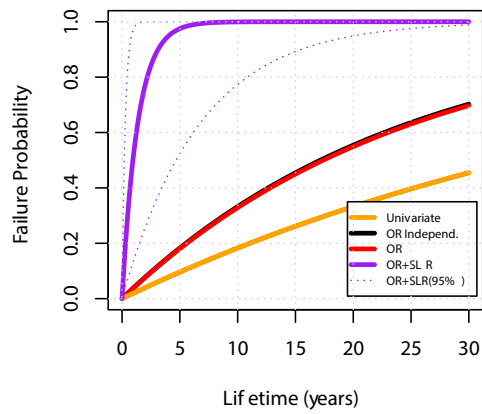
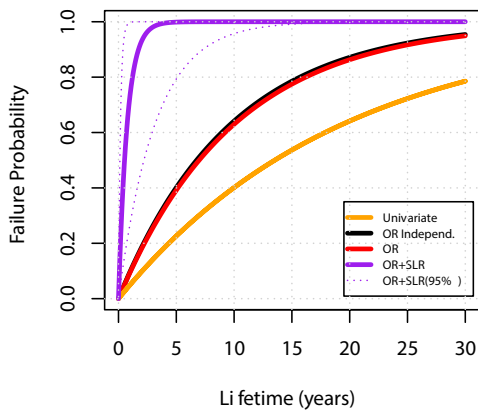
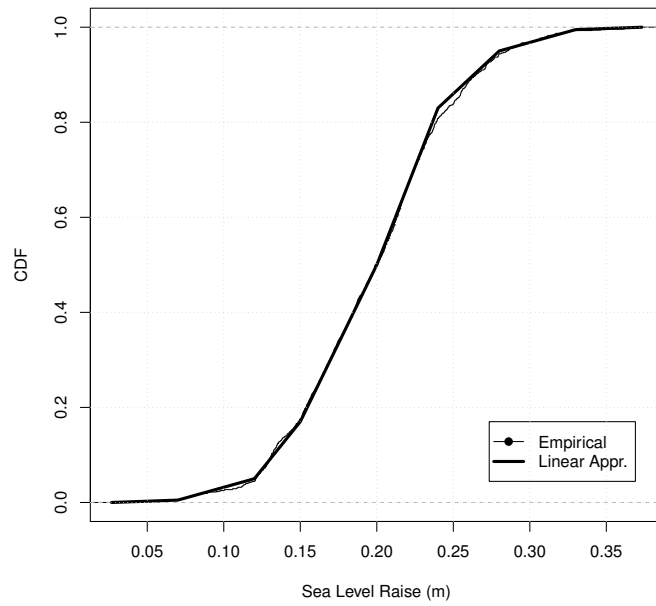


Figure SM.55: see text for explanation.

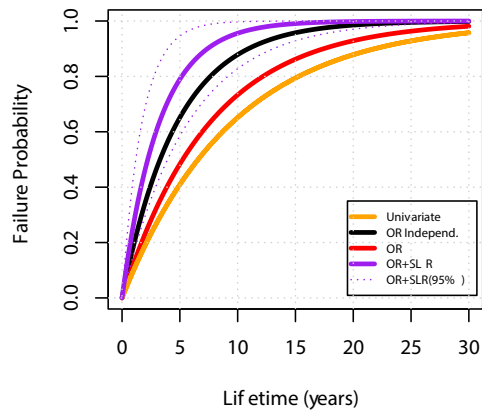
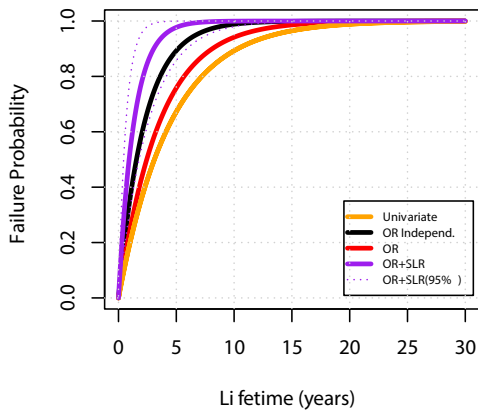
Washington (DC): RCP=4.5; Year=2030



Washington (DC) □ RCP=4.5; Year=2030

HS: (X_{5y} ,Y_{5y})

HS: (X_{10y} ,Y_{10y})



HS: (X_{20y} ,Y_{20y})

HS: (X_{50y} ,Y_{50y})

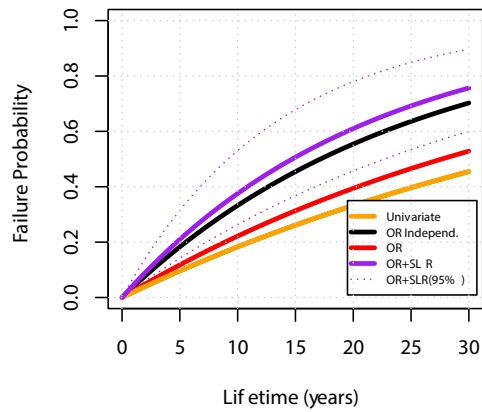
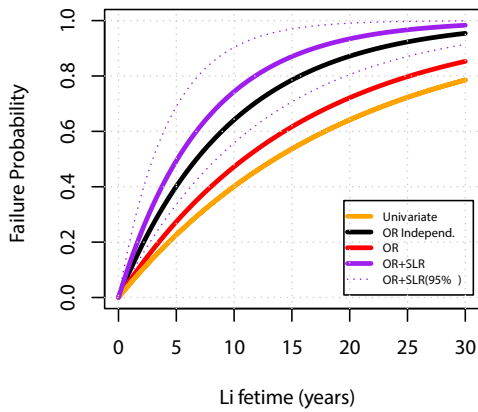
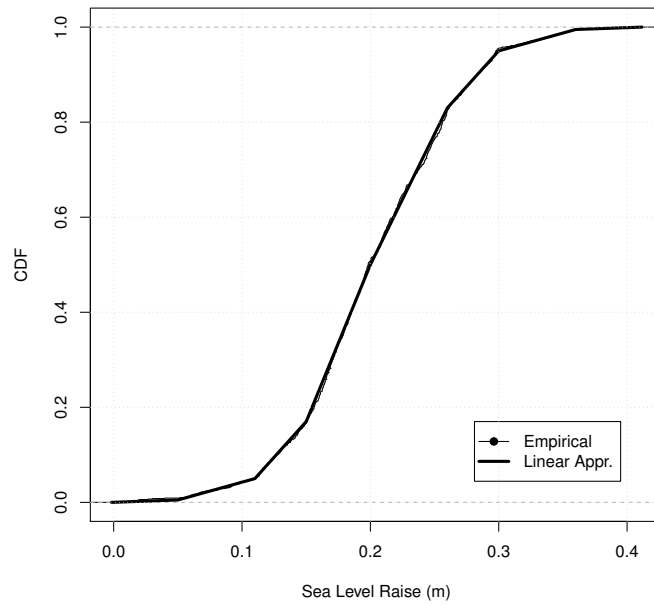


Figure SM.56: see text for explanation.

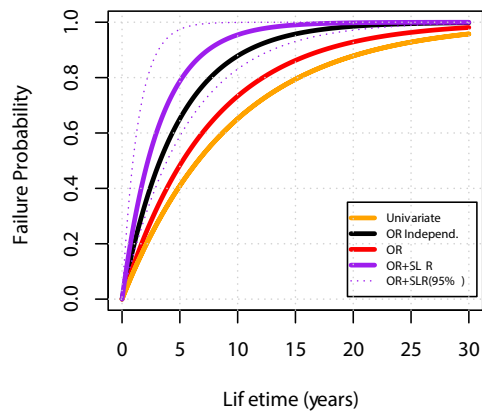
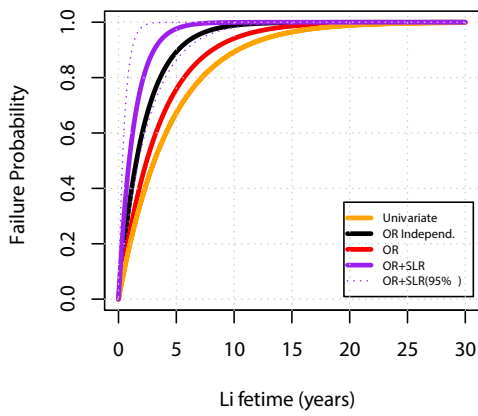
Washington (DC): RCP=8.5; Year=2030



Washington (DC) □ RCP=8.5; Year=2030

HS: (X_{5y} ,Y_{5y})

HS: (X_{10y} ,Y_{10y})



HS: (X_{20y} ,Y_{20y})

HS: (X_{50y} ,Y_{50y})

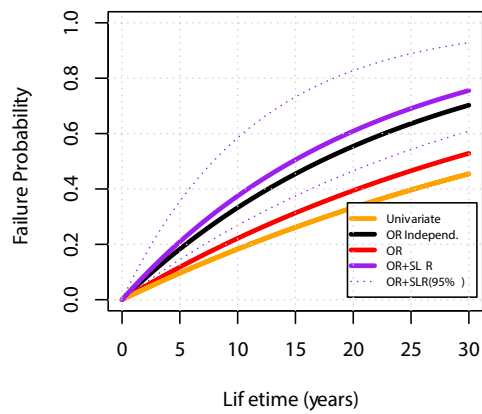
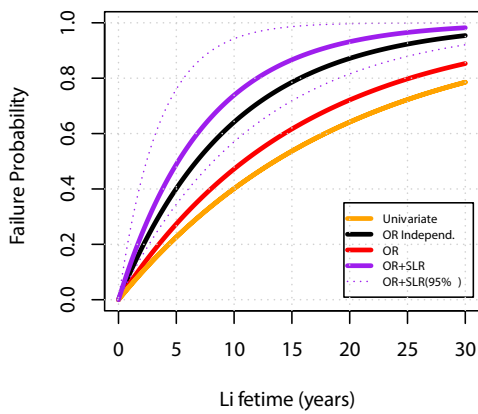
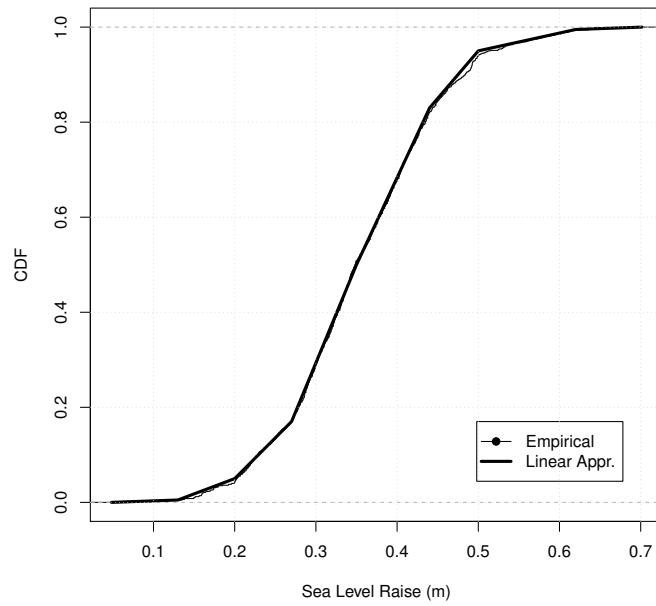
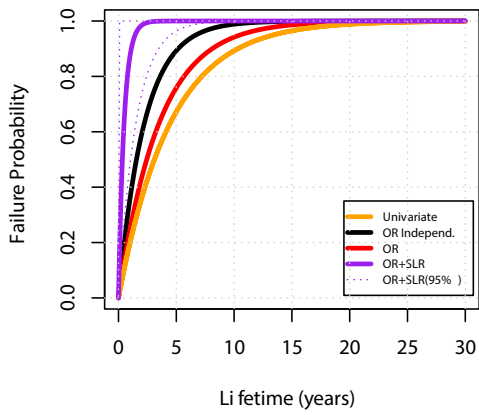


Figure SM.57: see text for explanation.

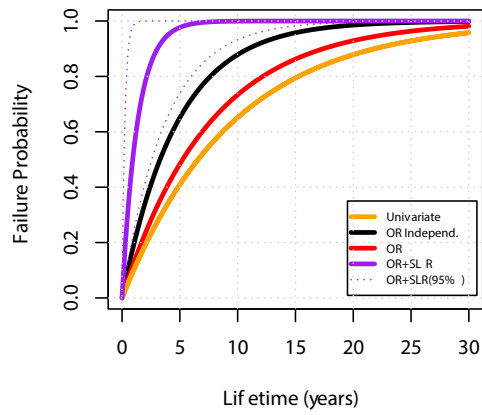
Washington (DC): RCP=4.5; Year=2050



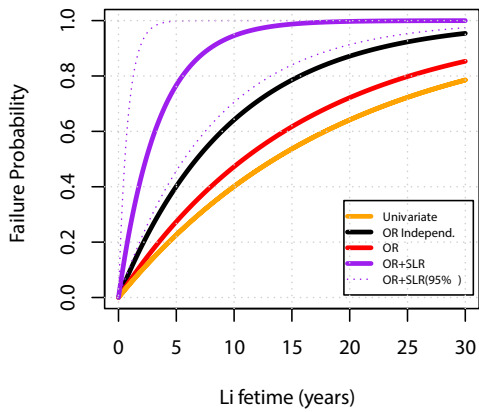
Washington (DC) □ RCP=4.5; Year=2050
 HS: (X_{5y} ,Y_{5y})



HS: (X_{10y} ,Y_{10y})



HS: (X_{20y} ,Y_{20y})



HS: (X_{50y} ,Y_{50y})

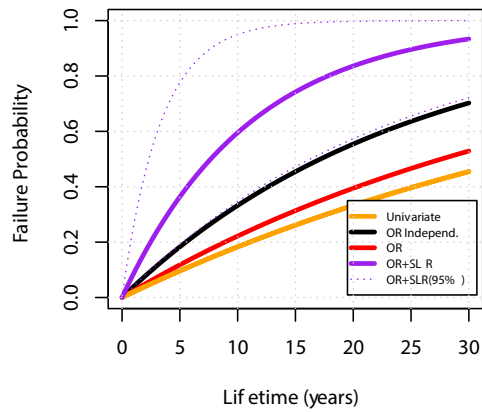
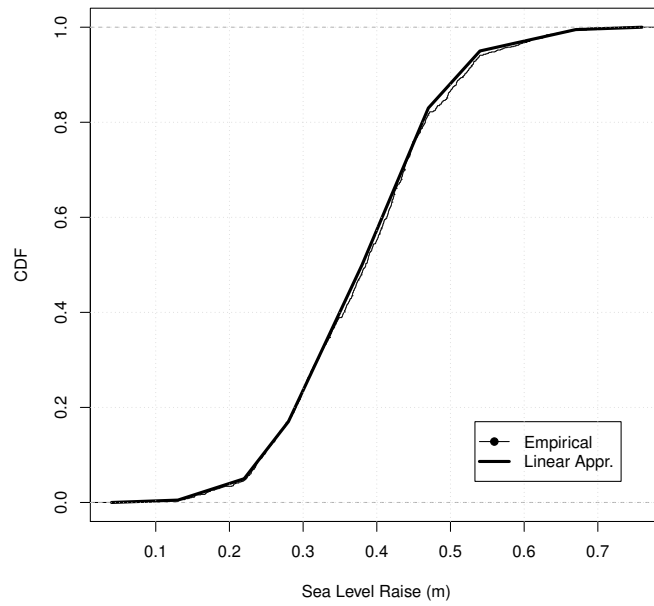


Figure SM.58: see text for explanation.

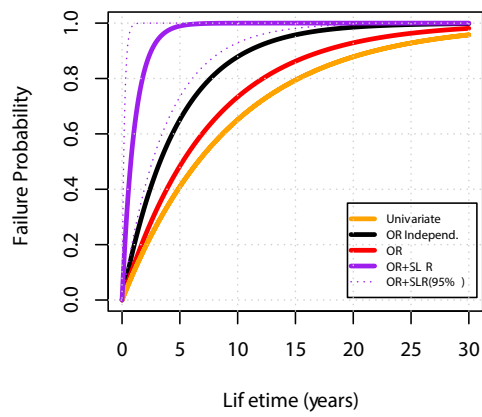
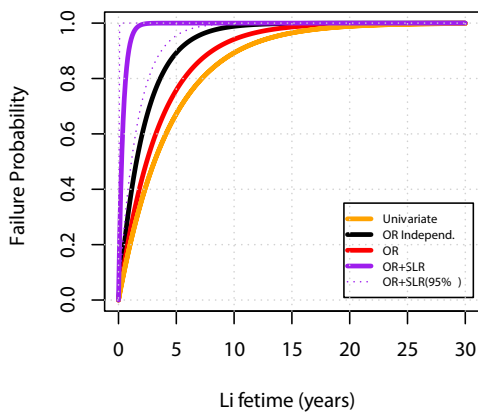
Washington (DC): RCP=8.5; Year=2050



Washington (DC) □ RCP=8.5; Year=2050

HS: (X_{5y} ,Y_{5y})

HS: (X_{10y} ,Y_{10y})



HS: (X_{20y} ,Y_{20y})

HS: (X_{50y} ,Y_{50y})

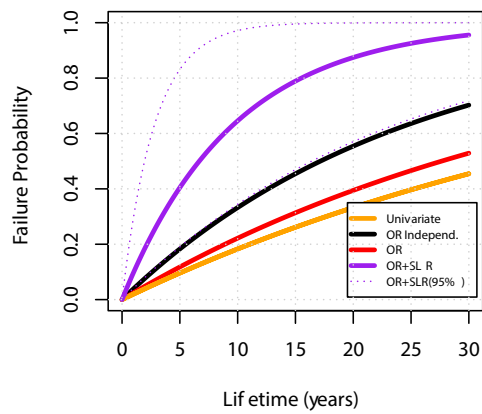
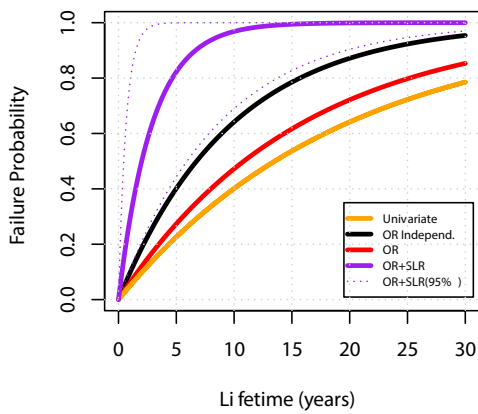


Figure SM.59: see text for explanation.

References

- Jens Bender, Thomas Wahl, Alfred Müller, and Jürgen Jensen. A multivariate design framework for river confluences. *Hydrological Sciences Journal*, 61(3):471–482, 2016.
- N Chini and PK Stansby. Extreme values of coastal wave overtopping accounting for climate change and sea level rise. *Coastal Engineering*, 65:27–37, 2012.
- S Corbella and DD Stretch. Multivariate return periods of sea storms for coastal erosion risk assessment. *Natural Hazards and Earth System Sciences*, 12(8):2699–2708, 2012.
- Stefano Corbella and Derek D Stretch. Simulating a multivariate sea storm using archimedean copulas. *Coastal Engineering*, 76:68–78, 2013.
- C De Michele, G Salvadori, G Passoni, and R Vezzoli. A multivariate model of sea storms using copulas. *Coastal Engineering*, 54(10):734–751, 2007.
- B Gouldby, FJ Méndez, Y Guanache, A Rueda, and R Mínguez. A methodology for deriving extreme nearshore sea conditions for structural design and flood risk analysis. *Coastal Engineering*, 88:15–26, 2014.
- Peter J Hawkes, Ben P Gouldby, Jonathan A Tawn, and Michael W Owen. The joint probability of waves and water levels in coastal engineering design. *Journal of hydraulic research*, 40(3):241–251, 2002.
- M. Hofert, I. Kojadinovic, M. Maechler, and J. Yan. *copula: Multivariate Dependence with Copulas*, R package version 0.999-15 edition, 2016. URL <http://CRAN.R-project.org/package=copula>.
- SF Kew, FM Selten, G Lenderink, and W Hazeleger. The simultaneous occurrence of surge and discharge extremes for the rhine delta. *Natural Hazards and Earth System Sciences*, 13(8):2017–2029, 2013.
- Wouter-Jan Klerk, HC Winsemius, WJ van Verseveld, AMR Bakker, and FLM Diermanse. The co-occurrence of storm surges and extreme discharges within the rhine–meuse delta. *Environmental Research Letters*, 10(3):035005, 2015.
- Rob Lamb, Caroline Keef, Jonathan Tawn, Stefan Laeger, I Meadowcroft, S Surendran, P Dunning, and C Batstone. A new method to assess the risk of local and widespread flooding on rivers and coasts. *Journal of Flood Risk Management*, 3(4):323–336, 2010.
- Ann Lehman, Norm ORourke, Larry Hatcher, and Edward Stepanski. *Jmp for basic univariate and multivariate statistics*. SAS Institute Inc., Cary, NC, page 481, 2005.
- F Li, PHAJM Van Gelder, R Ranasinghe, DP Callaghan, and RB Jongejan. Probabilistic modelling of extreme storms along the dutch coast. *Coastal Engineering*, 86:1–13, 2014a.
- F Li, PHAJM van Gelder, JK Vrijling, DP Callaghan, RB Jongejan, and R Ranasinghe. Probabilistic estimation of coastal dune erosion and recession by statistical simulation of storm events. *Applied Ocean Research*, 47:53–62, 2014b.
- JJ Lian, K Xu, and C Ma. Joint impact of rainfall and tidal level on flood risk in a coastal city with a complex river network: a case study of fuzhou city, china. *Hydrology and Earth System Sciences*, 17(2):679–689, 2013.
- A Rueda, P Camus, A Tomás, S Vitousek, and FJ Méndez. A multivariate extreme wave and storm surge climate emulator based on weather patterns. *Ocean Modelling*, 104:242–251, 2016.
- G. Salvadori, C. De Michele, and F. Durante. On the return period and design in a multivariate framework. *Hydrol. Earth Syst. Sci.*, 15:3293–3305, 2011. doi: 10.5194/hess-15-3293-2011.

- G Salvadori, GR Tomasicchio, and F D'Alessandro. Practical guidelines for multivariate analysis and design in coastal and off-shore engineering. *Coastal Engineering*, 88:1–14, 2014.
- G Salvadori, F Durante, GR Tomasicchio, and F D'Alessandro. Practical guidelines for the multivariate assessment of the structural risk in coastal and off-shore engineering. *Coastal Engineering*, 95:77–83, 2015.
- G. Salvadori, F. Durante, C. De Michele, M. Bernardi, and L. Petrella. A multivariate Copula-based framework for dealing with Hazard Scenarios and Failure Probabilities. *Water Resources Research*, 53:3701–3721, 2016. doi: 10.1002/2015WR017225. doi: 10.1002/2015WR017225.
- Katherine A Serafin and Peter Ruggiero. Simulating extreme total water levels using a time-dependent, extreme value approach. *Journal of Geophysical Research: Oceans*, 119(9):6305–6329, 2014.
- Cecilia Svensson and David A Jones. Dependence between extreme sea surge, river flow and precipitation in eastern britain. *International Journal of Climatology*, 22(10):1149–1168, 2002.
- Cecilia Svensson and David A Jones. Dependence between sea surge, river flow and precipitation in south and west britain. *Hydrology and Earth System Sciences Discussions*, 8(5):973–992, 2004.
- Bart van den Hurk, Erik van Meijgaard, Paul de Valk, Klaas-Jan van Heeringen, and Jan Gooijer. Analysis of a compounding surge and precipitation event in the netherlands. *Environmental Research Letters*, 10(3): 035001, 2015.
- T Wahl, C Mudersbach, and J Jensen. Assessing the hydrodynamic boundary conditions for risk analyses in coastal areas: a multivariate statistical approach based on copula functions. *Natural Hazards and Earth System Science*, 12(2):495–510, 2012.
- Thomas Wahl, Shaleen Jain, Jens Bender, Steven D Meyers, and Mark E Luther. Increasing risk of compound flooding from storm surge and rainfall for major us cities. *Nature Climate Change*, 5(12):1093–1097, 2015.
- Thomas Wahl, Nathaniel G Plant, and Joseph W Long. Probabilistic assessment of erosion and flooding risk in the northern gulf of mexico. *Journal of Geophysical Research: Oceans*, 2016.
- Feifei Zheng, Seth Westra, and Scott A Sisson. Quantifying the dependence between extreme rainfall and storm surge in the coastal zone. *Journal of Hydrology*, 505:172–187, 2013.
- Feifei Zheng, Seth Westra, Michael Leonard, and Scott A Sisson. Modeling dependence between extreme rainfall and storm surge to estimate coastal flooding risk. *Water Resources Research*, 50(3):2050–2071, 2014.
- Feifei Zheng, Michael Leonard, and Seth Westra. Application of the design variable method to estimate coastal flood risk. *Journal of Flood Risk Management*, 2015a.
- Feifei Zheng, Michael Leonard, and Seth Westra. Efficient joint probability analysis of flood risk. *Journal of Hydroinformatics*, 17(4):584–597, 2015b.